

Df31 protein and snoRNAs maintain accessible higher order structures of chromatin

Dissertation zur Erlangung des Doktorgrades der
Naturwissenschaften (Dr. rer. nat.) der Fakultät der Biologie und
vorklinischen Medizin der Universität Regensburg

vorgelegt von

Thomas Schubert

aus Regensburg

im Jahr 2012

Das Promotionsgesuch wurde eingereicht am: 16 Mai 2012

Die Arbeit wurde angeleitet von: Prof. Dr. Gernot Längst

Prüfungsausschuss:

Vorsitzender:	Prof. Dr. Herbert Tschochner
Erstgutachter:	Prof. Dr. Gernot Längst
Zweitgutachter:	Prof. Dr. Michael Rehli
Weiterer Gutachter:	Prof. Dr. Gunter Meister
Ersatzgutachter:	Prof. Dr. Reinhard Sterner

Unterschrift:

Table of Contents

List of figures.....	7
List of tables.....	9
List of abbreviations	10
1. Summary	17
2. Introduction	21
2.1. The nucleus, DNA and chromatin.....	21
2.2. The nucleosome, the basic unit of chromatin.....	22
2.3. Higher order structures of chromatin.....	23
2.4. Nuclear bodies, chromatin domains and chromosome territories...	28
2.5. Chromatin conformation and gene activity.....	30
2.6. Mechanisms regulating chromatin structure and function	31
2.6.1. Remodelling on the nucleosomal level.....	31
2.6.2. Remodelling higher order structures of chromatin.....	35
2.6.3. Chromatin marks define the functionality of chromatin domains.....	37
2.7. ncRNA functions in chromatin	39
2.7.1. Influence of RNA on chromatin function on the level of nucleosomes.....	40
2.7.2. RNA, an architectural component of chromatin influencing higher order structures of chromatin.....	43
2.8. Decondensation factor 31	46
3. Objectives	49
4. Results	51
4.1. RNA maintains chromatin accessible in <i>Drosophila in vivo</i>	51
4.2. Reconstituted chromatin recapitulates the RNA-dependent accessibility of chromatin	54
4.3. Chromatin associated RNA maintains accessible higher order structures of chromatin	60
4.4. Df31 is bound to chromatin and its associated RNA.....	65
4.5. Characterisation of Decondensation factor 31.....	66
4.6. Df31 is involved in RNA dependent chromatin opening.....	70
4.7. Chromatin associated snoRNAs open higher order structures of	

chromatin.....	77
4.8. Df31 specifically interacts with snoRNAs	80
4.9. Characterisation of the RNA binding domain of Df31	83
4.10. Generation and characterisation of Df31 antibodies.....	85
4.11. snoRNAs are enriched in the caRNA fraction of human chromatin	87
4.12. RNA maintains chromatin accessible <i>in vivo</i> human HeLa cells.....	89
4.13. The influence of RNA on the accessibility of the human ribosomal DNA locus	92
4.14. Human homologues of Df31	95
4.15. Bioinformatic analysis of HMGN5, a possible Df31 homologue.....	96
4.16. HMGN5 interacts with RNA	100
4.17. Characterisation of the RNA binding domain of HMGN5	101
5. Discussion.....	105
5.1. RNA maintains chromatin accessible in <i>Drosophila</i> cells.....	105
5.2. Chromatin associated RNAs decondense and open up higher order structures of chromatin	106
5.3. Df31 is involved in an RNA dependent mechanism opening up chromatin.....	109
5.4. Df31 specifically interacts with chromatin-associated snoRNAs	111
5.5. snoRNP mediated chromatin opening.....	111
5.6. Potential snoRNP dependent mechanisms to maintain accessible chromatin.....	112
5.7. A conserved RNA-dependent mechanism regulates accessibility of chromatin domains.....	115
5.8. Perspectives.....	117
6. Materials and Methods	123
6.1. Materials	123
6.1.1. technical devices	123
6.1.2. Software tools.....	124
6.1.3. Chemicals and consumables.....	126
6.1.4. Standard Solutions	128
6.1.5. Enzymes	132
6.1.6 Kits.....	133

6.1.7. Standard DNA, RNA and protein marker.....	133
6.1.8. Protease inhibitors, RNase inhibitors and antibiotics.....	134
6.1.9. Bacterial cell lines and media.....	134
6.1.10. Eukaryotic cell lines and media.....	136
6.1.11. Antibodies	137
6.1.12. Oligonucleotides.....	138
6.1.13. plasmids.....	143
6.2. Methods	144
6.2.1. Working with DNA.....	145
6.2.2. Working with RNA	150
6.2.3. Protein biochemical methods.....	151
6.2.4. E. coli culture and methods	155
6.2.5. Expression and purification of recombinant proteins from E. coli.....	156
6.2.6. Eukaryotic cell culture and methods.....	158
6.2.7. Chromatin methods.....	160
7. References	169
8. Appendix	187
8.1. Curriculum vitae.....	187
8.2. List of publications.....	188
8.3. Active participation at conferences	189
8.4. Grants and awards	190
9. Eidesstattliche Erklärung.....	191
10. Acknowledgements	192

List of figures

2. Introduction

Figure 2.1: Atomic structure of the nucleosome core particle (NCP).

Figure 2.2: Models of the 30nm chromatin fibre.

Figure 2.3: Scheme depicting the higher order structures of chromatin

Figure 2.4: Schematic representation of an interphase cell

Figure 2.5: Schematic representation of histone modifications

Figure 2.6: Simplified representation of RNA mediated chromatin remodelling mechanisms in different eukaryotic organisms

4.Results

Figure 4.1: RNA maintains accessible chromatin structures *in vivo Drosophila*

Figure 4.2: Pol II transcribed RNA maintains accessible chromatin structures *in vivo*

Figure 4.3: RNA maintains accessible chromatin structures *in vitro*

Figure 4.4: single stranded RNAs influence chromatin accessibility

Figure 4.5: Testing the activity of MNase in RNaseA treated chromatin.

Figure 4.6: Histone and nucleosome density do not change after RNA depletion.

Figure 4.7: RNA sedimentation is dependent on its interaction with chromatin.

Figure 4.8: The role of RNA in chromatin compaction.

Figure 4.9: Reversible opening of higher order chromatin structures with RNA

Figure 4.10: Quantitative analysis of proteins associated with accessible and inaccessible chromatin fractions.

Figure 4.11: Results of the quantitative analysis of proteins associated with accessible and inaccessible chromatin fractions.

Figure 4.12: Gene expression profiles of the Df31 gene.

Figure 4.13: Abundance of Df31 in *Drosophila melanogaster*

Figure 4.14: Folding prediction of Df31.

Figure 4.15: RNA binding sequence prediction of Df31

Figure 4.16: Df31 is a chromatin- and RNA-binding protein.

Figure 4.17: The interaction of Df31 to histones/chromatin

Figure 4.18: RNA enhances the interaction of Df31 with chromatin

- Figure 4.19: knock-down of Df31 condenses chromatin and decreases its accessibility
- Figure 4.20: Characterization of the caRNA-chromatin interaction.
- Figure 4.21: snoRNAs are highly enriched in caRNAs.
- Figure 4.22: Chromatin associated snoRNAs open up chromatin.
- Figure 4.23: RNA secondary structure prediction
- Figure 4.24: Df31 specifically interacts with snoRNAs
- Figure 4.25: Df31 snoRNA binding *in vitro*
- Figure 4.26: RNA binding prediction of Df31 and overview of Df31 deletion mutants
- Figure 4.27: purification of Df31 deletion mutants
- Figure 4.28: Identification of the binding regions of the Df31 antibodies
- Figure 4.29: snoRNA molecules are highly enriched in human chromatin
- Figure 4.30: RNA maintains accessible chromatin structures *in vivo* HeLa cells
- Figure 4.31: Pol II transcribed RNA maintains accessible chromatin structures *in vivo* HeLa
- Figure 4.32: RNA maintains the accessibility of the ribosomal DNA locus.
- Figure 4.33: Polymerase II inhibition decreases the accessibility of the ribosomal DNA locus.
- Figure 4.34: Sequence alignment between Df31 and HMGN5
- Figure 4.35: Abundance of HMGN5 in *Homo sapiens*
- Figure 4.36: Folding prediction of HMGN5.
- Figure 4.37: Nuclear and nucleolar localisation of HMGN5
- Figure 4.38: RNA binding sequence prediction of HMGN5 and purification
- Figure 4.39: RNA binding study of HMGN5.
- Figure 4.40: RNA binding prediction of HMGN5 and overview of HMGN5 deletion mutants

5. Discussion

- Figure 5.1: Working model how snoRNPs maintain accessible higher order structures of chromatin.

List of tables

- 4.14. structural homologues of Df31 in human
- 6.1.1. List of technical devices
- 6.1.2. List of software tools
- 6.1.3. List of chemicals and consumables
- 6.1.4. List of standard solutions and buffers
- 6.1.5. List of enzymes
- 6.1.6. List of kits
- 6.1.7. List of standard DNA/RNA and protein marker
- 6.1.8. List of RNase and proteinase inhibitors and antibiotics
- 6.1.9. List of bacterial cell lines and media
- 6.1.10. List of eukaryotic cell lines and media
- 6.1.11. List of antibodies
- 6.1.12. List of oligonucleotides
- 6.1.13. List of plasmids
- 6.2.1.8. reaction scheme for standard Polymerase chain reaction
- 6.2.1.9. reaction scheme for colony Polymerase chain reaction
- 6.2.2.2. reaction scheme for *in vitro* transcription

List of abbreviations

ADP	Adenosine-Di-Phosphate
Ago1/4	Argonaute 1/4
Amp	Ampicilin
APS	Ammonium Persulfate
Apro	Apronitin
ASH2	absent, small, or homeotic discs 2
ASF1	Alternative splicing factor 1
ATP	Adenosine-Tri-Phosphate
bp	base pair
BSA	Bovine Serum Albumin
caRNA	chromatin-associated RNA
CAF1	Chromatin assembly factor 1
C-terminal	carboxy terminal
CHD	Chromodomain/helicase/DNA-binding protein
Chp1/2	Chromo domain-containing protein 1/2
ChIP	chromatin imunoprecipitation
CpG	Cytosine-phospatidyl-guanosine
CT	Chromosome territories
Da	Dalton
DamID	DNA adenine methyltransferase identification
DBFs	DNA binding factors
Df31	Decondensation factor 31
DMSO	Dimethylsulfoxide
DNA	Deoxyribonucleic acid
DNMT1	DNA-Cytosine-5-Methyltransferase
DRM1/2	domains rearranged methylase 1/2

dNTP	2'deoynucleotide triphosphate
DTT	dithiothreitol
D1	D1 chromosomal protein
E. coli	Escherichia coli
EDTA	Ethyleneiaminotetraacetate
EGFP	Enhanced green fluorescent protein
EGTA	Ethylene-Glycol-Tetraacetic acid
EM	Electron microscopy
EMANIC	EM-assisted nucleosome interaction capture
EMSA	Electromobility shift assay
EtBr	Ethidium bromide
E(Z)	Enhancer of zeste
FCS	Fetal calf serum
Fig.	Figure
FISH	fluorescence in situ hybridisation
g	gram
g	relative centrifugation force
GH	growth hormone
G1	Gap phase 1
h	hour
hnRNA	heterogeneous nuclear RNAs
H1	Histone 1
H2A	Histone 2A
H2B	Histone 2B
H3	Histone 3
H4	Histone 4
H5	Histone 5

H3K(x)me(y)	mono, di or tri (y) methylation of lysine x of histone 3
H4Kxac	Acetylation of lysine x of histone 4
HAT	Histone-acetylase
HDAC	Histone-deacetylase
HMT	Histone-methyltransferase
His-Tag	Octahistidine Tag
HCNE	highly conserved non-coding element
HDAC	Histone-deacetylase
HIRA	Histone regulatory protein A
HMGN5	High mobility group nucleosomal binding domain 5, also nucleosome binding protein 1
HMT	Histone methyltransferase
HOTAIR	HOX antisense intergenic RNA
HOTTIP	HOXA transcript at the distal tip
HP1	Heterochromatin binding protein 1
HSR1	Heat shock response RNA 1
IAL	IplI-aurora-like kinase
IP	Immuno-precipitation
IPTG	Isopropylthiogalactoside
ISWI	Imitating switch
JARID1	jumanji like demethylase 1
Kd	half maximal binding constant#
Kb	kilobase
kDa	kilo Dalton
l	litre
lincRNA	long interspersed non coding RNA
LB	Luria-Broth

m	meter
M	molar
MARs	matrix-attached regions
MeCP	Methyl-CpG binding protein
MED31	Mediator complex subunit 31
MiCCS	mitotic chromosome coating spheres
Min	minute
miRNA	microRNA
MNase	Micrococcal nuclease
MW	Molecular Weight
MWCO	Molecular Weight cut off
n	Hill coefficient
ncRNA	non coding RNA
N-terminal	amino terminal
NAP1	Nucleosome assembly protein 1
NCP	Nucleosome core particle
Ni-NTA	Nickel-nitroacetic acid
NFAT	nuclear factor of activated T cells
NLP	nucleoplasmin-like proteins
NLS	nuclear localisation sequence
Nop56	nucleolar protein 5A (56kD with KKE/D repeat)
NoRC	Nucleolar remodelling complex
NPM1	B23, nucleophosmin
NPM2	nucleoplasmin
NRON	non-protein coding RNA, repressor of NFAT
NSBP1	nucleosome binding protein 1, also HMGN5

nt	nucleotide
NTD	amino-terminal domain
NuRF	Nucleosome remodelling factor
PAA	Polyacrylamid
PAGE	Polyacrylamid-gel
PBS	Phosphate buffered saline
PBST	Phosphate buffered saline tween
PCR	Polymerase chain reaction
PC	Polycomb protein
PCR	Polymerase chain reaction
PHD	Plant homeodomain
piRNAs	PIWI-interacting RNAs
PML-bodies	promyelocytic leukaemia protein containing nuclear body
PMSF	phenylmethylsulfonyl fluoride
RPD3	Histone deacetylase 1
PRC1/2	Polycomb-group repressive complex 1/2
pRNA	promoter associated RNA
PTM	posttranslational modification
RCC1	regulator of chromatin structure 1
rcf	relative centrifugal speed
rDNA	ribosomal DNA
rec	recombinant
RITS	RNA-induced transcriptional silencing
RNA	Ribonucleic acid
RNAPI	RNA-Polymerase I
RNAPII	RNA-Polymerase II
RNP	Ribonucleoprotein

roX1/2	RNA on the X 1
rpm	rounds per minute
rRNA	ribosomal RNA
RT	room temperature
s, sec	second
SAM	S-adenosyl-L-methionine
sdRNAs	sno-derived RNAs
SINE	short interspersed nuclear elements
Sir2	Silent Information Regulator 2
SDS	Sodium-dodecyl-sulfate
SDS-PAGE	Sodium-dodecyl-sulfate Polyacrylamid-gel
Snf2H	Snf2 homolog protein
snRNA	small nuclear RNA
snoRNA	small nucleolar RNA
snoRNP	small nucleolar ribonucleoprotein
S-phase	synthesis phase
Su(var2-10)	suppressor of variegation 2-10
Su(var3-9)	suppressor of variegation 3-9
SUUR	Suppressor of Under-Replication
SWI/SNF	Switching defective/ sucrose non
TBE	Tris Borate EDTA
TCA	Trichloric acid
TE	Tris/EDTA
TEM	Transmission electron microscopy
TEMED	N,N,N',N'-tetramethylethylenediamine
TF	Transcription factor
TIP5	TTFI-interacting protein
Tris	tris(hydroxymethyl)aminomethane

tRNA	transfer RNA
TSS	Transcription start site
TTF1	Transcription Termination factor 1
U	unit
UV	ultra violet
WCE	Whole cell extract
WDR5	WD repeat-containing protein 5
Wt	wild type
XIST	X (inactive)-specific transcript

1. Summary

The genetic information of the eukaryotic cell is encoded in the DNA. Chromatin represents the form of packaging of DNA, compacting the DNA to fit into the nucleus. However, chromatin has to allow access to the underlying genetic information as it represents the template for all DNA-dependent processes like replication, repair or transcription (van-Holde, 1989; Woodcock and Ghosh, 2010). Recent studies indicate RNA to play a major role in chromatin organisation. The existence of RNA co-fractionating with chromatin was shown more than four decades ago (Bonner and Widholm, 1967; Holoubek et al., 1983; Huang and Bonner, 1965; Huang and Huang, 1969). It is supposed that this chromatin-associated RNA (caRNA) serves as a structural component of chromatin. Despite the high abundance of caRNAs, their functional role and how they assist in chromatin folding remained enigmatic.

In this study, the influence of RNA on *Drosophila* chromatin structure and accessibility was determined. Chromatin accessibility was measured by the sensitivity of chromatin towards the endonuclease Micrococcal nuclease (MNase). Depletion of cellular RNA resulted in decreased chromatin accessibility *in vitro* and *in vivo*, monitored by nuclease sensitivity assays. Decreased chromatin accessibility correlated clearly with RNA depletion and was shown to be due to a change in chromatin conformation. Sucrose gradient sedimentation experiments revealed a proportion of RNA being tightly associated to chromatin. Chromatin containing caRNA adopted an open, decondensed conformation, whereas chromatin that lacked caRNA exhibited a compacted, condensed conformation. Re-addition of caRNA to compact, inaccessible chromatin resulted in subsequent opening of the higher order structures of chromatin. Thus, caRNAs were shown to play a key role in a reversible mechanism organizing higher order structures of chromatin. High-throughput sequencing assays of isolated caRNAs exposed that snoRNA molecules are highly enriched in chromatin compared to the transcriptome *in vitro*. Furthermore, snoRNAs were demonstrated to be capable of opening up higher order structures of chromatin in sucrose gradient sedimentation experiments.

In a mass spectrometric search for possible mediator proteins, the Decondensation factor 31 (Df31) was identified to be RNA dependently bound to chromatin. Here, Df31 specifically interacted with snoRNA molecules while discriminating random RNAs. The Df31 protein is depicted to tether RNAs to chromatin by simultaneous interactions with H3 tails. Knock-down of the protein resulted in a decrease of chromatin accessibility reminiscent to the depletion of RNA. It is proposed that snoRNA molecules bind to larger genomic domains, targeted by Df31 that distinctively recognizes euchromatic regions to maintain these domains accessible and active.

This molecular mechanism seems to be evolutionary conserved across eukaryotes, as the analysis of caRNAs in human cells also revealed a strong enrichment of snoRNA molecules. Comparable to *Drosophila*, depletion of cellular RNA in the human system resulted in decreased chromatin accessibility. In search for Df31 homologues in human, the high mobility group protein HMGN5 was identified being the most conserved based on sequence. In this study, HMGN5 was shown to be an RNA-binding protein, localised in both the nucleus and the nucleolus. Furthermore, recent studies describe HMGN5 to maintain euchromatic regions open and accessible (Rochman et al., 2010; Rochman et al., 2009), resembling the localisation and function of Df31. This study reports a novel role for chromatin-associated snoRNAs in the regulation of higher order structures of chromatin. The working model suggests that snoRNAs in complex with mediator proteins like Df31 cross-link chromatin fibers by protein-mediated interactions with H3 tails. This net-like structure maintains accessible higher order structures of chromatin.

2. Introduction

2.1. The nucleus, DNA and chromatin

The nucleus is the seat of the genetic information in an eukaryotic cell.

A deoxyribonucleic acid (DNA) double strand, which is in human in total around 1.7 m in length, encodes the information. This DNA molecule has to fit into the nuclear compartment with a median diameter of 10µm, making a 10000 fold compaction of the DNA strand necessary. In the same moment this compacted DNA strand has to be highly accessible to enable the fast read out of the genetic information (Felsenfeld and Groudine, 2003). At the end of the 19th century, Walter Flemming discovered a stainable substance filling the nucleus of an eukaryotic cell. He named this substance „chromatin“ deduced from the greek word „chroma“, meaning coloured. Chromatin represents a form of packaging, on the one hand compacting the DNA strand to fit into the nucleus and on the other hand leaving it accessible for all DNA dependent processes. Essentially chromatin consists of DNA, histone proteins and non-histone proteins. Due to its staining abilities, chromatin was historically divided in two different classes, heterochromatin and euchromatin. The strongly stained chromatin domains also referred to as heterochromatin were found mainly in the periphery of the nucleus, whereas the unstained regions in the center of the nucleus were named euchromatin. In a simplistic manner it was thought that euchromatin, possessing a more decondensed chromatin structure, is accessible for DNA dependent processes like replication, transcription or repair. In contrast the condensed heterochromatin was thought to be less accessible for these cellular processes (Felsenfeld, 1978; Woodcock and Ghosh, 2010).

2.2. The nucleosome, the basic unit of chromatin

In general, the first level of DNA packaging into chromatin is represented by the nucleosome, compacting the DNA strand five- to tenfold. 147 base pairs (bp) of DNA are wrapped around an octameric building block of two copies of each core histone H2A, H2B, H3 and H4 in a 1.65 left-handed, superhelical turn (Figure 2.1) (Luger et al., 1997; McGhee and Felsenfeld, 1980; McGhee et al., 1980a).

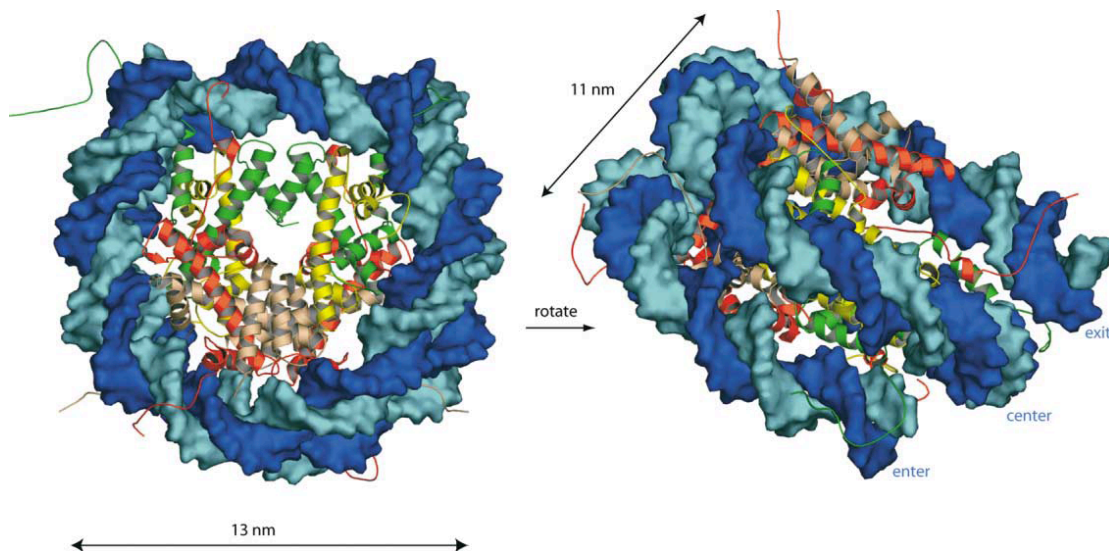


Figure 2.1: Atomic structure of the nucleosome core particle (NCP).

The blue DNA strand is wrapped around the central multicoloured histone octamer.

(After Khorasanizadeh, 2004)

These small, basic molecules (11-17kDa) are highly conserved throughout evolution. The nucleosome core particle (NCP) is organised as a $(H3/H4)_2$ tetramer and two $(H2A/H2B)$ dimers interacting with the DNA strand in 14 major DNA/histone contact clusters (Kornberg, 1977; Luger and Richmond, 1998a; McGhee and Felsenfeld, 1980). The histones bind to the phosphodiester skeleton of the DNA, whereas the points of contact are separated by 10bp, in which the small groove of DNA is turned inside (McGhee et al., 1980a). Histones are bipartite proteins composed of an N-terminal domain and a C-terminal, globular domain. In contrast to the highly conserved C-terminal domain, the N-terminal domain is variable, unstructured and easily accessible as it is protruding outward of the nucleosome (Luger and Richmond, 1998b). Due to several arginine and lysine residues, these positively charged „tails“ facilitate the interaction with the negative charged DNA. H3 and H4 tails interact

intranucleosomal with DNA, whereas H2A and H2B tails can interact with the DNA of a neighbouring nucleosome. (Fletcher and Hansen, 1995; Kan et al., 2009; Luger, 2006). Furthermore, H3 tails play crucial roles in intra-array interactions indicated by crosslinking experiments with reconstituted chromatin arrays (Kan et al., 2007). Nucleosome core particles are separated by the linker DNA, varying in length between 10 to 80bp dependent on the species, the developmental stage and the cell type (van-Holde, 1989). These repetitive units resembles a „beads on a string“ structure in electron microscopic pictures (McGhee et al., 1980b). Despite the fact possessing a diameter of 5-7nm, literature commonly uses „11nm fibre“ to describe this structure.

2.3. Higher order structures of chromatin

Under physiological conditions in the cell, chromatin is not linear in structure, it rather folds into a three-dimensional higher order structure.

Intermolecular interactions between the core histones H2A and the N-terminal domain of H4 of adjacent nucleosomes organize regular higher order structures of chromatin. Furthermore, H3 tails play crucial roles in inter-array interactions indicated by crosslinking experiments with reconstituted chromatin arrays (Kan et al., 2007). The direct internucleosomal contact within a nucleosomal array is thought to be necessary to form the first higher order structure, called „30nm fibre“(Grigoryev and Woodcock, 2012; Robinson and Rhodes, 2006). However, the precise structure of the 30nm fibre and also of the following higher order structures are controversially discussed and still remain elusive.

Two models for the 30nm fibre, the „one start“ and the „two start“ model were proposed (Schalch et al., 2005; Widom and Klug, 1985).

In the “one start” model, the fibre resembles a solenoid wherein the nucleosomes are spooled around a central axis of 6-8 nucleosomes per turn and bent linker DNA (Figure 2.2 left)(Finch and Klug, 1976; Robinson and Rhodes, 2006).

The „two start“ model favours nucleosomes forming a „zigzag“ loop, either twisted or supercoiled and a straight linker DNA (Figure 2.2 right) (Dorigo et al., 2004; Schalch et al., 2005).

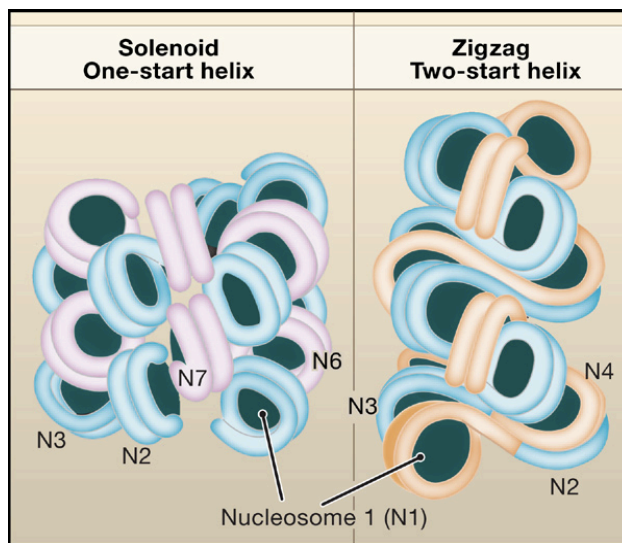


Figure 2.2: Models of the 30nm chromatin fibre.

(Left) In the solenoid model proposed by Rhodes and colleagues, the fibre is an interdigitated one-start helix. Alternative helical gyres are colored blue and magenta. The linker DNA has not been modelled.

(Right) In the zigzag model suggested by Richmond and colleagues, the fibre is a two-start helix with the linker DNA criss crossing between the adjacent

rows of nucleosomes. Alternative gyres are colored blue and orange. Views have the fibre axis running vertically. (After Trementhick 2007)

Long *in vitro* reconstituted, regular chromatin fibres, containing linker histone H1, were analysed by electron microscopy (EM) and cryo-EM under different solution conditions (Robinson and Rhodes, 2006). Measuring the dimensions of the chromatin structures supported the „solenoid – one start“ model.

In contrast, based on *in vitro* studies, using electron microscopy and crystal structures of a tetranucleosome core array, lacking the linker histone, the „two start“ model was strengthened. Furthermore an elegant *in vitro* chemical crosslinking experiment supported the two-start model. Here the H4 and H2A tail were chemically modified to be crosslinked when chromatin was compacted in salt dependent manner. TEM based analysis of these fibres revealed the zigzag conformation (Dorigo et al., 2004).

However, in general agreement the *in vitro* studies indicated that the folding of the nucleosomal array into the 30nm fibre is promoted by low ionic strength and the lack of histone 4 lysine 16 acetylation (McBryant et al., 2009; Wang and Hayes, 2008).

As an alternative approach determining the conformation of chromatin *in vivo*, DNA breaks induced by ionizing radiation indicates cellular chromatin to adopt a zigzag conformation (Rydberg et al., 1998). Transmission electron microscopy (TEM) studies of a special class of nuclei revealed the presence of 30nm fibre like

structures. These nuclei include nucleated erythrocytes and echinoderm sperm and share several features. They lack transcription, possess a special highly charged type of H1, longer nucleosomal repeat length and offer a low portion of non-histone proteins. In thin section TEM of these nuclei 30nm fibres are observed to be organized in the zigzag conformation (Horowitz et al., 1994; Woodcock, 1994).

Studies using optical tweezers measuring the force/length relationship of an isolated chromatin fibre ended up with controversial results arguing for both models (Cui and Bustamante, 2000; Kruithof et al., 2009). A recent study combining computational modelling and EM-assisted nucleosome interaction capture (EMANIC) indicate both types of 30nm fibres being present in chromatin, implying chromatin to be heterogeneous in structure (Grigoryev et al., 2009). The possible transition between the two proposed 30nm fibre chromatin structures may depend on ionic conditions (McBryant et al., 2009), on the position of the H4 tail (Kan et al., 2009), nucleosomal repeat length (Routh et al., 2008), architectural proteins (Georgel et al., 2003; Phillips and Corces, 2009; Rochman et al., 2010; Verschure et al., 2005), histone variants (Fan et al., 2004) and the amount and type of linker histones (Routh et al., 2008). The linker histone H1, representing a highly abundant protein in the cell, which is present in comparable amount to the core histones, binds to entry and exit sites of the adjacent nucleosomes. H1 is thought to bring linker DNA segments together, thereby strengthening and stabilizing the compacted form of the „30nm fibre“ adopting the zigzag conformation (Noll and Kornberg, 1977; Wolffe, 1997; Wolffe et al., 1997). In this way, compacted 30nm fibres are mainly found in gene-poor chromatin regions, decorated with H1. Modest depletion of H1 in fruit fly and mouse, achieved by knock out of several of the six H1 genes, resulted in a reduced nucleosomal repeat length, whereas complete knock out was lethal in both organisms (Fan et al., 2003; Lu et al., 2009). In contrast, open, nucleosomal array resembling, decondensed 30nm fibres are mainly found at gene-dense regions, marking genes to be activated, by creating a potent transcriptional environment (Gilbert et al., 2004).

A large proportion of mammalian chromatin is further packed into higher order structures beyond the „30nm fibre“. A recent EM study clearly shows chromatin being organized into higher order fibre-like structures. Gold-labelled antibodies against the EGFP epitope of a tagged Lac-repressor protein were injected into chinese hamster ovary (CHO) cells, exhibiting a stably integrated Lac-array. The Lac-repressor was detected to bind to the Lac-array in fluorescence microscopy and electron microscopy. Interestingly the EM analysis clearly showed chromatin to be arranged in fibres with a diameter of 120-170nm (Kireev et al., 2008). These fibre-like structures are based on fibre-fibre interactions (Li and Reinberg, 2011). Different fibres are cross-linked by nucleosomal contacts between H2A and H4 sitting on one or the other fibre. Furthermore, the H3 tail plays crucial roles in interarray interactions and fibre formation, as shown by crosslinking studies using reconstituted nucleosomal arrays (Kan et al., 2007; Zheng et al., 2005). In addition, H1 influences fibre formation by criss crossing of different fibres (Thoma et al., 1979). However, the fine structure of these „chromonema“ fibres still remains enigmatic (Belmont et al., 1989; Belmont and Bruce, 1994).

Several studies using different techniques including fluorescence in situ hybridisation (FISH) or conformation capture (3C, 4C, 5C or Hi-C) methods suggest that chromatin fibres can form chromatin loops (Dekker et al., 2002). The high flexibility of chromatin fibres allows physical contacts between distant genomic regions in *cis* and *trans* by looping (Figure 2.3). In this manner regulatory elements like enhancers and promoters or terminators and promoters get into contact, by this regulating the transcription rate of a specific gene (Carter et al., 2002) (Németh et al., 2008). Noteworthy chromatin loops can be found in active and inactive genes, whereas the loops are not only limited to enhancer-promoter contacts, but also contain insulator regions (Tolhuis et al., 2002). Several factors are implicated in regulatory chromatin loop formation, like insulator proteins, transcription factors, polycomb proteins, chromatin remodelling factors and architectural proteins (Cai et al., 2006; Deuring et al., 2000; Splinter et al., 2006). Chromatin loops are frequently formed between the chromatin binding sites of these factors. Some studies suppose that chromatin

loops are anchored at a filamentous nuclear scaffold, called the „nuclear matrix“ (Pederson, 2000). This nuclear skeleton can be detected when nuclei are extracted according to specific protocols and it is thought to contribute to higher order structure formation (Belgrader et al., 1991). However, the existence of this framework is highly discussed and some studies indicate it might be an artefact. Experimental proofs for the actual presence of the „nuclear matrix“ and its function are still missing.

The highest level of DNA compaction is found during M phase in the mitotic metaphase chromosomes. The metaphase chromosome, condensing chromatin 10000-20000 times, represents the most consistent and best-studied higher order structure of chromatin (Figure 2.3).

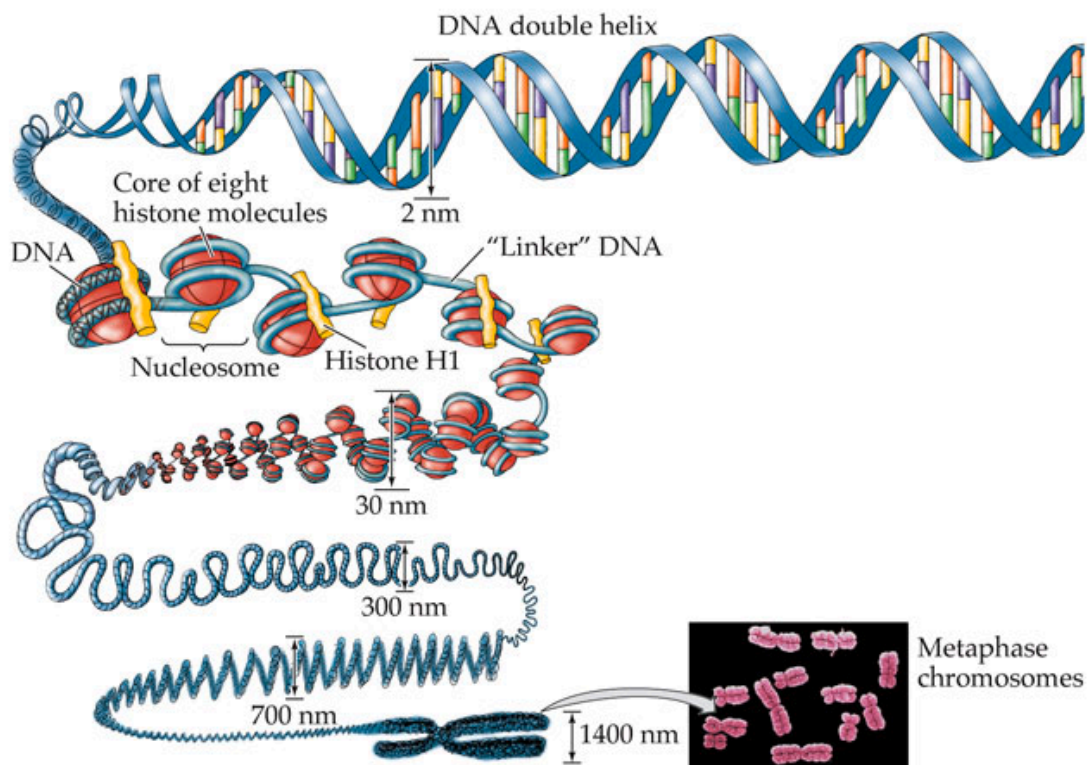


Figure 2.3: Scheme depicting the higher order structures of chromatin

DNA compaction is maintained at different levels of higher order structures: the beads on a string structure, 30nm fibre, chromatin fibres, chromatin loops to metaphase chromosome. (After Life: The science of biology edition 7)

2.4. Nuclear bodies, chromatin domains and chromosome territories

During interphase, the cell nucleus is compartmentalized into different substructures, the morphologically and functionally distinct chromatin domains and nuclear bodies (Figure 2.4) (Nemeth and Langst, 2011). Chromatin domains are dynamic nucleoprotein structures, assembled together with RNA, on interphase chromosomes. These domains specifically interact with each other depending on the physiological state of the cell. Nuclear bodies are protein assemblies like PML-bodies with unknown function, Cajal bodies playing a role in nuclear RNA processing and in assembly of spliceosomal components, nuclear speckles involved in pre-mRNA processing, or nucleoli as the seat of ribosome biogenesis and transcription factories (Cook, 1999; Eskiw and Bazett-Jones, 2002; Lamond and Spector, 2003; Olson et al., 2000; Platani et al., 2000).

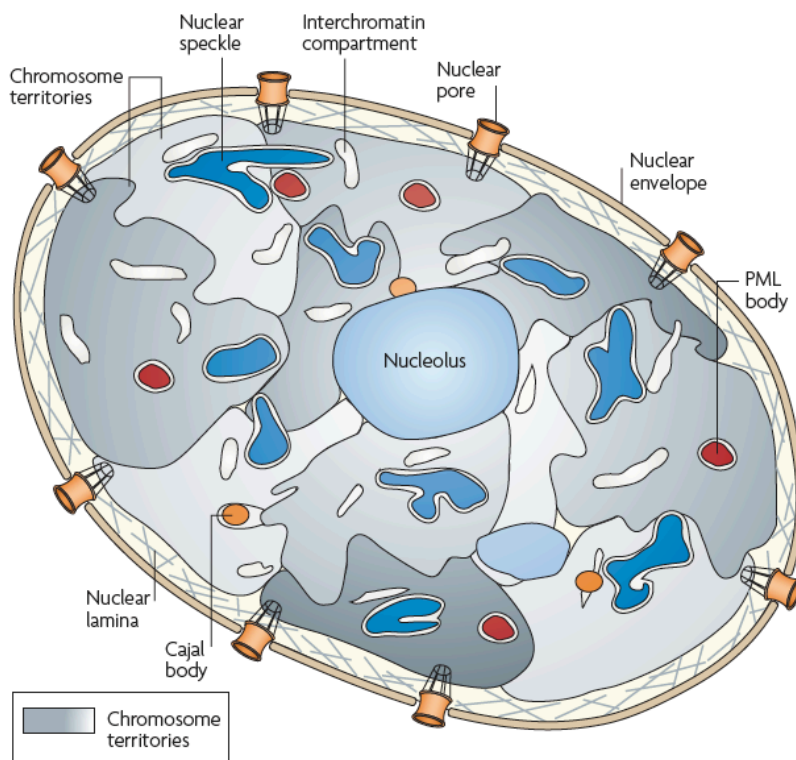


Figure 2.4: Schematic representation of an interphase cell

Chromatin territories, nuclear bodies (PML bodies, Cajal bodies, nuclear speckles and nucleoli) nuclear pores and nuclear lamina are indicated. (After Lanctot 2007)

Early experiments analysing DNA damage provide insights into the distribution of interphase chromosomes in the cell. Microlaser induced DNA damage in

interphase, was analysed and localized in the subsequent metaphase. These experiments revealed that only a small fraction of chromosomes was damaged and that the number was dependent on the irradiated area (Cremer et al., 1982). Underlining this, recent chromosome painting experiments as well as Hi-C analyses show that, in general, interactions within chromosomes are more frequent as interactions between chromosomes, postulating each chromosome adopts a specific area in the nucleus, its chromosome territory (Figure 2.4) (Cremer et al., 2000; Lieberman-Aiden et al., 2009). Chromosome territories are built up by chromatin domains with an average DNA content of 1Mb. Chromatin domains are interconnected by chromatin fibres and may be based on smaller chromatin loop domains. The boundaries of chromosome territories are thought to be fussy and undefined, allowing inter- and intrachromosomal interactions (Cremer et al., 2000). Dependent on the activity and functionality of the underlying chromatin domains, chromatin territories are functionally compartmentalized. Recently, a fractal globule model was described which shows how chromatin domains form chromosome territories (Lieberman-Aiden et al., 2009; Sexton et al., 2012). In this model the genome is a knot-free polymer capable on the one hand to be highly compacted and on the other hand to be very flexible and accessible due to rapid folding and unfolding events. This model explains how the genome is handling its duties in expression and storage. In general, FISH experiments show that gene-rich, chromatin domains are found preferentially in the centre of the nucleus and gene-poor domains in the periphery of the nuclear space (Shopland et al., 2006). Supporting this, chromatin domains associated with the nuclear lamina are largely gene-poor (Guelen et al., 2008). Resembling the localisation of chromatin domains, historically euchromatin was defined to reside in the nuclear centre, whereas heterochromatin can be found in the periphery of an interphase cell. Euchromatin is characterized by high nuclease-accessibility due to a low condensation stage of chromatin, making it suitable for gene-expression, but not necessarily transcriptionally active. Furthermore euchromatin is replicated in early S-phase. In contrast, heterochromatin shows a highly condensed state of chromatin, low gene activity and is replicated in middle to late S-phase. It can be further subdivided into constitutive and facultative heterochromatin (Richards

and Elgin, 2002). Constitutive heterochromatin is mainly formed in repetitive DNA sequences, such as centromeric satellites, pericentromeric repeats, telomeres and contains a low number of genes. Facultative heterochromatin represents regions of chromatin that are targets for transcriptional silencing triggered by external stimuli. The heterochromatin regions found at the inactivated X-chromosome in female mammalian cells, at inactive mating type loci in yeast and at genes silenced by the position variation effect are examples for facultative heterochromatin (Grewal and Jia, 2007).

2.5. Chromatin conformation and gene activity

Systematic FISH studies used to determine chromatin accessibility/compaction compare the physical distance between two genomic sites on a chromosome and the genomic distance of the two probes. Artificial targeting of transcriptional regulators to the mammalian genome resulted in unfolding and decondensation of the chromatin fibres (Muller et al., 2001; Tumbar et al., 1999). In addition chromatin from a plasmid-borne gene in yeast sediments slower in sucrose gradient sedimentation experiments when induced compared to the non-induced state (Kim and Clark, 2002). Moreover, mouse centromeric chromatin sediments faster than bulk chromatin, suggesting a compacted conformation of chromatin at these sites (Fedorov et al., 2001). DNase I hypersensitive site mapping studies strengthen the hypothesis that active genes are in a more accessible, open structural conformation (Stalder et al., 1980). Summing up, these experiments indicate a clear correlation between transcriptional activity of a gene and the chromatin higher order structure of the surrounding chromatin (Chambeyron and Bickmore, 2004). Hence, actively transcribed genes possess a decondensed, open chromatin conformation, whereas transcriptionally silent genes are mainly found in condensed, compacted structures.

Nevertheless, there is growing evidence that decondensed chromatin fibres are not necessarily transcriptionally active (Gilbert et al., 2004). It is assumed that the open conformation only indicates genes that are poised for transcription and can be transcriptionally activated by specific transcription factors if required. Supporting this, active genes are also found in heterochromatic regions that do

not possess open, decondensed chromatin conformations. However, in general agreement, gene-rich chromatin domains are found in an open, decondensed chromatin structure, whereas gene-poor regions adopt a more compacted structure.

2.6. Mechanisms regulating chromatin structure and function

Chromatin structure and organisation is directly linked to its functionality and activity. As a consequence, changes in chromatin structure directly influence chromatin activity and function. The cell possesses several active remodelling mechanisms to alter chromatin structure and function, thereby regulating the biological output of the genome.

2.6.1. Remodelling on the nucleosomal level

The most prominent chromatin remodelling mechanisms that impart variations in chromatin on a nucleosomal level include DNA methylation, ATP-dependent remodelling complexes, chromatin assembly/histone chaperones, variant histone proteins and covalent histone modifications. These well known mechanisms have remarkably impact on the biological output of the genetic information.

2.6.1.1. DNA methylation

Methylation of cytosines in the DNA represents a highly studied chromatin remodelling mechanisms. Out of 56 million CG sites in human, 60-80% are methylated, representing 4-6% of all cytosines in the genome. CpG sites are enriched at hotspots in the genome, called CpG islands. They are found in promoter regions of about 70% of all human genes, including housekeeping genes (Saxonov et al., 2006). DNA methylation of promoter regions leads to repressed gene activity (lister 2009, laurent 2010). Usually active genes show hypomethylation at the transcription start site (TSS) and hypermethylation throughout the coding region. DNA methylation signals can on the one hand be recognized and interpreted by methyl-binding proteins, serving as scaffold

proteins to recruit effector proteins and on the other hand interfere transcription factor binding. Thereby, DNA methylation regulates cellular mechanisms like proliferation, differentiation and development of cells.

2.6.1.2. ATP-dependent nucleosome remodelling complexes

The genome is packed into chromatin by nucleosomes, thereby organising genome activity. Necessary regulatory elements in the genome like promoters, enhancers or replication origins have to be exposed in a regulative manner. Therefore, nucleosome positions within the chromatin fibres have to be changed. To maintain accessibility of these regulatory elements, the cell possesses specialized proteins, which move nucleosomes in an ATP-dependent manner, called nucleosome-remodelling complexes. Remodelers are multisubunit complexes, whereat the associated subunits alter and modify the activity and affinity of the ATPase motor subunit. Studies indicate that remodelling complexes individually interpret the DNA sequence underlying a nucleosome and move the respective nucleosome to a preferred position (Rippe et al., 2007). A model is proposed in which nucleosome remodelers continuously sample a large number of nucleosomes by transiently binding and dissociation without nucleosome translocation (Erdel et al., 2010). Upon identification of histone modifications like acetylation or methylation, that mark a nucleosome to be moved, the remodelling complex translocates the target nucleosome.

2.6.1.3. Chromatin assembly – Histone chaperones

As the basic unit of chromatin is represented by the nucleosome, the assembly and disassembly of nucleosomes highly influences the accessibility of the underlying DNA sequence and its biological activity. Histone chaperones are proteins with specific functions in chromatin assembly and disassembly processes during DNA repair, replication and transcription. Chaperones associate with histones upon their synthesis, shuttle them into the nucleus and help them in association with DNA (Eitoku et al., 2008). In addition the chaperones evict and help to recycle old or damaged histone molecules, thereby playing crucial roles in the establishment of new chromatin states and erasing or

re-establishment of existing chromatin states (Avvakumov et al., 2011; Park and Luger, 2008).

This broad group of proteins is characterized by its histone binding affinity and a histone-dependent, but ATP-independent nucleosome assembly or disassembly activity. Notably, most of the histone chaperones bind preferentially H2A-H2B and H3-H4, but some histone chaperones are known to specifically interact with variant histones and establish these variants into chromatin.

2.6.1.4. Histone variants

Besides the core nucleosomes, specialized non-allelic variant histone proteins evolved. The incorporation of these histone proteins increases the complexity of chromatin and changes the accessibility of the DNA by changing particular properties like the stability, the DNA bendability or the exit and entry sites of the NCP. In addition, the positioning of affected nucleosomes in the genome varies and they can carry posttranslational modifications that differ from the modifications of core histones. While core histones are only expressed and incorporated during S-phase in a replication dependent manner, the histones variants are synthesized and incorporated throughout the cell cycle in a replication independent manner (Sarma and Reinberg, 2005; Talbert and Henikoff, 2010). Mainly variant versions of H3 and H2A are described so far, whereas the incorporation of these histone variants often requires specialized, co-evolved histone chaperone proteins.

Histone variants fulfil various activating or repressing roles in chromatin structure and function.

2.6.1.5. Posttranslational histone modifications (PTMs)

The N-terminal tails of core histones show a highly unstructured composition and do not contribute to the NCP formation. However they are highly conserved across different species. A possible explanation for the high conservation of these sequences lies in the posttranslational modifications, the histone N-termini carry, which highly influence chromatin structure (Imhof, 2006). The deletion of N-termini of H3 and H4 is lethal in yeast (Ling et al., 1996), whereas the

mutations of individual lysine residues changes the expression pattern (Dion et al., 2005).

Histone modifications can be categorised into two groups. The first group, characterized by modifying small chemical groups, includes lysine acetylation, lysine and arginine methylation, serine and threonine phosphorylation, arginine deimination and proline isomerisation. The second group comprises larger modifications like lysine ubiquitylation, glutamate poly-ADP-ribosylation and lysine sumoylation, (Wang et al., 2007). Noteworthy, methylation occurs in a mono-, di- and tri-manner, symmetrically or asymmetrically for lysines, respectively arginines (Wang et al., 2004). Mainly the histone tails of H3 and H4 are modified, whereas only few modifications of H2A and H2B are described. In addition to the core histones also the linker histone H1 is also subject of intense modifications (Figure 2.5) (Godde and Ura, 2008; Greaves et al., 2007).

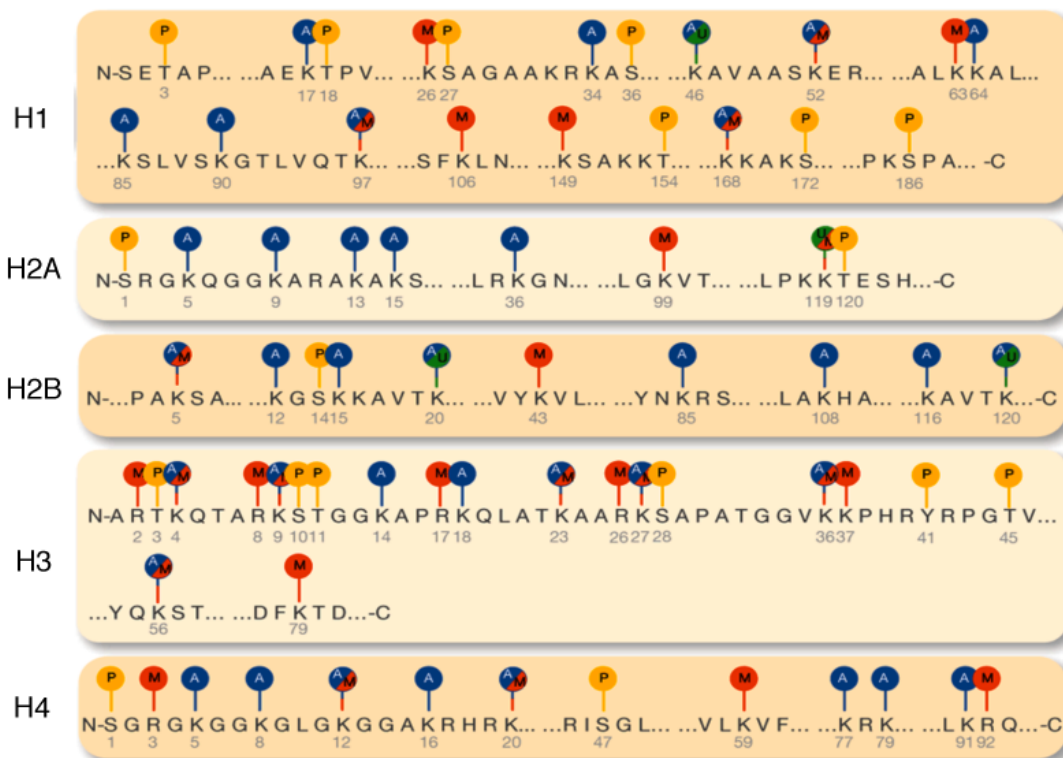


Figure 2.5: Schematic representation of histone modifications.

The main modifications are depicted in different colours. Histone methylation is highlighted in red, acetylation in blue, phosphorylation in orange and ubiquitylation in green. (After Portela and Esteller, 2010)

The molecular mechanisms behind the different histone modifications can be categorised into „cis“ and „trans“ mechanisms (Wang et al., 2007). Cis

mechanisms like acetylation influence chromatin structure via the alteration of intra and internucleosomal contacts by changing steric or ionic interactions. Trans acting modifications, like methylation, recruit „reader“ proteins, which represent the effector molecules, thus influencing chromatin structure like histone modifications writers, remodelling complexes, chromatin architectural proteins or DNA methyltransferases. Growing evidence strengthens the idea of a „histone code“ established by the combination of different histone modifications. In this hypothesis the „writers“ establish the code, the „erasers“ remove the code and the „readers“ bind to specific codes via specialized domains and finally remodel chromatin structure, thereby establishing the optimal chromatin environment for chromatin dependent processes (Wang et al., 2004). Another level of complexity of chromatin remodelling by histone modifications is given by the cross-talk between different modifications, which influence and regulate each other. This cross-talk occurs not only intranucleosomal, but different studies also suggest an internucleosomal cross-talk.

2.6.2. Remodelling higher order structures of chromatin

Influenced by the various effects on chromatin structure on the level of nucleosomes, higher order structures highly affect the activity of chromatin domains. Several factors are shown to organize higher order structures of chromatin: histone modifications, histone variants, presence of H1, non-histone architectural proteins, histone chaperones and ATP-dependent nucleosome remodelling complexes.

Posttranslational Histone modifications

Several studies indicate that histone modifications affect higher order structures of chromatin. Histone acetylation represents a key regulator in folding of chromatin structures. In general, acetylation prevents chromatin to fold into the 30nm fibre and in addition it blocks interarray self-association into higher order structures. H4 lysine 16 acetylation, a mark for transcriptional activity, is sufficient to abolish formation of condensed higher order structures of chromatin (Shogren-Knaak et al., 2006). The acetylation inhibits the interarray interaction mediated by the charged N-terminal tail of H4. Moreover, histone

modifications can recruit architectural proteins to chromatin regions. These effector proteins later contribute to the folding of higher order structures. Exemplarily HP1 preferentially binds to H3K9 me3 and forms inaccessible, compact chromatin domains (Fischle et al., 2005).

Histone variants

Furthermore variant histone proteins influence higher order structures of chromatin. H2A.Z was shown to cooperate with the HP1, thereby establishing a condensed, compacted structure of chromatin, found mostly at constitutive heterochromatin (Fan et al., 2004). The H3 variant H3.3 is mainly detected in active chromatin regions and it is suggested that H3.3 influences the higher order folding of chromatin, establishing active environments (Hake and Allis, 2006).

Linker histone 1

H1 as key regulator of 30nm fibre folding is predominantly found decorating and crosslinking condensed, compacted chromatin domains. In addition to the amount of H1, also the affinity of H1 to chromatin has an impact on chromatin higher order structures. Phosphorylation of H1 residues decreases its affinity to nucleosomes, thus decondensing chromatin fibres (Hendzel et al., 2004).

Architectural, non-histone proteins

Non-histone proteins change the architecture of chromatin. High mobility group proteins increase the accessibility of chromatin, by opening up higher order structures. The nucleosomal binding protein 1, also called HMGN5, interferes with H5 compaction by competing interaction to the linker histone (Rochman et al., 2009). Other architectural proteins like PRC1, MeCP2 and HP1 are mainly involved in the formation of condensed fibres and compacted higher order structures by various mechanisms (Francis et al., 2004) (Georgel et al., 2003) (Verschure et al., 2005).

Histone chaperones

Regular nucleosomal arrays are a prerequisite for compacted chromatin folding. Arrays and also chromatin fibres that display nucleosome free regions are improper substrates for condensed higher order structures of chromatin. Histone chaperones depositing and evicting histones change the array integrity and thereby also higher order structures. In addition histone chaperones exchange core histones by histone variant proteins, which affect higher order structures of chromatin.

ATP-dependent nucleosome remodelling complexes

The nucleosomal repeat length and the periodicity and spacing of the nucleosomes control the higher order structures of chromatin. ATP-dependent remodelling complexes establish the spacing and also the repeat length of the nucleosomal array. In this way highly condensed chromatin fibres characterized by a narrow spacing of the nucleosomes can be established (Deuring et al., 2000) (Varga-Weisz and Becker, 2006). Moreover, nucleosome remodelling factors promote chromatin loop formation and interconnect chromatin regions (Strohner et al., 2005).

2.6.3. Chromatin marks define the functionality of chromatin domains

Recent technical advantages in high throughput sequencing techniques and in bioinformatic analyses of the resulting data, enable the localisation of different epigenetic chromatin marks on a genome wide level. Chromatin immunoprecipitation (ChIP) experiments and related techniques targeting chromatin marks like histone modifications, histone variants or chromatin modifying enzymes generate genome wide binding maps. Furthermore DNase-sequencing or MNase-sequencing methods allow to determine nucleosome positions in the genome. Comparing the different genome wide localisation maps to transcriptome data and RNA-polymerase binding maps indicate correlations between different chromatin marks, nucleosome positions and the activity of the local chromatin region. In addition, correlations and anti-correlations between different chromatin marks are found, suggesting local chromatin functionality

being defined by the sum/combination of the chromatin marks at a specific chromatin region. Hence, the combination of different chromatin modifications characterizes the specific local chromatin environment and its potential transcriptional state. Several studies in different organisms categorised chromatin states by combinatorial analysis of chromatin marks (Ernst and Kellis, 2010; Ernst et al., 2011; Gerstein et al., 2010; Roudier et al., 2011).

Recently, the van Steensel group defined five distinct chromatin types in *Drosophila* by the overlapping combinations of non-histone proteins, histone H1 and H3 and histone marks, that form chromatin domains able to extend more than 100kbp (Filion et al., 2010). Therefore, the genome wide binding sites of 53 broadly selected chromatin components were analysed by techniques like DAM-ID (van Steensel et al., 2001) or ChIP method and compared to the interaction sites of H3 and the histone marks H3K4me2, H3K9me2, H3K27me3 and H3K79me3 in *Drosophila*. Prominent members of the selected proteins were histone modifying enzymes, proteins that bind to histone modifications, general transcription machinery components, nucleosome remodelers, insulator proteins, heterochromatin proteins, structural components of chromatin and DNA-binding factors. Interestingly this bioinformatical approach identified two already well-studied heterochromatin types. But in addition this study defined a third type of inactive chromatin as well as two active types. The interesting model proposed, describes how the constraints of chromatin in highly packaging and giving access are solved by structural modification.

The overlapping, combinatorial analyses of the non-histone proteins, histone H1 and H3 and histone modifications as well as their underlying mechanisms result in new insights into the organisation of functional chromatin domains and territories. However, the high impact of RNA on the organisation of functional chromatin domains is not taken into account.

2.7. ncRNA functions in chromatin

It becomes more and more evident that the transcriptional output of the genome is dominated by RNA molecules lacking the potential to encode for proteins (non-coding RNAs, ncRNAs) rather than by protein-coding RNAs. 98% of the cellular transcription results in ncRNA, but the biological relevance of these pervasive transcribed ncRNAs was long time a matter of debate (Wilusz et al., 2009).

But there is growing evidence that these molecules, former called evolutionary “junk”, possess biological functions. In agreement to this, many ncRNAs are highly regulated during development, exhibit celltype specific expression, localize to specific nuclear compartments and are linked to specific diseases. Of fundamental importance are the functions of these ncRNAs in regulation of gene-expression and development. Various modes of action for ncRNAs exist, but it was shown that even the ncRNA transcription itself can influence and co-regulate adjacent genes by modulating the promoter structure of these adjacent genes (Katayama et al., 2005). Furthermore, ncRNAs can directly modulate the activity and localisation of transcription factors. The long ncRNA HSR1 (Heat shock response RNA 1) for example binds to the heat shock transcription factor 1 (HSF1), enabling it to induce expression of heat shock response genes (Shamovsky et al., 2006). Conversely under heat shock conditions ncRNAs derived from retrotransposon repeat elements (SINEs) inhibit overall gene transcription by interaction to RNA polymerase II (Allen et al., 2004).

The transcription factor NFTA is actively localized to the nucleus upon external calcium signals, thereby upregulating gene transcription. The ncRNA NRON, however, inhibits NFTA nuclear accumulation by binding and blocking of to the trafficking machinery (Willingham et al., 2005).

2.7.1. Influence of RNA on chromatin function on the level of nucleosomes

Despite the aforementioned “classical” chromatin remodelling mechanisms, a great variety of studies clearly show that RNA to plays a major role in chromatin organisation. Many cellular mechanisms based on chromatin structures are directed and organised by short (<200nt) as well as long (>200nt) ncRNAs.

Short ncRNAs

In plants and yeast, an RNA dependent mechanism, based on short ncRNAs, was discovered, being responsible for heterochromatin formation and gene silencing. Heterochromatin formation by H3K9 me2/3 and the binding of HP1 (or the yeast homologues Swi6 /Chp1/Chp2) is targeted by small interfering RNAs (siRNAs), derived from the RNA-interference mechanism (Hall et al., 2002). The RNA-induced transcriptional silencing complex (RITS) consists of Ago1, Chp1, the adaptor protein Tas3 and the associated siRNA. The complex is recruited to chromatin most likely via the RNA-DNA hybrid formation (Nakama et al., 2012). A histone-methyltransferase is attracted and subsequently H3K9 is methylated. The epigenetic mark is read by Swi6, promoting centromeric heterochromatin formation and subsequent gene silencing (Figure 2.6A) (Grewal and Jia, 2007). Another class of small RNAs the piRNAs (PIWI-interacting RNAs), known to repress transposon activity in animals, are also involved in heterochromatin formation. These RNAi independent RNAs interact with the Argonaute-like Piwi proteins and recruit histone-methyltransferase activity and HP1 to target transposons, thereby silencing them (Figure 2.6A)(Brower-Toland et al., 2007). In plants, RNA-directed DNA methylation is a common mechanism to silence target genes. RNA-Polymerase IV transcripts processed by the RNAi machinery are incorporated into Ago4 to guide DRM1/2 DNA methyltransferases to the RNA complementary sites. As a result, promoter directed siRNAs silence plant promoters and their genes, or plants inactivate transposons in this manner (Figure 2.6B) (Meins et al., 2005).

Tissue-specific transcription of SINEs in the murine growth hormone (GH) locus is required to activate the gene locus. The repeat element, serving as a boundary between active and inactive domains, generates short RNA-Polymerase II and III

transcripts that are necessary and sufficient to reposition the GH locus in euchromatic environment. However, the exact mechanism, how these ncRNA influence chromatin domain positioning and activity remains elusive (Figure 2.6C) (Lunyak et al., 2007).

Long ncRNAs

To ensure equal gene expression in both genders while possessing different numbers of sex chromosomes, cells exhibit RNA-dependent compensation mechanisms.

The first example showing long ncRNAs to possess regulatory function was the discovery of the 17kb Xist ncRNA (Brockdorff et al., 1992). This RNA is involved in the X-chromosome inactivation mechanism of female mammalian cells. A complex regulation mediated by the ncRNAs, Xist and its antisense transcript and counterpart Tsix results in the inactivation of one of the X-chromosomes by packing it into condensed heterochromatin. The Xist ncRNA recruits repressive chromatin modifying enzymes like polycomb proteins or methyltransferases to the X-chromosome and coats the whole chromosome to ensure its genetic inactivity (Figure 2.6D) (Chow and Heard, 2009).

In contrast to the downregulation of one sex chromosome in mammals, in *Drosophila* the male cells upregulate the single X-chromosome to achieve the same gene activity than the female flies. Reminiscent to mammals, ncRNAs participate in a regulative manner. RoX1 and roX2 RNAs recruit their binding partners to specific target sites, where the RNP complex acts as histone acetylase opening up and activating chromatin higher order structures and upregulate gene expression (Figure 2.6D) (Franke and Baker, 1999).

A recent high-throughput RNA analysis implies, that in mouse more than 1300 loci are expressed in a parent-of-origin-specific manner, as subject to parental imprinting mechanisms (Gregg et al., 2010). In this vein, one or the other gene loci, dependent on the parental origin, is silenced. Kcnq1ot1, a long ncRNA, is required to downregulate a set of gene loci with paternal origin. Polycomb-group proteins, G9a and DNMTs are recruited to the paternal loci to silence the genes by histone modifications (H3K27me3, H3K9me3 respectively) and DNA-methylation (Kanduri, 2011).

A novel class of long non-translated RNAs, the long intervening non-coding RNAs (lincRNAs), serves as molecular scaffolds to coordinate the action of histone-modifying enzymes (Figure 2.6D) (Khalil et al., 2009). More than 1600 lincRNAs were found in chromatin signature analysis across four mouse cell lines, exhibiting high conservation in mammals (Guttman et al., 2009). Different studies indicate lincRNA molecules to fulfil different functions in the chromatin context. Exemplarily for a repressive mechanism influencing chromatin structure and function, the lincRNA HOTAIR mediates the recruitment of PRC2, which silences genes by the chromatin modification H3K27me3 (Figure 2.6D) (Tsai et al., 2010). In contrast, the WDR5 subunit of the WDR5/MLL complex, which activates gene transcription by H3K4me3, is recruited to the specific loci by the lincRNA HOTTIP (Wang et al., 2011).

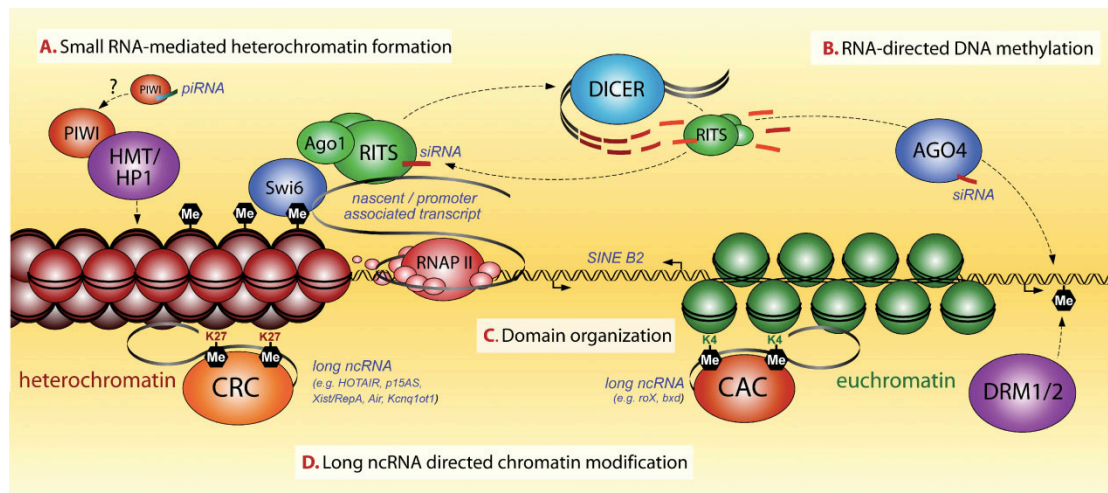


Figure 2.6: Simplified representation of RNA mediated chromatin remodelling mechanisms in different eukaryotic organisms. (A) Mechanisms mediated by small RNAs: PIWI associated RNAs in complex with PIWI proteins interact with HP1 and HMT and induce heterochromatin dependent silencing in *Drosophila* and direct histone methylation in mammals. siRNAs produced by DICER direct histone methylation by RITS recruitment in heterochromatin and centromeres of yeast. The methylation signal is recognized by Swi6 a HP1 homologue in yeast and heterochromatin formation is propagated. (B) In plants siRNAs transcribed by Pol IV recruit a DNMT that methylates DNA. (C) The transcription of the SINE B2 RNA element in mouse establishes boundaries between active and inactive chromatin domains. (D) Long ncRNA serve as scaffolds to recruit activating or repressing effector proteins in cis or trans regulating chromatin structure and activity. (After Mattick 2009)

In general agreement, RNA directed processes help to orchestrate chromatin architecture and epigenetic memory. Many proteins involved in chromatin

remodelling and modification have the capacity to bind RNA directly or interact to complexes that contain RNA (Mattick et al., 2009). The binding of HP1, a major structural component of heterochromatin, for example, is highly e.g. dependent on the presence of RNA (Maison et al., 2002). Moreover, DNMTs and DNA methyl binding proteins recognize and interact with RNA (Jeffery and Nakielny, 2004). Other chromatin proteins binding RNA contain multi KH domains, like DPP1 which suppresses heterochromatin-mediated silencing in *Drosophila* (Birchler et al., 2004), Tudor domains, Set domains or Chromodomains (Bernstein et al., 2006; Shimojo et al., 2008; Tresaugues et al., 2006). Interestingly, only a few of these chromatin remodelling proteins are described to possess a preference for particular DNA sequences. However the modifications have to be purposefully directed to “different positions, in different loci, in different cells” (Mattick et al., 2009), implying another layer of information to guide these processes, which seems to be RNA-based.

Moreover, RNA represents an architectural component of chromatin and therefore may directly influence chromatin organisation and structure (Pederson and Bhorjee, 1979; Rodríguez-Campos and Azorín, 2007).

2.7.2. RNA, an architectural component of chromatin influencing higher order structures of chromatin

Early reports showing RNA being associated to chromatin date back to the late 60s of the last century. James Bonner and colleagues showed that 10% of the total nucleic acids found in chromatin of pea buds were RNA (Huang and Bonner, 1965). Many other groups, working on different model organisms, confirmed their results in various organisms (Arnold and Young, 1972; Getz and Saunders, 1973; Huang and Huang, 1969; Mondal et al., 2010; Rodríguez-Campos and Azorín, 2007; von Heyden and Zachau, 1971). The fraction of chromatin-associated RNA (caRNA) has been reported to be about 1% of the DNA level in calf thymus, 2-5% in *Drosophila* and chicken embryos (Rodríguez-Campos and Azorín, 2007).

RNA is supposed to be an integral component of chromatin. Defined as nuclear body, paraspeckles comprise several RNA-binding proteins. RNase A treatment

resulted in disrupted structures, as paraspeckles are formed out of several long ncRNAs (Clemson et al., 2009; Fox et al., 2005).

In addition, RNA fulfils important roles in the organisation of the cellular cytoskeleton and highly affects chromosome and spindle formation in mitosis. In *Xenopus* oocytes, the cytoskeleton is dependent on two ncRNAs, whereas their depletion results in severe defects in the cytokeratin network, but not in the actin network (Kloc et al., 2005). Furthermore, the mitotic spindle assembly requires an RNP-complex. The necessary ncRNA acts transcription independent, implying to be an integral component of the spindle (Blower et al., 2005).

Interestingly, RNAs are also participating in the structure of the mitotic chromosomes. RNA molecules coat whole chromosomes as detected by immunofluorescence, enoting a structural role of the RNA. In addition, RNAs form „mitotic chromosome coating spheres“ (MiCCS), which are necessary for proper chromosome separation (Chiba and Tanabe, 2010).

Early studies indicate that RNA plays a crucial role in the suggested nuclear skeleton, the „nuclear matrix“. A heterogeneous group of high molecular weight, heterogeneous nuclear RNAs (hnRNA) is found being tightly connected to the matrix structures after high salt extraction of nuclei in complex with matrix binding proteins (van Eekelen and van Venrooij, 1981). RNaseA treatment disrupted this framework and lead to the collapse of chromatin, implying a functional role of RNA in the organisation of chromatin higher order structures (Belgrader et al., 1991; Bouvier et al., 1985). In support of this, a study by Penman and colleagues showed changed nuclear and chromatin structures after the inhibition of transcription (Nickerson et al., 1989).

A study by Berezney and colleagues clearly indicates a role of RNA in organisation of chromosome territories. RNA depletion resulted in a disruption and break down of chromosome territories, assuming that RNP complexes regulate the organisation of chromosome territories (Ma et al., 1999).

In addition to the above mentioned RNA-mediated mechanisms, it was recently suggested, that a fraction of soluble RNA molecules alter higher order structures of chromatin (Caudron-Herger et al., 2011). Depletion of cellular RNA by RNase A treatment resulted in compaction of cellular chromatin, detected in fluorescence microscopy.

Models from the late 1970s describe a positive role of caRNA in the regulation of transcription (Britten and Davidson, 1969). Herein, caRNA functions as an “activator” for the transcription of an “acceptor gene” by sequence specific interaction between RNA and DNA; however, studies to strengthen the model are rare. Other studies showed that caRNA activates the template chromatin and thereby increases transcriptional activity of chicken liver chromatin. It was assumed that the caRNA interferes with the binding of histones and the eviction of these would lead to a changed structure of chromatin favouring transcription (Kanehisa et al., 1971) (Tanaka and Kanehisa, 1972). Recently, a group focused on the identification of caRNAs in human fibroblasts. The identified RNAs exhibit high conservation across species and the preliminary functional characterisation of one selected RNA molecule suggested a positive regulatory influence on neighbouring genes. It was supposed that the modulation of the chromatin structure in *cis* via the RNA results in increased gene activity, suggesting that RNA is an integral component of chromatin (Mondal et al., 2010).

In contrast to the studies and models suggesting an activating function of caRNA in transcription, there are in addition studies implying caRNA to promote transcriptional silencing. RNA was found being associated with inactive heterochromatin of avian erythrocytes and with inactive bull sperm chromatin (Paul and Duerksen, 1975). Therefore, it was claimed that caRNA is a structural component of heterochromatin. Underlining this, a study determining the influence of RNA on chromatin accessibility of, Micrococcal Nuclease (MNase) released, chicken and fruit fly chromatin, indicates a correlation between RNA content and inaccessibility (Rodríguez-Campos and Azorín, 2007).

Despite the high abundance of chromatin-associated RNAs, their functional role in chromatin and how they assist in chromatin folding is controversially discussed and still remains enigmatic.

2.8. Decondensation factor 31

As the decondensation factor 31 (Df31) was identified in this study as an adaptor protein binding RNA and chromatin, a detailed description is given.

Originally identified decondensing compacted sperm chromatin *in vitro*, Df31 was purified of *Drosophila* embryonic extracts. The 183aa protein is highly abundant in the embryonic extracts representing around 0,1% of the total protein content, comparable to the amount of H1 (Crevel and Cotterill, 1995). The 1,6kbp mRNA (CG2207, FBgn0022893) of Df31 is transcribed from a fast evolving gene, located at position 39e in chromosome 2 (Schmid and Tautz, 1997). Moreover, Df31 is expressed in a wide range of cell types, throughout differentiation and is present in dividing and non dividing cells (Crevel et al., 2001). In addition, the 18,8kDa protein migrates in SDS PAGE as a doublet with apparent sizes of 18 and 31kDa.

Df31 is shown to be phosphorylated, whereas one identified serine phosphorylation site of Df31 is serine at position 41. The phosphorylating enzyme is predicted to be casein kinase II. In addition to this phosphorylation site, further unidentified modifications are suggested by mass spectrometric analysis (Crevel et al., 2001). Moreover, Df31 possesses a bipartite nuclear localisation sequence (NLS) at amino acid 95-108. A biochemical characterisation study showed that Df31 is an intrinsically disordered protein, explaining the unexpected electromobility in SDS PAGE and its heat stability (Szollosi et al., 2008). The combination of NMR analysis, limited proteolysis, CD spectroscopy, bioinformatics, gel-filtration techniques, chemical crosslinking and differential scanning calorimetry clearly demonstrates Df31 to exhibit a flexible, unstructured, monomeric architecture, prevalent for protein or RNA chaperone proteins. In general intrinsic disorder allows proteins to adapt to the structure of several binding partners, a phenomenon termed binding promiscuity or „moonlightening“ (Szollosi et al., 2008). Originally, the function of Df31 was defined to remove sperm specific chromatin proteins and exchange them with core histones (Crevel and Cotterill, 1995). However, recent studies indicate Df31 to play a more general role in the organisation of higher order structures of chromatin (Crevel et al., 2001; Guillebault and Cotterill, 2007). Microinjection of antisense oligonucleotides into *Drosophila* embryos depleting Df31 mRNA, lead

to a general condensation of chromatin. In addition, Df31 protein seems to be chromatin associated throughout the cell cycle in microscopic analyses as well as chromatin fractionation experiments. However, cross-linking experiments indicate that the association to chromatin is not due to direct interaction with DNA (Guillebault and Cotterill, 2007). The interaction of Df31 to oligonucleosomes is salt resistant as shown *in vitro* and *in vivo*. However, the binding of Df31 to the oligonucleosomal template happens in a transient manner (Guillebault and Cotterill, 2007). Column based assays indicate H3 to be the primary binding partner of Df31 in chromatin. Analysis of the binding behaviour of deletion mutants of Df31 to chromatin suggested several parts of the protein (aa1-21, 49-75, 130-183) to contribute to the chromatin interaction *in vitro*. Furthermore, Df31 binding to chromatin showed no significant influence on H1-chromatin interaction. Df31 may be involved in the organisation of higher order structures as it can interlink different chromatin fibres by bridging (Guillebault and Cotterill, 2007). In a genome wide DAM-ID study Df31 was localized exclusively to euchromatic regions as defined by epigenetic marks, implying a possible role in establishing or maintaining open, decondensed chromatin regions (Filion et al., 2010). However, this important role of Df31 in chromatin structure is still elusive and remains to be further characterized.

3. Objectives

Several studies suggested a stable interaction of RNA with chromatin. However the function of this fraction of RNA in chromatin structure and function is unclear.

The aim of this study is to identify functions of chromatin associated RNA molecules that affect properties of chromatin, like accessibility, conformation and structure in *Drosophila* and human.

In order to shed light on a possible function of RNA in chromatin organisation and structure, chromatin accessibility will be monitored *in vitro* and *in vivo* by nuclease sensitivity assays. In this regard, RNA depletion should unravel the influence on the accessibility of chromatin. Moreover, chromatin-associated RNA molecules (caRNAs) will be identified and their function in regulating the global chromatin structure *in vitro* and *in vivo* will be investigated. In addition, possible effector-proteins interacting with caRNAs can be identified. Furthermore, potential mechanisms of how caRNAs affect chromatin structure and function should be characterized.

4. Results

4.1. RNA maintains chromatin accessible in *Drosophila* *in vivo*

To examine whether RNA affects chromatin structure in *Drosophila* cells, cellular RNA was hydrolysed and chromatin structure was probed by its accessibility to the endonuclease micrococcal nuclease (MNase).

Drosophila S2 cells were permeabilised with 0.1% NP40, a concentration that does not affect the overall cellular integrity (Iborra et al., 2001; Stewart et al., 1991). MNase was added to the permeabilised cells and the chromatin accessibility was monitored. Limited MNase digestion typically creates a ladder of DNA fragments, where the median length of nucleosomal fragments depends on the MNase concentration and incubation time (Figure 4.1A, lanes 2-7).

Digestion of the cellular chromatin with 10 U of MNase for 2 minutes gives rise to a DNA ladder, reaching from the small DNA fragments protected by mononucleosomes, to large DNA fragments (Figure 4.1B, lane 2). The addition of increasing amounts of RNaseA for 5 minutes, prior to MNase digestion, resulted in decreased sensitivity of chromatin towards MNase (Figure 4.1B, lanes 3-7).

Supporting this, permeabilised *Drosophila* S2 cells were incubated with RNaseA (150 µg/ml) for increasing time (0 to 15 min) and subsequently monitored for changes in chromatin accessibility by MNase digestion. This revealed a decreased accessibility after 6min of RNaseA incubation (Figure 4.1C).

Furthermore, the accessibility of cellular chromatin correlates with the depletion of RNA, as shown by visualisation of RNA and DNA after the MNase accessibility assay (Figure 4.1D). Nucleic acid purification was performed in the absence (lanes 1 to 5) or in the presence of RNaseA (lanes 7 to 11) in the stop buffer, revealing the levels of RNA remaining in the chromatin fraction.

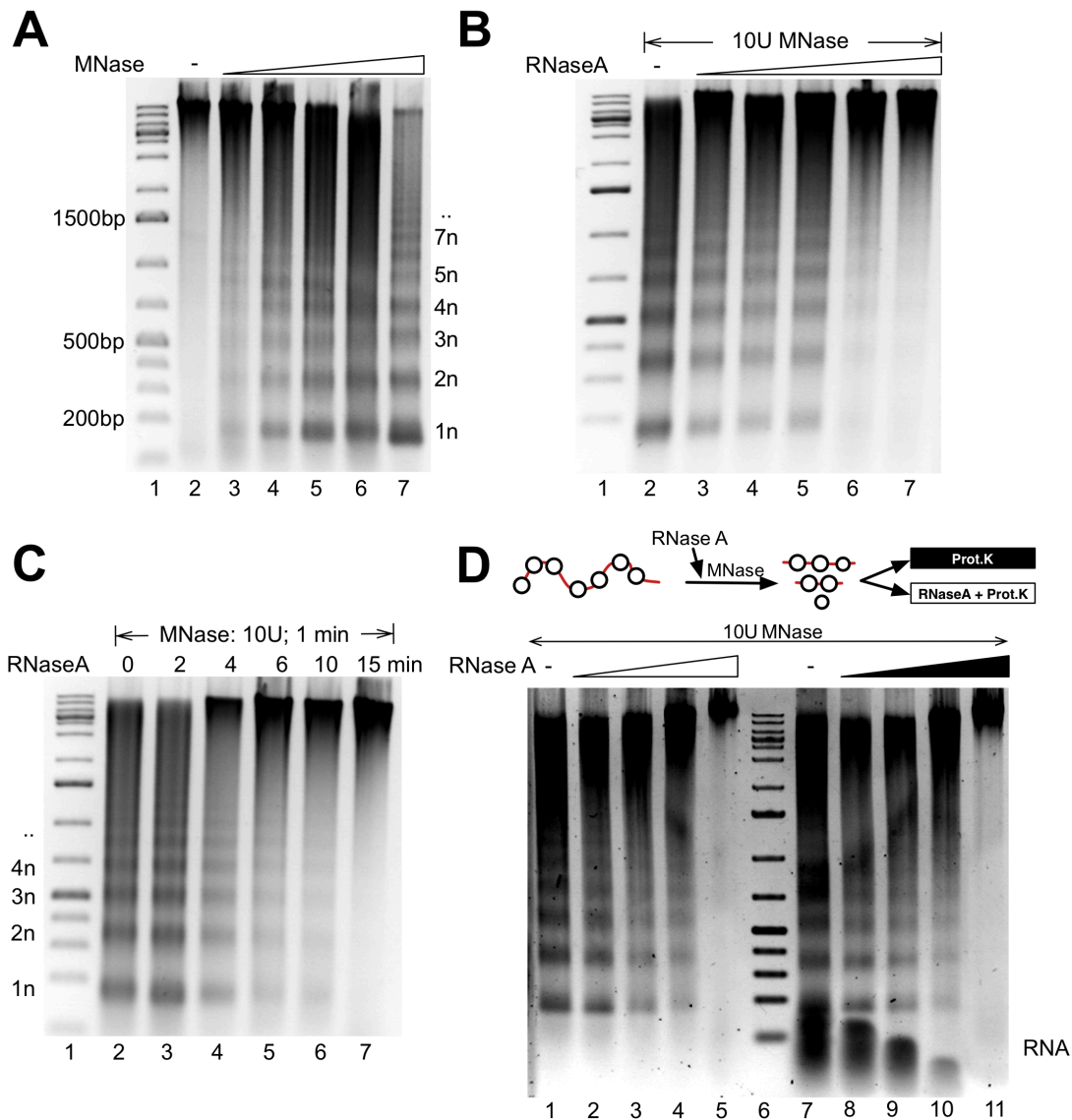


Figure 4.1: RNA maintains accessible chromatin structures in *Drosophila* cells

(A) Permeabilised *Drosophila* S2 cells were incubated with increasing concentrations of MNase (1 to 10 U) for 2 min. Reactions were stopped, RNA and proteins were digested, and the DNA was visualised by agarose gel electrophoresis. The positions of the monomers and multimers of the nucleosomal DNA (1n, 2n,...) and the DNA marker (lane 1) are indicated. **(B)** RNaseA treatment of permeabilised *Drosophila* S2 cells prior to MNase accessibility analysis. Permeabilised *Drosophila* S2 cells were incubated for 5 minutes without (lane 2) or with RNaseA (lanes 3 to 7), MNase accessibility was analysed with 10U MNase. Analysis of the DNA was performed as described in (A). The positions of the monomers and multimers of the nucleosomal DNA (1n, 2n,...) and the DNA marker (lane 1) are indicated. **(C)** Monitoring the RNaseA dependent kinetics of chromatin accessibility *in vivo*. Permeabilised *Drosophila* cells were treated with 150 µg/ml RNaseA for 0 to 15 min (lanes 2 to 7) and then incubated with 10 U MNase for 2 min. The reaction was stopped, nucleic acids were purified and analyzed by agarose gel-electrophoresis. The DNA marker is shown in lane 1. **(D)** Chromatin compaction correlates with the loss of RNA. S2 cells were

incubated for 5 min with increasing amounts of RNaseA (10 to 150 $\mu\text{g/ml}$) and subsequently incubated with 10 U MNase for 2 min, as indicated. Reactions were stopped and split in two halves. One half was depleted of proteins only (black box), in the other half both RNA and proteins (white box) were hydrolyzed. Nucleic acids were analyzed as described.

Moreover, higher concentrations of MNase are again capable of generating a nucleosomal ladder, suggesting that in the absence of RNA, chromatin forms a more compact structure (Figure 4.2A).

To test whether Pol II transcribes the RNA involved in chromatin opening, cells were treated with α -amanitin for up to 6 hrs and assayed for MNase accessibility (Figure 4.2B; compare panels 2 and 3). The accessibility analysis lead to the conclusion, that chromatin of treated cells is less accessible towards the nuclease than the chromatin of untreated cells. Structural changes of nuclear chromatin was visualised by DAPI staining of the DNA in *Drosophila* S2 cells and fluorescence microscopy (Figure 4.2B). Whereas DNA staining in non-treated cells appears homogenous, increasing incubation time with α -amanitin results in a rough, compacted DNA staining pattern correlating with chromatin condensation. The MNase accessibility analysis and the fluorescence microscopy suggest that a RNA fraction synthesized by RNA Pol II is required to maintain chromatin structures in an accessible form.

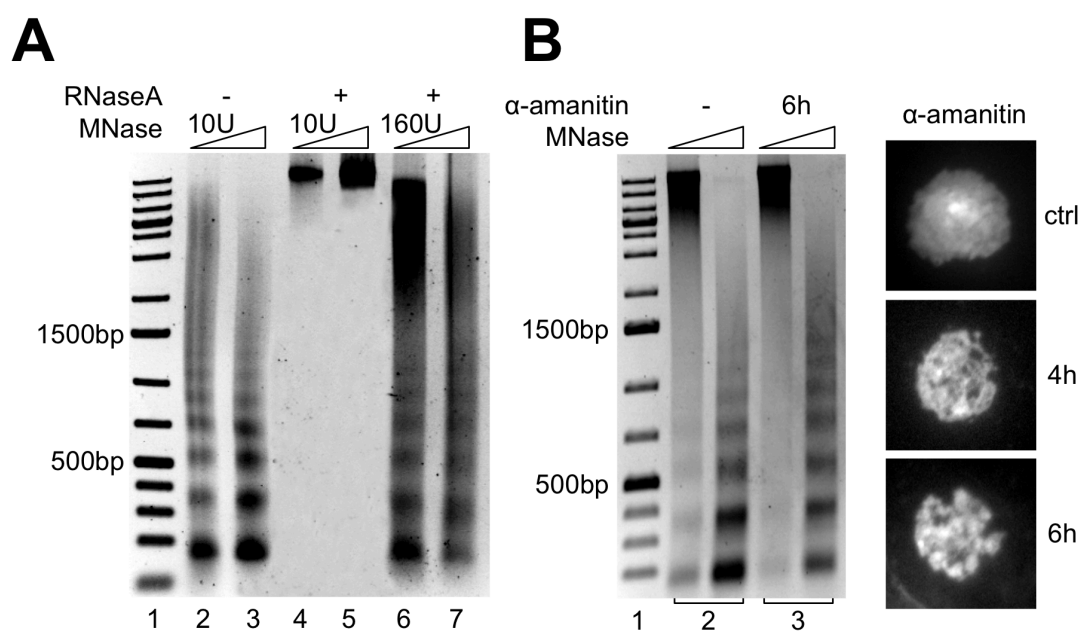


Figure 4.2: Pol II transcribed RNA maintains accessible chromatin structures *in vivo*

(A) S2 cells were treated without or with RNaseA and chromatin was subsequently hydrolysed with different doses of MNase as indicated. Analysis of the DNA was performed as described in (A). **(B)** *Drosophila* S2 cells were incubated with α -amanitin (50 μ g/ml) for 6 h. Chromatin accessibility was assessed as described in (1B) with a identical number of cells. The right panel shows the DNA staining of α -amanitin treated *Drosophila* cells by fluorescence microscopy.

Taken together the *in vivo* studies show that depletion of cellular RNA influences the accessibility of chromatin. The accessibility of chromatin correlates with the RNA content, whereas the RNA seems to be transcribed by RNA Polymerase II.

4.2. Reconstituted chromatin recapitulates the RNA-dependent accessibility of chromatin

To address the role of RNA in the organisation of higher order structures of chromatin, a cell-free chromatin assembly system derived from *Drosophila* embryos was used (Becker and Wu, 1992). Incubation of circular plasmid DNA with the *Drosophila* extract led to efficient chromatin assembly, as visualised by partial MNase digestion (Figure 4.3A, panel 2). The extract contains high levels of RNA, which is not required for chromatin assembly (Figure 4.3A, panel 3 and 5). Similar to what was observed in *Drosophila* cells, RNaseA treatment of the reconstituted chromatin results in decreased MNase accessibility, which strictly correlates with the disappearance of the small RNA molecules in the chromatin preparation (Figure 4.3B; Figure 4.3C). To monitor whether DNA aggregated non-specifically and whether nucleosomes were still organised in a regular array, RNaseA treated chromatin was incubated with a 16-fold higher concentration of MNase (Figure 4.3C, panels 10 and 11). Like in the *Drosophila* cells, elevated MNase concentrations lead to the generation of a regular nucleosomal ladder, indicating that RNA depletion also results in chromatin compaction *in vitro*.

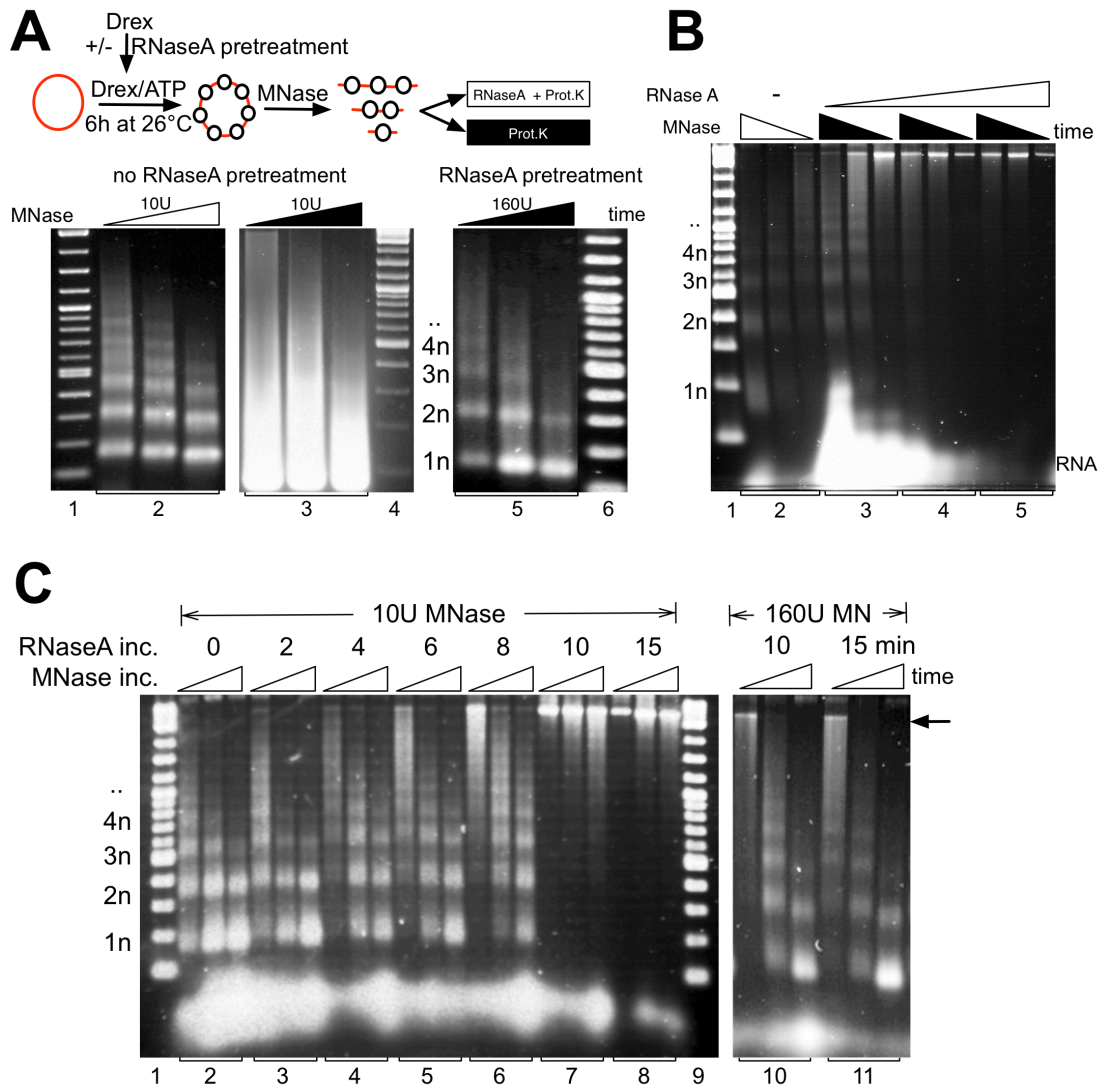


Figure 4.3: RNA maintains accessible chromatin structures *in vitro*

(A) As indicated by the scheme, DNA was incubated for 6h at 26°C with *Drosophila* embryo extract (Drex) and an ATP regenerating system to form chromatin. Chromatin was digested for 0.5 to 3 min with 10 U MNase, the reaction was stopped and incubated with RNaseA and proteinase K (white triangles) to hydrolyze RNA and proteins. DNA was purified and analyzed by agarose gel electrophoresis (panel 2). Leaving out RNaseA from the stop buffer (black triangles) reveals the high levels of RNA being present in the chromatin assembly reaction (panel 3). Preincubation of the Drex with RNaseA prior to the chromatin assembly reaction does not affect nucleosome assembly (panel 5). (B) Reconstituted chromatin was incubated without (panel 2) or with 10 to 150 µg/ml RNaseA (panels 3-5) for 15 min and then subjected to MNase accessibility analysis (10U MNase; 0.5 to 3 min). The reaction was stopped and either proteins and RNA (white triangles) or only the proteins (black triangles) were digested as indicated. The remaining nucleic acids were purified and analyzed by agarose gel electrophoresis. (C) Chromatin reconstituted with a *Drosophila* embryo extract was incubated with RNaseA in a time course as indicated and subsequently used for MNase accessibility analysis. Chromatin was

incubated with 10 U of MNase (panels 2 to 8) for 0.5 to 3 min, the reaction was stopped, and proteins were digested with proteinase K. DNA and the remaining RNA were purified and analysed by agarose gel electrophoresis. Chromatin fractions incubated with RNaseA for 10 and 15 min were analysed as described above, albeit high doses of MNase were used (panels 10 and 11). The non-digested DNA (arrow) and the positions of the nucleosomal ladder are indicated (1n, 2n,...).

To address the nature of the RNA that is required to maintain accessible chromatin, RNase H hydrolysing RNA-DNA hybrids, or RNase T1 digesting single-stranded RNA was used. Chromatin was incubated with these enzymes prior to MNase digestion analysis. The experiment reveal decreased MNase sensitivity after treatment with RNaseA and RNase T1 (Figure 4.4A), but not with RNase H (Figure 4.4B), demonstrating that single-stranded RNA regions and not RNA-DNA hybrids modulate chromatin structure.

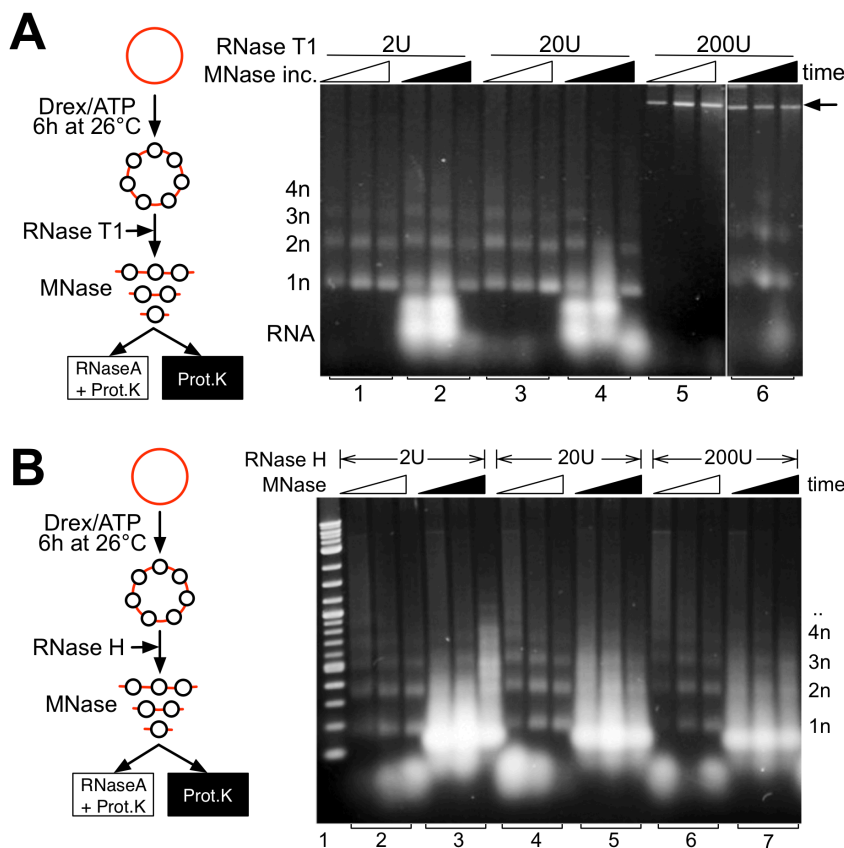


Figure 4.4: single stranded RNAs influence chromatin accessibility

(A) The MNase accessibility of reconstituted chromatin was probed after incubation with RNase T1. As described by the scheme, chromatin assembly reactions were incubated with RNase T1 for 15 min and subsequently analysed by partial MNase digestion. Reactions were stopped and incubated either with proteinase K (black triangles) or proteinase K and RNaseA (white

triangles) as indicated. Remaining nucleic acids were purified and analysed by agarose gel electrophoresis. The undigested DNA (arrow) and the nucleosomal ladder (1n, 2n,...) are indicated. **(B)** MNase accessibility assay of reconstituted chromatin after incubation with RNase H. As indicated by the scheme, chromatin assembly reactions were incubated with RNase H for 15 min and subsequently analyzed by partial MNase digestion. Remaining nucleic acids were purified and analyzed by agarose gel electrophoresis as described in (B). The nucleosomal ladder (1n, 2n, ..) is indicated.

To further exclude the possibility that the enzymatic activity of MNase was inhibited due to our experimental conditions, several control experiments were performed. To rule out the inactivation of MNase by RNaseA treatment, the RNaseA treated chromatin was supplemented with naked DNA to monitor the MNase dependent hydrolysis of the highly accessible DNA (Figure 4.5A). As shown in panel 6, free DNA was efficiently hydrolyzed, clearly showing that MNase remains active in the RNaseA treated samples. In addition, incubation of an MNase reaction with excess of RNaseA (Figure 4.5B) or excess of the released nucleotides (Figure 4.5C) had no effect on the overall activity of the enzyme. Moreover EDTA present in the RNase A reaction buffer has no impact on the activity of the MNase (Figure 4.5D). Compaction of the chromatin fibre was specific for the enzymatic activity of RNaseA as revealed by the inhibition of RNaseA with RNasin (Figure 4.5E). Partial MNase digestion of chromatin was performed without (lane 2), with RNaseA (lane 3) and with RNaseA in the presence of RNasin (lane 4). Analysis of the DNA by agarose gel electrophoresis revealed that RNaseA dependent chromatin compaction was not induced in the presence of RNaseA and RNasin, showing that the enzymatic activity of RNaseA is essential.

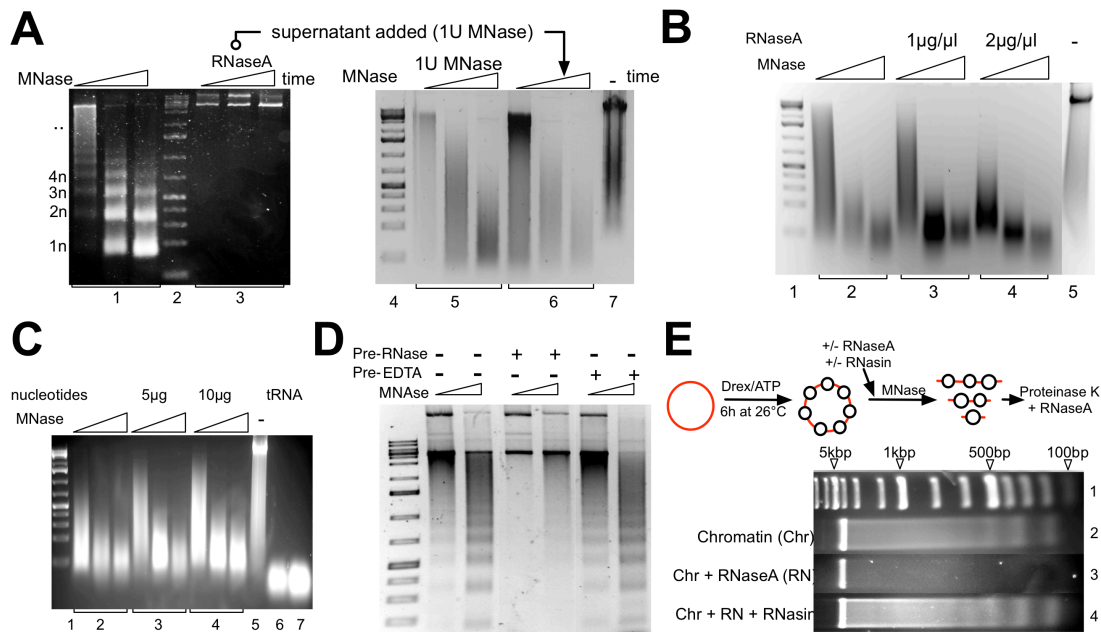


Figure 4.5: Testing the activity of MNase in RNaseA treated chromatin.

(A) MNase activity is not inactivated by the reaction conditions. Drex reconstituted chromatin was incubated without or with 100 $\mu\text{g}/\text{ml}$ RNaseA for 15 min (panel 1 and 3) and analyzed for chromatin accessibility. To test the activity of the MNase within the RNaseA treated sample, the supernatant was used to hydrolyze genomic DNA (panel 6). 2 μg HeLa genomic DNA was digested with either 1 U MNase (panel 5) or supernatant of the reaction shown in panel 3 corresponding to 1 U MNase (panel 6). DNA hydrolysis was stopped after 0.5 to 3 min and the nucleic acid was analyzed by agarose gel electrophoresis. A DNA marker is shown in lanes 2 and 4. Genomic HeLa DNA input is shown in lane 7. **(B)** RNaseA does not inhibit MNase activity. 0.1 U MNase was incubated without (panel 2) or with RNaseA as indicated (panels 3 and 4). Enzyme mixtures were used to hydrolyze genomic DNA for 0.5 to 3 min. Purified DNA was analyzed as described before. DNA marker is shown in lane 1. Input genomic HeLa DNA is shown in lane 5. **(C)** RNaseA degradation products do not inhibit the activity of MNase. 0.1 U MNase was incubated without (panel 2) or with rising concentrations of RNaseA digested yeast tRNA (panels 3 and 4). MNase nucleotide mixtures were used for the partial digestion of genomic DNA as described before. Lane 5 shows genomic DNA input and lanes 5 and 6 show the undigested amounts of tRNA used for the assay. **(D)** EDTA in the RNase A reaction buffer does not influence the MNase activity. Drex assembled chromatin was pre-treated with RNase A as described before. In a separate sample, chromatin was incubated with EDTA equal the amounts present in the RNase A reaction buffer. The accessibility of chromatin was assayed as described before. **(E)** RNaseA mediated change in chromatin accessibility of reconstituted chromatin is dependent on the RNaseA activity. As indicated by the scheme, reconstituted chromatin was either treated with 100 $\mu\text{g}/\text{ml}$ RNase A (lane 3) or with 100 $\mu\text{g}/\text{ml}$ RNase A in addition to RNasin (lane 4) and subjected to the MNase accessibility assay. Chromatin was incubated with 10 U of MNase (panel 2 to 4) for 1 min. Purified DNA was analyzed by agarose gel electrophoresis. The positions of the

monomers and multimers of the nucleosomal DNA (1n, 2n..) and the DNA marker (lane 1) are indicated.

A previous study reported that hydrolysis of the RNA within assembly extracts increases the efficiency of histone deposition, an effect that could lead to reduced MNase sensitivity due to an “over”-assembly of chromatin (Sekiguchi and Kmiec, 1992). To test this possibility, chromatin assembly with increased histone levels (Figure 4.6A) or incubated salt-assembled chromatin with either untreated or RNaseA-treated *Drosophila* extract (Figure 4.6B) were performed. In both cases, the accessibility of chromatin towards the nuclease did not significantly change. In addition, RNaseA treatment did not alter the density of nucleosomes on circular DNA analysed by topoisomerase I assays, showing that chromatin compaction is not an effect of additional nucleosome assembly and unspecific histone association (Figure 4.6C,D).

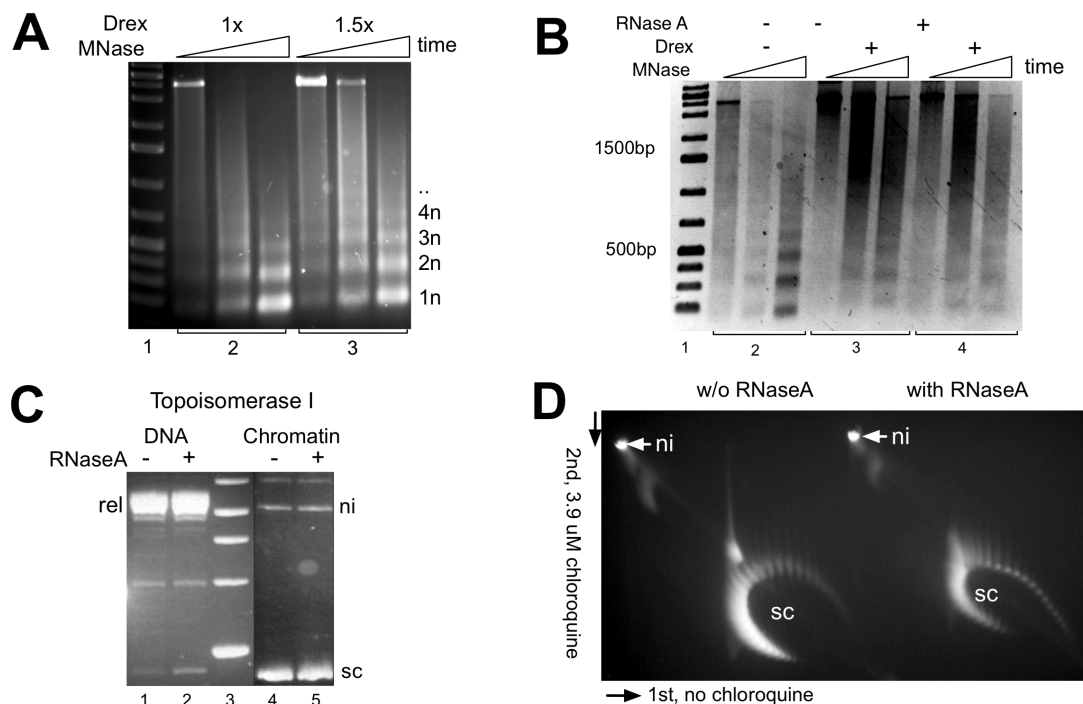


Figure 4.6: Histone and nucleosome density do not change after RNA depletion.

(A) Chromatin reconstituted with an excess of histones and Drex does not exhibit decreased MNase sensitivity. Chromatin reconstitution with optimal and excessive (150%) levels of Drex were incubated with 10 U of MNase for 0.5 to 3 min. Nucleic acids were purified and analyzed by agarose gel electrophoresis and ethidium bromide staining. The nucleosomal ladder (1n, 2n, ..) and the DNA marker (lane 1) are indicated. (B) Chromatin reconstituted by salt dialysis was incubated with additional Drex and RNaseA treated Drex as indicated. Salt dialysed chromatin (panel 2) and salt dialysed chromatin incubated with Drex (panels 3 and 4) were analyzed for

chromatin accessibility with MNase (5 U; 0.5 to 3 min). DNA was purified and analyzed as described. (C) The *Drosophila* extract contains topoisomerases, allowing the direct evaluation of DNA supercoiling degrees by 1D and 2D supercoiling assays. Chromatin assembly reactions were incubated without (lane 4) or with RNaseA (lane 5) and the superhelical DNA was purified. 1D supercoiling analysis was performed on a tris/glycine gel in the presence of 3.9 μ M chloroquine. Free DNA treated with topoisomerase I served as an internal control (lanes 2 and 3). The positions of the nicked (ni), the supercoiled (sc) and the relaxed (rel) DNA are indicated. (D) 2D supercoiling assay of RNaseA treated chromatin. Chromatin assembly reactions were incubated without (w/o) or with RNaseA and the superhelical DNA was purified. In the first dimension the tris/glycine gel was run without chloroquine, soaked with chloroquine (3.9 μ M) for 2 h, the gel was turned by 90 degree and electrophoresed in the presence of 3.9 μ M chloroquine. The location of the nicked (ni) and the topoisomeres (sc) of DNA are indicated.

Taken together, these experiments proof perfect activity of the micrococcus nuclease under the used conditions. In addition, it is shown that no changes in histone occupancy or density occurred while the RNase A treatment. Indirect effects resulting in chromatin inaccessibility, like histone overassembly or precipitation effects can be excluded.

Furthermore these experiments show that single stranded RNA molecules have a direct role in the maintenance of open chromatin structures.

4.3. Chromatin associated RNA maintains accessible higher order structures of chromatin

To further investigate the effect of RNA on chromatin structure, *in vitro* reconstituted chromatin was analysed by density gradient centrifugation. Condensed chromatin structures sediment in fractions of higher sucrose concentrations as compared to open chromatin structures (Hansen et al., 1997). Individual fractions of the linear sucrose gradient (15 to 40%) were subjected to total nucleic acid extraction and analysis by agarose gel electrophoresis. Most of the RNA in the extract sediments with fractions of low density, but a substantial portion of RNA co-purifies with the assembled chromatin (Figure 4.7A). The interaction of this chromatin associated RNA fraction (caRNA) is chromatin specific, as free RNA, the extract-RNA in the absence of reconstituted chromatin and also free DNA migrate with fractions of lower density, distinct from the

chromatin fractions (Figure 4.7B, C, D). RNA-chromatin interactions are dependent on reconstituted chromatin as a mere mixing of DNA and RNA does not result in a sedimentation shift of RNA (Figure 4.7E). Yeast tRNA sediments with very light fractions of the sucrose gradient (Figure 4.7F).

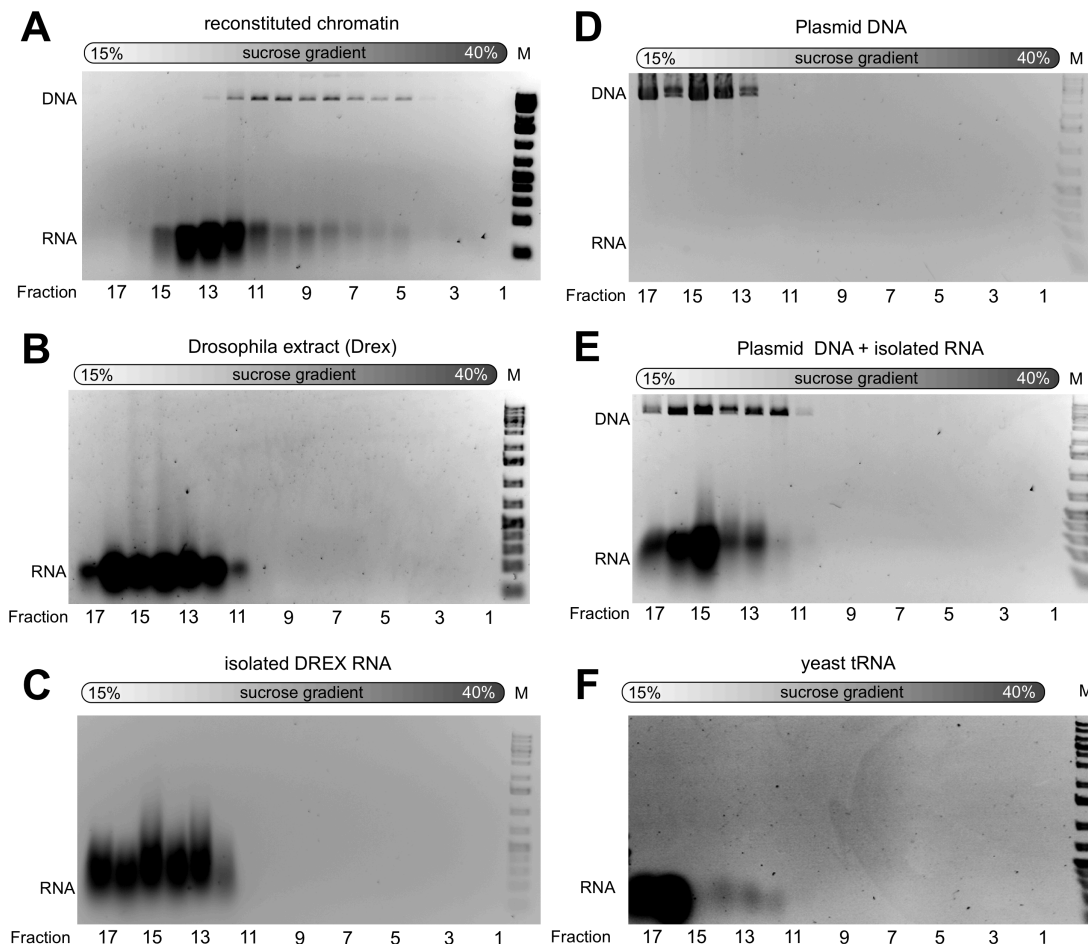


Figure 4.7: RNA sedimentation is dependent on its interaction with chromatin.

Reconstituted chromatin (A), *Drosophila* embryo extract without plasmid DNA (B), isolated *Drosophila* embryo extract RNA (C), plasmid DNA (D) and a mixture of plasmid DNA, isolated RNA (E) and yeast tRNA (F) were analyzed by sucrose density gradient centrifugation. The samples were applied to a linear 15-40% sucrose gradient, individual fractions (500 μ l) were isolated and nucleic acids were purified. DNA and RNA were analyzed by agarose gel electrophoresis. The locations of the nucleic acids and the DNA marker are indicated (M).

Interestingly, the hydrolysis of chromatin associated RNAs with RNaseA results in a shift of chromatin to higher density fractions (fractions 1 and 2), suggesting the formation of a more compact chromatin structure (Figure 4.8). This experiment shows that the caRNA fraction is responsible for the observed RNaseA dependent chromatin compaction observed in *Drosophila* cells and in

the reconstituted chromatin. In order to test whether the chromatin condensation effect is a reversible process, the compacted, RNaseA treated chromatin was purified by gel filtration, to exclude the RNase A enzyme, and subsequently incubated with RNase inhibitors to allow rescue experiments. Compacted chromatin was incubated for 15 min with either fresh *Drosophila* assembly extract (Drex) or total RNA purified from the extract. It is noted that incubation with Drex or RNA resulted in efficient re-opening of the compacted chromatin as revealed by density gradient fractionation (Figure 4.8). Chromatin migrates again with fractions of lower sucrose density and significant levels of RNA were again stably associated with chromatin.

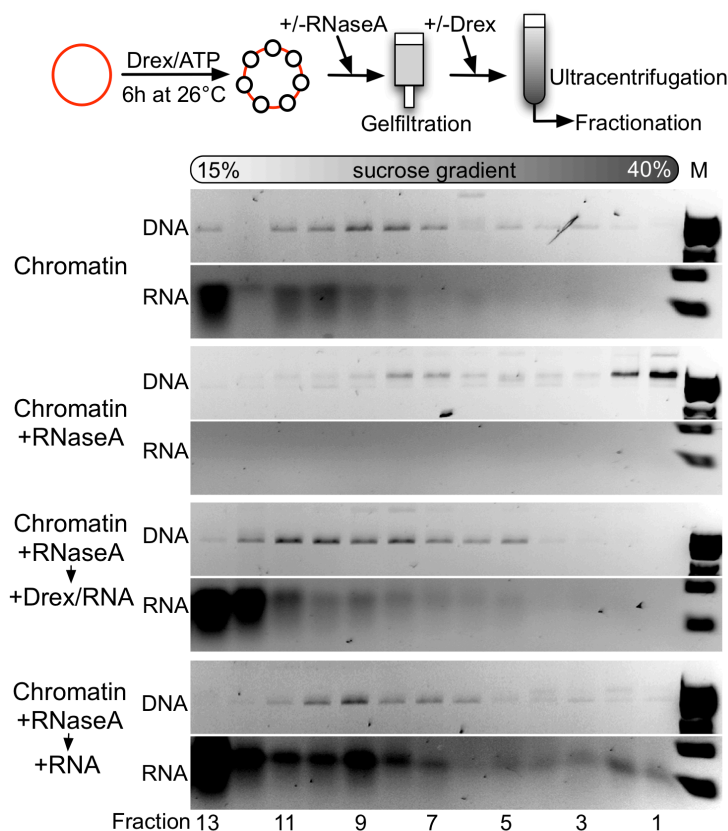


Figure 4.8: The role of RNA in chromatin compaction.

The scheme describes the experimental setup. Chromatin was incubated with or without RNaseA as indicated and purified by gel filtration. The remaining RNaseA activity was inhibited by the addition of RNasin. Chromatin fractions were subsequently incubated with fresh *Drosophila* extract (Drex/RNA) or purified Drex RNA (RNA) for 15 min as indicated. Chromatin conformation was analysed by density gradient centrifugation on a linear sucrose gradient (15 to 40%). Individual fractions were collected, proteins were digested, and nucleic acids were analysed on a 1.3% agarose gel. The positions of DNA and RNA within the individual fractions are indicated.

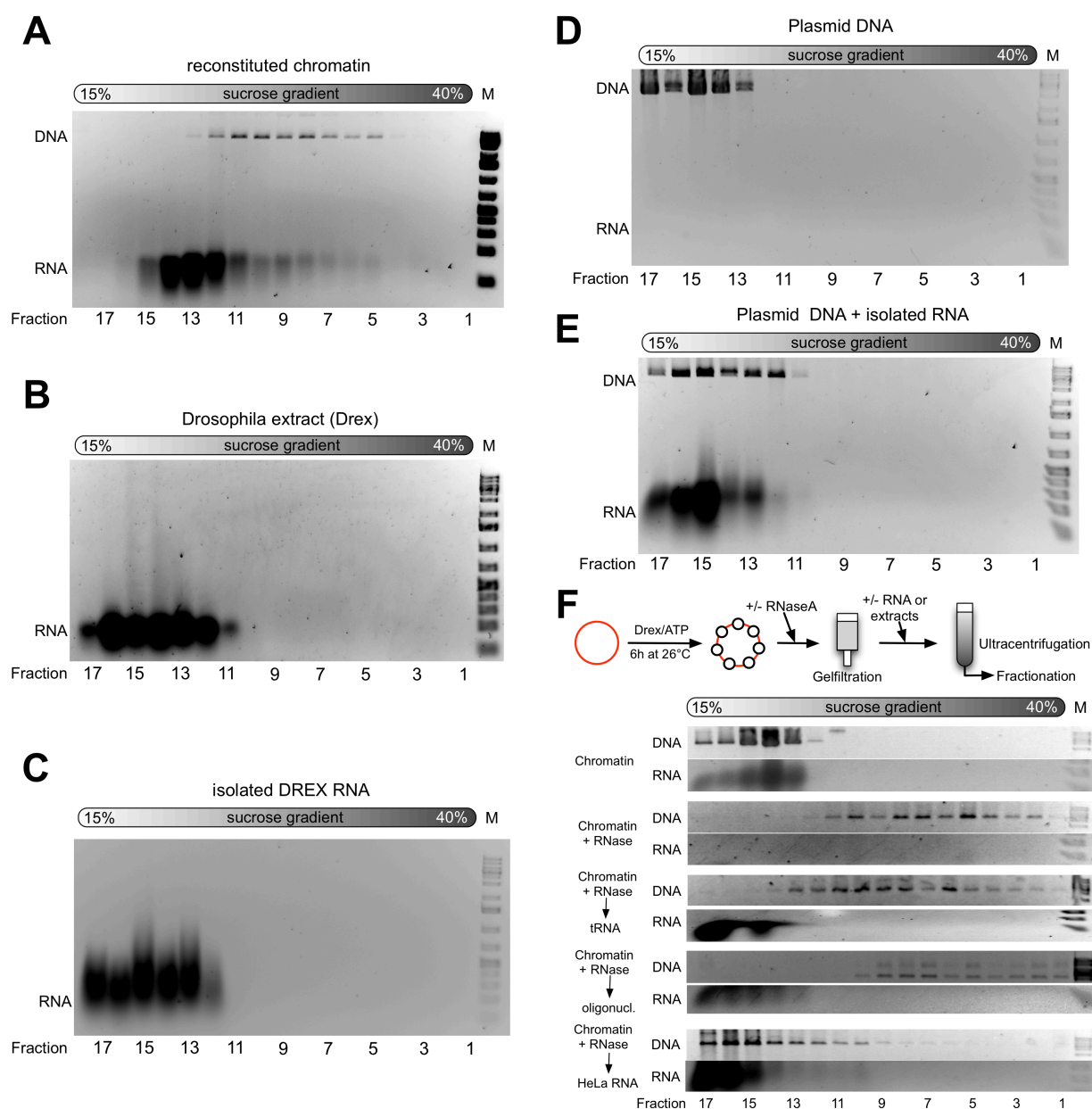


Figure 4.9: Reversible opening of higher order chromatin structures with RNA

Chromatin was treated with or without RNaseA as indicated, purified by gel filtration and remaining RNaseA activity was inhibited by the addition of RNasin. Chromatin fractions were subsequently incubated with yeast tRNA, oligonucleotides or isolated HeLa nuclear RNA for 15 min. Chromatin conformation was analyzed by density gradient centrifugation on a linear sucrose gradient (15 to 40%). Individual fractions were collected, proteins were digested and nucleic acids were analyzed on a 1.3% agarose gel. The positions of DNA and RNA within the individual fractions are indicated.

These rescue experiments show that chromatin compaction is a reversible and specific effect because the compacted chromatin is efficiently converted to an open structure by the addition of caRNA. In contrast to active changes in chromatin structure by chromatin remodelling enzymes (Langst et al., 1999), caRNA mediated chromatin opening does not require ATP hydrolysis. However, chromatin opening is dependent on the presence of additional factors associated with chromatin, as chromatin reconstituted by salt dialysis did not exhibit this behaviour. It is therefore hypothesised that caRNAs in conjunction with specific chromatin-associated factors form a structural component of chromatin leading to a stable de-condensed state.

4.4. Df31 is bound to chromatin and its associated RNA.

To determine the nature of potential RNA binding proteins, chromatin-bound proteins in the presence or absence of RNA were analysed (performed by Miriam Pusch, Imhof group). Therefore, biotinylated DNA was immobilised as template to magnetic streptavidin beads and reconstituted this template into chromatin. The chromatinized template was purified and then chromatin was treated with or without RNaseA. Bound proteins were then separated via SDS-PAGE and identified by LC MS/MS (Figure 4.10).

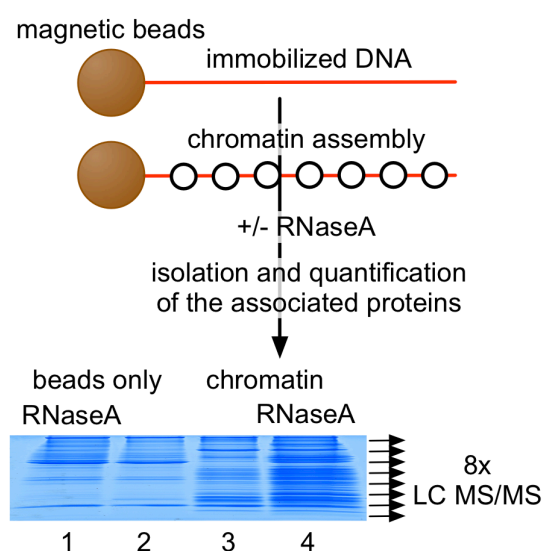


Figure 4.10: Quantitative analysis of proteins associated with accessible and inaccessible chromatin fractions.

As indicated in the scheme, biotinylated DNA was immobilised on magnetic beads, and chromatin was assembled on it by Drex reconstitution. Purified chromatin, untreated or treated with RNaseA, was washed before separation on an SDS PAGE. Bands were cut out and submitted to liquid chromatography before MS/MS analysis, followed by label free quantification using the Xcalibur™ and Proteome Discoverer™ software packages (Thermo Scientific).

The quantitative mass spectrometry approach revealed many RNA binding proteins and also proteins that were previously not shown to interact with RNA (Figure 4.11A). One of the factors among others that showed reduced affinity to chromatin after removal of RNA is the chromatin decondensation factor Df31 (Figure 4.11B).

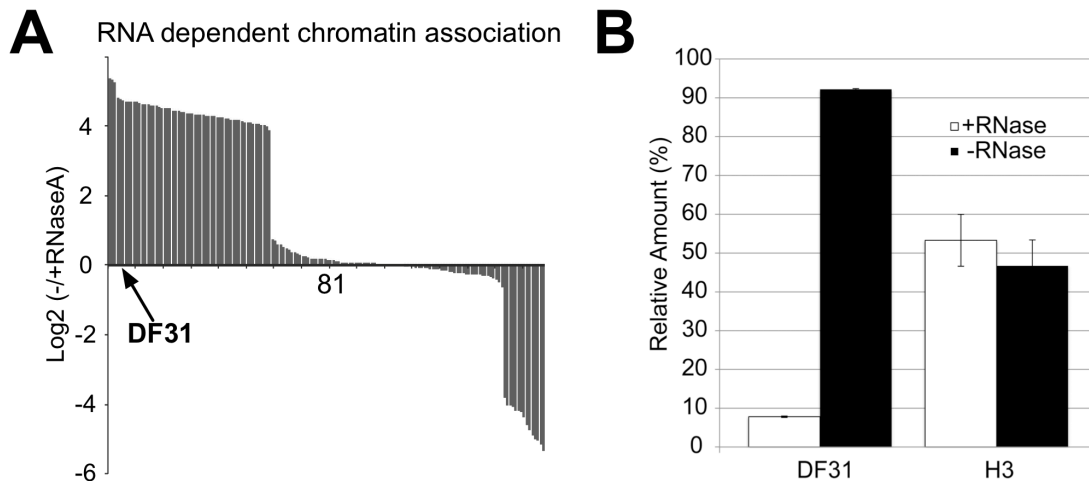


Figure 4.11: Results of the quantitative analysis of proteins associated with accessible and inaccessible chromatin fractions.

(A) Histogram of the number of proteins identified by chromatin pull-downs. Chromatin bound proteins were identified by combining Mascot and Sequest search algorithms searches of LC MS/MS runs from 8 slices of an SDS PAA gel separating chromatin bound proteins. Shown are only proteins that were identified in the presence of at least 2 unique peptides with high confidence. Quantification was performed by calculating the average intensity values of the XICs of two most intense ions for each protein. For a comparison, the intensity values of the -RNase sample were divided by the value of the +RNase sample and the Log₂ of this ratio displayed. **(B)** Quantification of DF31 and histone H3 in assembly reactions using extracted ion chromatograms of the peptides carrying amino acids 17-26, 29-39 and 40-55 for Df31 and 41-49 and 54-63 for H3. The relative ratio of the respective protein amount comparing RNaseA-treated (+RNase) and mock-treated fractions (-RNase) is shown.

4.5. Characterisation of Decondensation factor 31

Df31 mRNA transcripts are highly abundant in *Drosophila* as indicated in expression profiles (The modENCODE Consortium, (2010). DataS14: Gene co-expression clusters. [Science 330\(6012\)](#)). Df31 mRNA can be found in all developmental stages of *Drosophila* (flybase expression atlas). The highest expression level of the transcripts is detected in 4-6 h embryos, being classified into the highest expression class. In adult males the expression of Df31 mRNA is significantly reduced, placing it into the class of moderate expression (Figure 4.12 A).

In larval and adult expression in different tissues, Df31 mRNA is detected in all tissues, with ovaries exhibiting most Df31 mRNA transcripts. In contrast, testis express Df31 only moderately (Figure 4.12B).

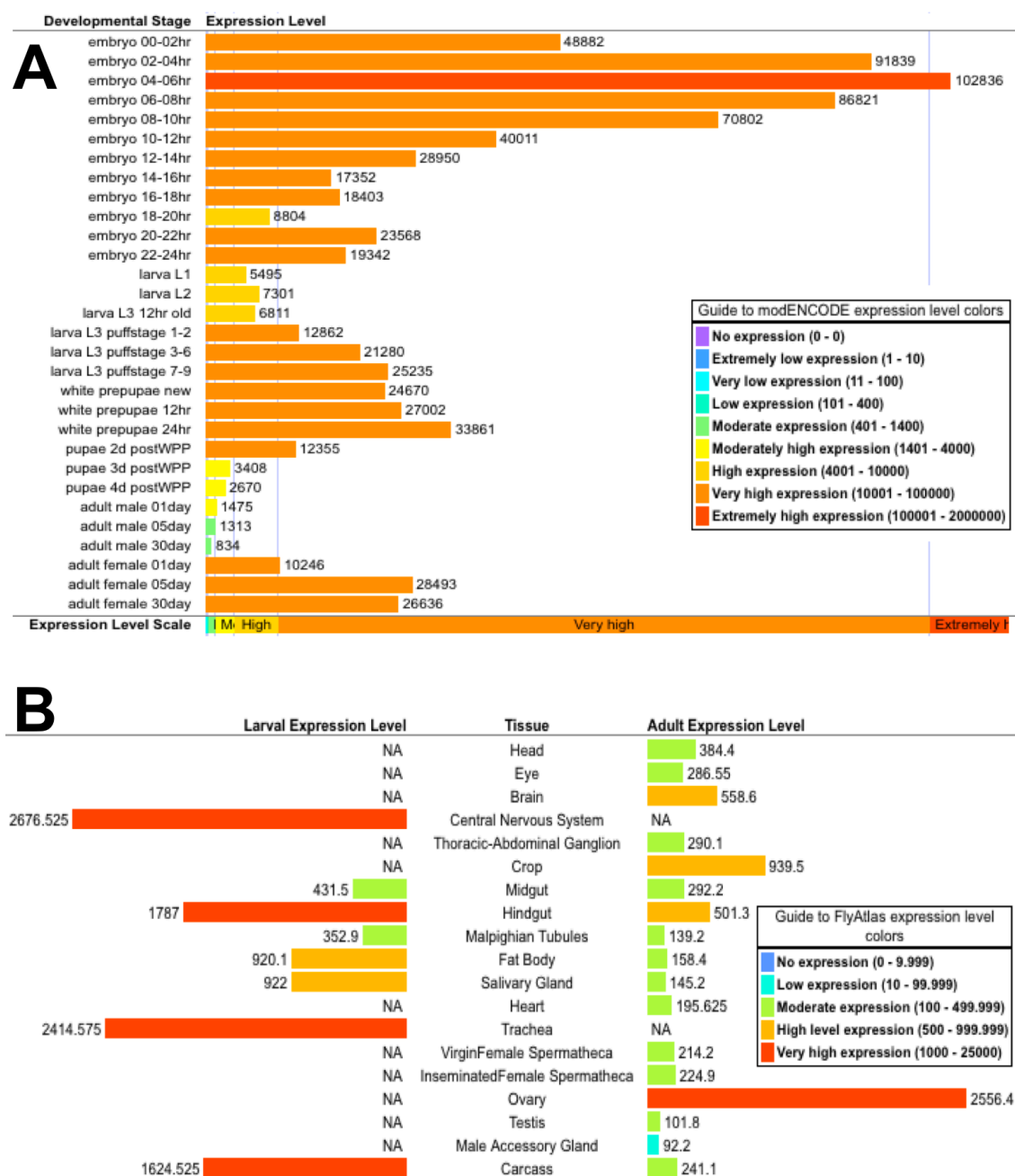


Figure 4.12: Gene expression profiles of the Df31 gene.

(A) The expression level of the Df31 gene is indicated in a developmental dependent manner. The colour code (description see box) indicates the expression level of the transcript. **(B)** The expression level of the Df31 gene in adults and larvae is indicated in a tissue dependent manner. The colour code (description see box) indicates the expression level of the transcript. (gene expression data from Flybase: <http://flybase.org/>)

The high abundance of Df31 is further confirmed on protein level as the *Drosophila* peptide atlas indicates (Brunner et al., 2007). The analysis was performed using the web based PaxDb software at the university of Zurich (<http://pax-db.org/#!home>) (Figure 4.13). The proteome atlas of *Drosophila* comprises more than 9000 proteins, whereas Df31 (17) is found in the Top 20 of the most abundant proteins. Comparatively, H3 is found at position 2960 and H1 at position 2774 of the protein abundance ranking.

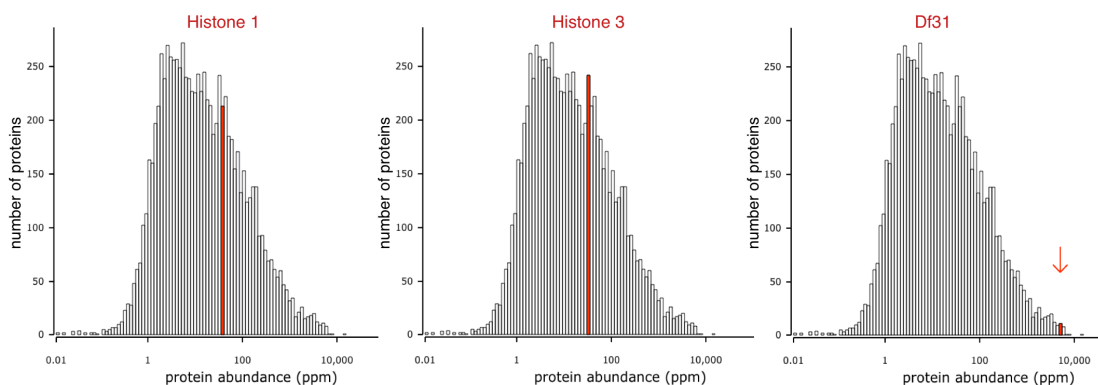


Figure 4.13: Abundance of Df31 in *Drosophila melanogaster*

The graphs indicate the abundance of H1, H3 and Df31 (red) in *Drosophila melanogaster* according to the *Drosophila* peptide atlas. The analysis was performed with the web based software PaxDb provided by the university of Zurich. The number of proteins is plotted on the y-axis, whereas the protein abundance is plotted on the x-axis whereas the abundance increases to the right.

Computational analysis of protein parameters using the ProtParam software, revealed Df31 being highly charged (Arg+Lys = 22, Asp+Glu = 52) and possessing a theoretical pI of 4.17 (Wilkins et al., 1999).

A recent study indicates that Df31 is highly unstructured and unfolded (Szollosi et al., 2008). This is further strengthened by the FoldIndex algorithm (Prilusky et al., 2005)

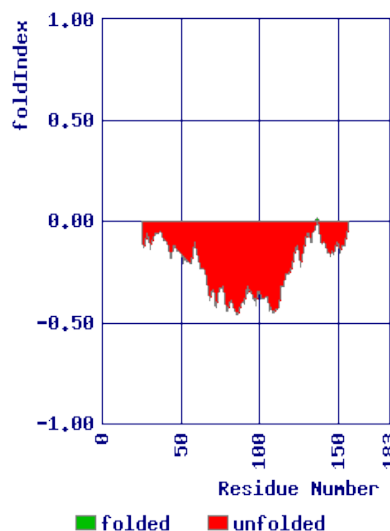


Figure 4.14: Folding prediction of Df31. The graph shows the folding prediction (red) based on the FoldIndex algorithm. The x-axis represents the 183 aa residues of Df31, whereas at the y-axis the FoldIndex is plotted. The negative Index (red) suggests that the protein is unfolded and disordered at certain residues.

This algorithm, which is based on the average residue hydrophobicity and net charge of the sequence, predicted Df31 to be unstructured and unfolded (Figure 4.14).

Hence, lacking structured domains, possible RNA binding sequences within Df31 could not be predicted by domain prediction algorithms like Dompred (Marsden et al., 2002) or SMART7 (Letunic et al., 2012)

RNA binding prediction using primary sequence were performed. BindN (Wang and Brown, 2006) and RNAbindR (Terribilini et al., 2007) showed overlapping results for predicted RNA binding residues. BindN predicts the propability of protein-RNA interaction by combinatory analysis of the pKa value of the aminoacid side chain, the hydrophobicity index and the molecular mass.

RNAbindR predicts the distances between the RNA and protein atoms. Protein residues with a distance to the RNA residues smaller than 5 Angström (default settings) are predicted to be interacting. Four possible RNA binding regions could be identified by both algorithms, besides the known nuclear localisation sequence and the phosphorylation site (Figure 4.15).

Decondensation factor 31

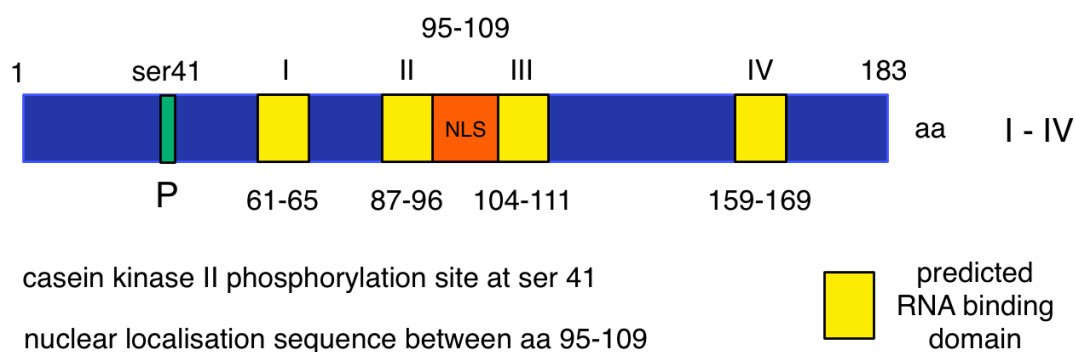


Figure 4.15: RNA binding sequence prediction of Df31

Based on primary sequence the RNA binding regions of Df31 were predicted with BindN and RNAbindR. Detected, overlapping RNA binding regions (red) are shown in the scheme as well as the nuclear localisation sequence (NLS, orange) and the site of phosphorylation (green).

The primary sequence analysis indicates Df31 possibly being a RNA binding protein. GO-term prediction using the CombFunc software indicates Df31 being a

histone binding protein with a probability of 38%. Furthermore Df31 acts in nucleosome assembly with a probability of 48% (Wass and Sternberg, 2008).

4.6. Df31 is involved in RNA dependent chromatin opening

To proof whether Df31 interacts with chromatin in an RNA-dependent manner, the assembly extract was mixed with recombinant, his-tagged Df31 (Figure 4.16A) prior to the chromatin assembly reaction. Reconstituted chromatin was either mock treated or treated with RNaseA to hydrolyse the caRNAs and purified via Ni-NTA agarose. Nucleic acids from the flow-through, wash and bound fractions were purified and analysed by agarose gel electrophoresis to determine the levels of Df31-bound chromatin. Consistent with our proteomic approach, Df31 binding to chromatin was RNA dependent (Figure 4.16B, lanes 5 to 7).

Next it was assessed whether Df31 can directly bind to RNA. Hence, its binding affinity to fluorescently labelled 39 nt long fragments of dsDNA, ssDNA or ssRNA was measured using microscale thermophoresis (Baaske et al., 2010). Df31 specifically binds the RNA molecule and fails to recognize the single-stranded or double-stranded DNA molecules (Figure 4.16C). Df31-RNA binding has a K_D value of 24 μM ($\pm 3.1 \mu\text{M}$) for the interaction with non-specific RNA. Worth mentioning, the his-tag has no influence on the RNA binding ability of Df31_{his}, as TEV cleaved Df31 (lacking his) showed not changed binding ability to a non-specific sal-RNA (Figure 4.16D).

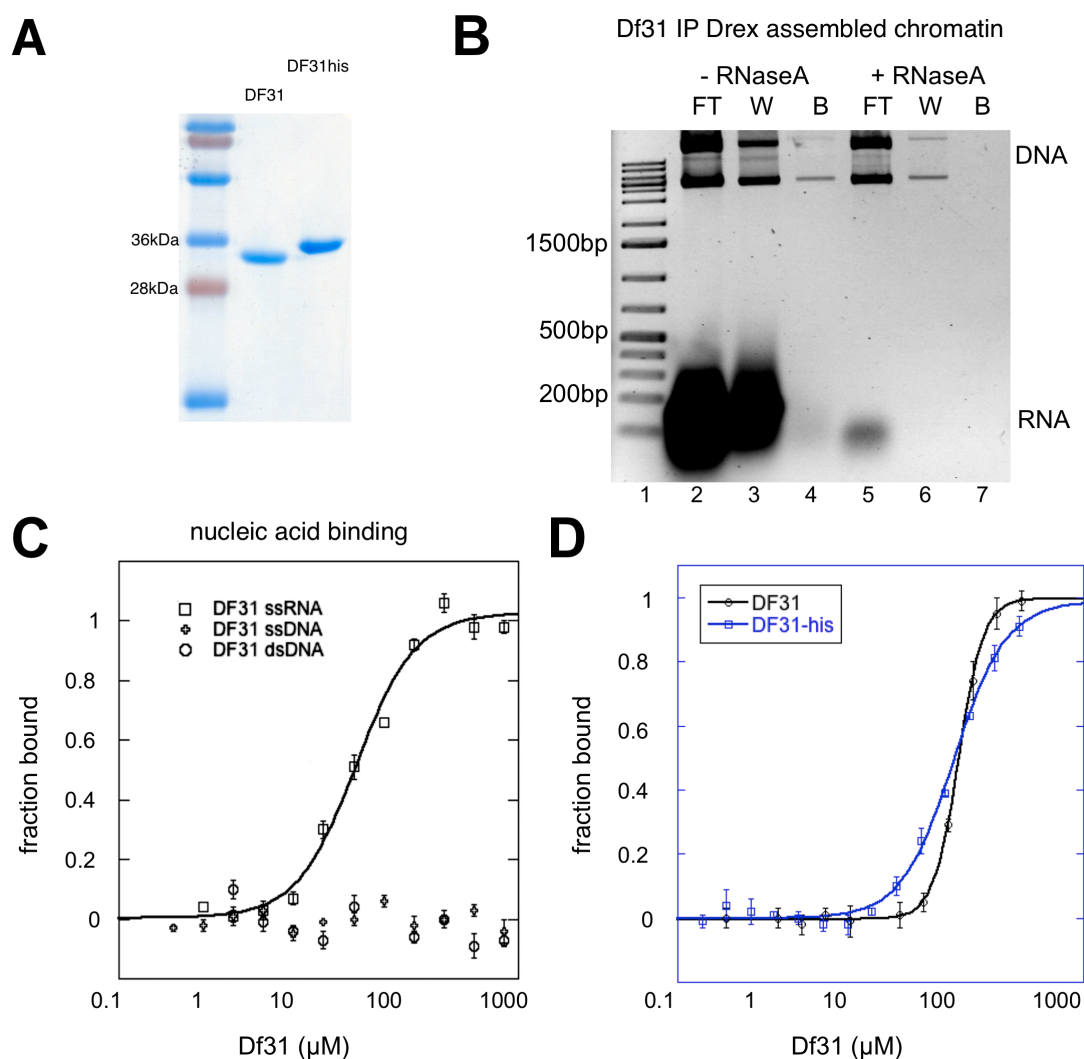


Figure 4.16: Df31 is a chromatin- and RNA-binding protein.

(A) Bacterially expressed Df31-his was purified using Ni-NTA beads. Df31 protein was analysed by SDS-PAGE and Coomassie blue staining. **(B)** The interaction between Df31 and chromatin is RNA-dependent. Df31-his (10 μg) was included in a chromatin assembly reaction and subsequently incubated without (lanes 2-4) or with RNaseA (lanes 5-7). His-tagged Df31 was purified using Ni-NTA beads, and the RNA-dependent binding of chromatin was monitored. Purified nucleic acids in the flow-through (FT), the wash (W) and the bead fraction (b) were visualised by agarose gel electrophoresis. **(C)** Analysis of Df31-nucleic acid interactions by microscale thermophoresis. Fluorescently labelled ssRNA, ssDNA and dsDNA templates of the same sequence and length (39 nucleotides, 50 nM) were incubated with increasing concentrations of Df31. Specific interactions were quantified by microscale thermophoresis. ssRNA binding was plotted using the Hill equation, where K_d is the peptide concentration where half of the oligonucleotides are bound. **(D)** Influence of the Tag on the RNA binding. The RNA binding abilities of Df31-his and Df31 were analysed by microscale thermophoresis as described in (C).

In addition, binding studies using microscale thermophoresis show that Df31 is able to bind to histone molecules. Therefore recombinant Df31-EGFP protein and EGFP protein as binding control (Figure 4.17A) were incubated with increasing amounts of the single core histones H2A, H2B, H3 and H4. Df31 interacts specifically with H3 exhibiting a K_D of $1.5\mu\text{M}$ ($\pm 0.4\mu\text{M}$), binds weakly to H4 with a K_D of $12\mu\text{M}$ ($\pm 0.6\mu\text{M}$) and does not bind to H2A and H2B (Figure 4.17B), confirming the data of Guillebault (Guillebault and Cotterill, 2007).

Electromobility shift assays (EMSA) demonstrate that Df31 interacts with mononucleosomes. Mononucleosomes were reconstituted on the strong nucleosome positioning sequence 601 Not, which was Cy5 labeled via salt dialysis. Cy5-601-Not Mononucleosomes were incubated with increasing amounts of Df31. Correlating with increasing amounts of Df31, more free nucleosomes were bound as the shift to slower electromobility indicates. This mobility shift is due to specific interaction between mononucleosomes and Df31, exhibiting the ability of Df31 to bind chromatin. (Figure 4.17C).

The ability of Df31 to bind to chromatin was further underlined by microscale thermophoresis experiments. Cy5-labeled reconstituted mononucleosomes were incubated with increasing amounts of Df31 or BSA, as control for specific binding. Df31 interacts with mononucleosomes exhibiting a K_D of $3.7\mu\text{M}$ ($\pm 0.6\mu\text{M}$) (Figure 4.17D).

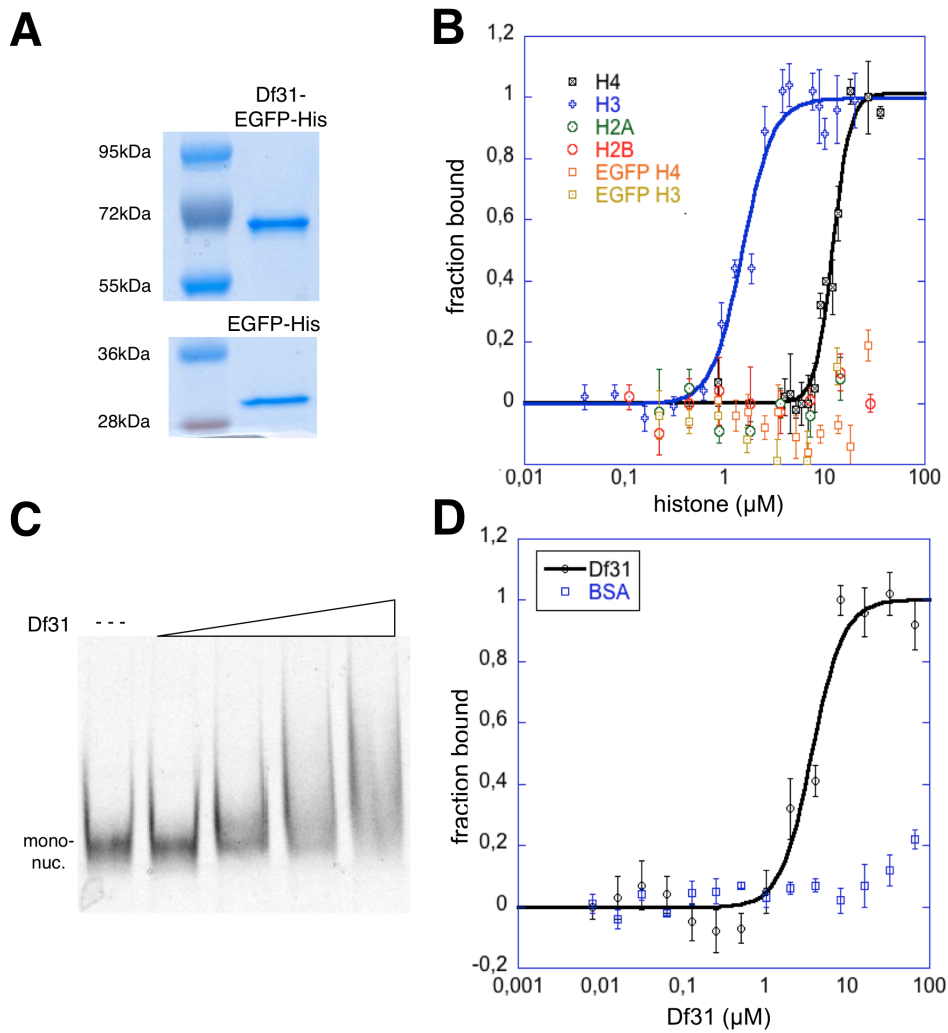


Figure 4.17: The interaction of Df31 to histones/chromatin

(A) Bacterially expressed Df31-EGFP-his and EGFP-his was purified using Ni-NTA beads. The Df31 protein was analysed by SDS-PAGE and Coomassie blue staining. **(B)** Analysis of Df31-histone interactions by microscale thermophoresis. Df31-EGFP was incubated with increasing amounts of core histone molecules. Specific interactions were quantified by microscale thermophoresis. Histone binding was plotted using the Hill equation, where K_d is the peptide concentration where half of the proteins are bound. EGFP protein served as control for specific binding. **(C)** Electromobility shift assay showing the interaction between Df31 and Cy5-labeled 601-Not-mononucleosomes. Mononucleosomes were incubated with increasing amounts of Df31 molecules and analysed in native polyacrylamide gel electrophoresis. **(D)** Analysis of Df31-mononucleosome interactions by microscale thermophoresis. Cy5-labeled 601-Not-mononucleosomes were incubated with increasing amounts of Df31 molecules. Specific interactions were quantified by microscale thermophoresis. Df31 binding was plotted using the Hill equation, where K_d is the peptide concentration where half of the proteins are bound. BSA served as control for specific binding.

Furthermore, it was tested in *in vitro* pull-down assays whether Df31 is capable of binding simultaneously to histones and RNA (Figure 4.18A). His-tagged Df31 was incubated with recombinant histone octameres and increasing amounts of total RNA. The RNA and Df31 dependent interaction with histones was monitored after binding of Df31 to Ni-NTA beads by analysing the fraction of histones bound to Df31. Bead-bound Df31 already binds significantly to histones in the absence of RNA (- RNA lane; compare panels 3 and 6). However, histone binding was further enhanced by the addition of increasing levels of RNA, suggesting cooperative binding of Df31 to histones in the presence of RNA. A continuative experiment was performed testing a possible influence of RNA on the interaction between Df31 and reconstituted chromatin (Figure 4.18B). The RNA and Df31 dependent interaction with salt assembled chromatin was monitored after binding of Df31 to Ni-NTA beads by analysing the fraction of chromatin bound to Df31. Bead-bound Df31 already binds weakly to chromatin in the absence of RNA (- RNA lane). However, chromatin binding was further enhanced by the addition of increasing levels of RNA, suggesting cooperative binding of Df31 to chromatin in the presence of RNA.

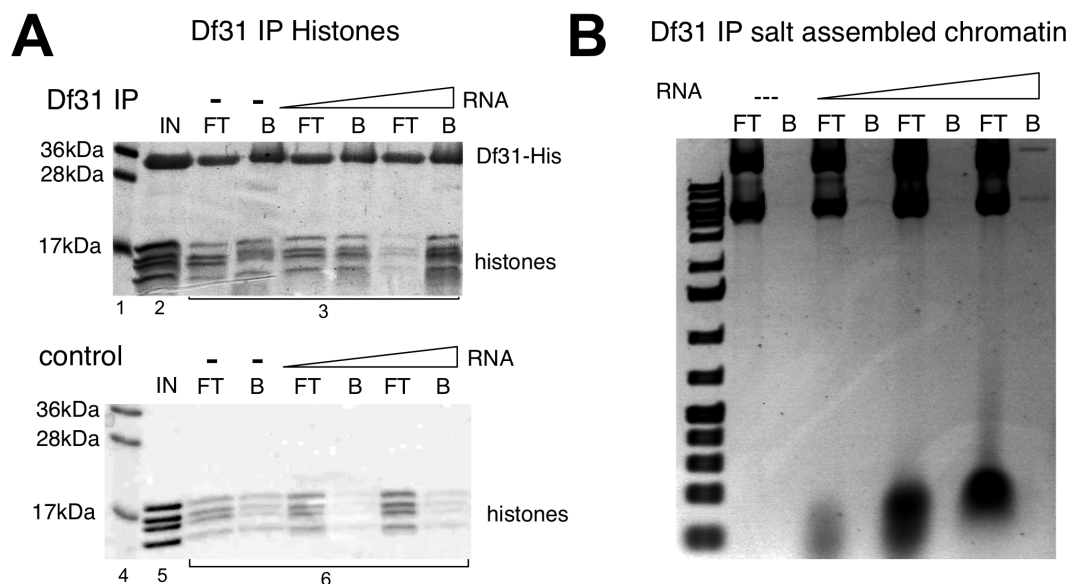


Figure 4.18: RNA enhances the interaction of Df31 with chromatin

(A) Df31-histone interactions are enhanced in the presence of RNA. Df31 (2 µg) and histone octameres (2.5 µg) were used for *in vitro* pull down studies. Df31 was incubated with histones and increasing amounts of RNA (300 ng and 1 µg) as indicated and subsequently purified with Ni-NTA beads. Bead bound proteins (B) and proteins present in the flowthrough fraction (FT) were

analyzed by SDS-PAGE (17%) and Coomassie blue staining. The lower panel shows the control experiment performed in the absence of Df31. The protein input (IN) is shown in lane 2, 5. **(B)** The interaction between Df31 and salt assembled chromatin is enhanced by RNA. 2µg reconstituted chromatin was incubated with 5µg Df31 without or with RNaseA (as indicated). His-tagged Df31 was purified using Ni-NTA beads, and the RNA-dependent binding of chromatin was monitored. Purified nucleic acids in the flow-through (FT), the bead fraction (B) were visualised by agarose gel electrophoresis.

These results imply a cooperative binding mechanism of Df31 and caRNA together to chromatin to exert their effect on chromatin opening.

To reveal the function of Df31 on chromatin structure *in vivo*, endogenous mRNA was depleted by dsRNA -mediated knock-down. Transcript levels were reduced by 93% after 5 days of incubation (Figure 4.19A), the time point when the chromatin structure of the *Drosophila* S2 cells was analysed (Figure 4.19B,C). MNase digestion of untreated cells, control knock-down cells and Df31 knock-down cells revealed that a fraction of genomic DNA showed lower accessibility to MNase in the absence of Df31 (Figure 4.19B, arrows). The results show that Df31 is required to maintain a cellular fraction of chromatin accessible, as suggested by the *in vitro* experiments. To prove the results, the effects of Df31 knock-down on chromatin compaction was also quantified by microscopic evaluation. 3D and stack cell reconstruction of four times 90 cells were performed, corresponding to control cells, control and specific knock down reactions. Cells were grouped into three categories (normal, intermediate and condensed) according to the roughness of the DNA staining with DAPI. Knock down of Df31 revealed a more than twofold increase of cells with compacted DAPI stain. As shown for the inhibition of Pol II transcription (Figure 4.2B), the knock-down of Df31 results in a prominent compaction of chromatin (Figure 4.19C).

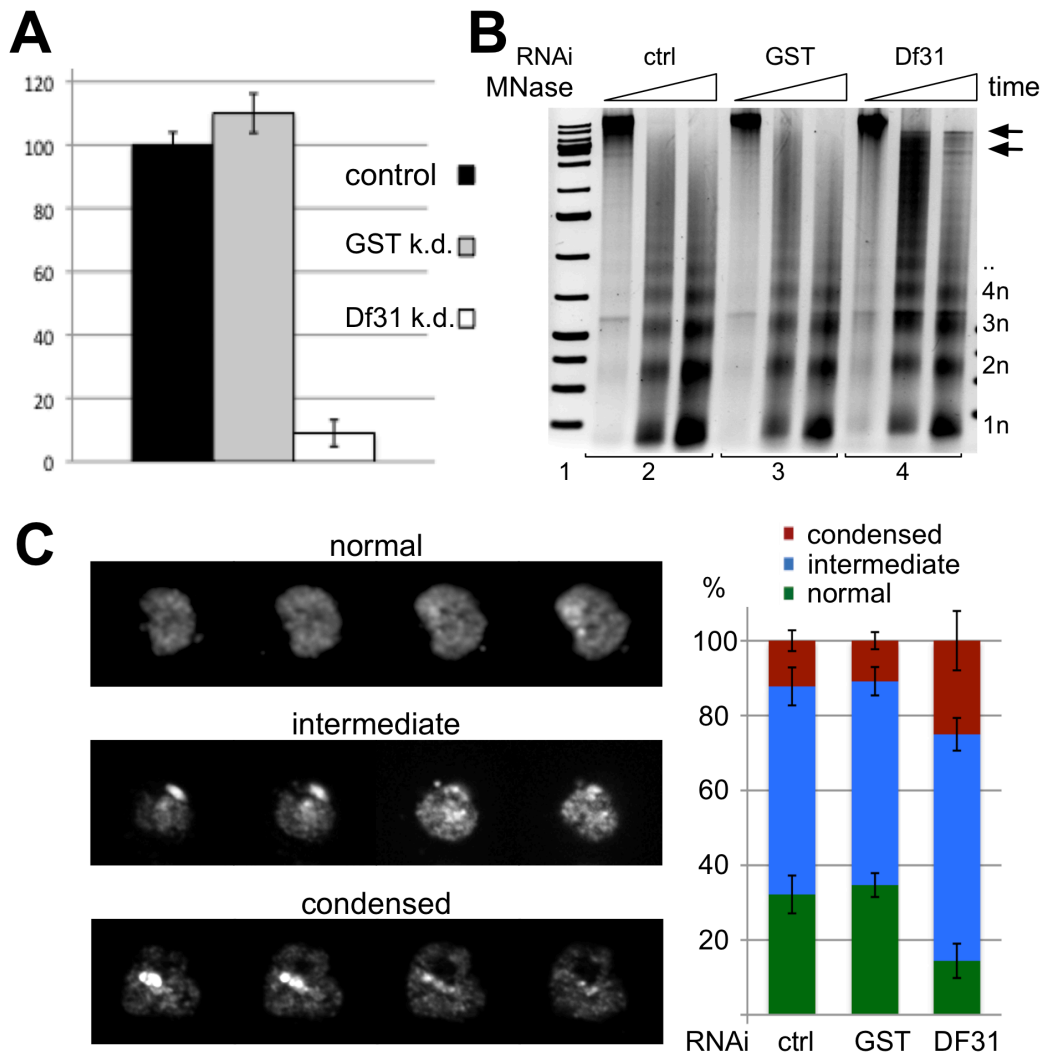


Figure 4.19: knock-down of Df31 condenses chromatin and decreases its accessibility

(A) Knock-down of the Df31 mRNA in S2 cells. After 1 h of starvation, cells were provided with dsRNA oligos and incubated for 5 days. Df31 mRNA levels were then analyzed by qPCR using 2 different primer pairs. Df31 mRNA levels were quantified in control cells, GST scramble knock-down and Df31 knock-down cells. Df31 mRNA level of the control cells was set to 100% as indicated in the graph. **(B)** Df31 knock-down in *Drosophila* cells results in decreased chromatin accessibility. *Drosophila* cells were incubated without (control) or with dsRNA directed against GST and Df31 for 5 days. Identical cell numbers were incubated with 20 U MNase for 30 to 270 sec. The reaction was stopped, and DNA was purified and visualised by agarose gel electrophoresis. The positions of the monomers and multimers of the nucleosomal DNA (1n, 2n,...) and the DNA marker (lane 1) are indicated. The arrows indicate inaccessible genomic DNA arising after Df31 knock-down. **(C)** Knock-down of Df31 results in chromatin condensation. Df31 depletion was performed as described in **(A)**, and cells were stained with DAPI and analysed by confocal microscopy with a Zeiss Imager ApoTome device. Nuclear stainings were grouped into three classes (even, intermediate and condensed) according to cellular staining properties. The

numbers of cells with even, intermediate and compacted staining patterns are given on the right. For each experimental condition, 90 cells were evaluated in four independent replicates.

The knock-down experiments imply Df31 to play a direct role in chromatin organisation and structure.

4.7. Chromatin associated snoRNAs open higher order structures of chromatin

Df31 interacts with caRNA and both molecules are tethered to chromatin, resulting in opening of the higher order structures of chromatin. In order to reveal whether the caRNAs belong to a specific RNA species, the caRNA pool was characterized. Initial characterisations show that the chromatin-caRNA interaction is stable at high salt concentrations (600mM NaCl) and does not require supercoiled chromatin templates for its interaction (Figure 4.20A). Isolated caRNA pool from density gradient purified chromatin fractions (Figure left) and total RNA purified from *Drosophila* embryo extracts (Figure 4.20B right) were used for library preparation and high throughput sequencing on the Illumina platform (lbp. and hts. performed by Sarah Diermeier).

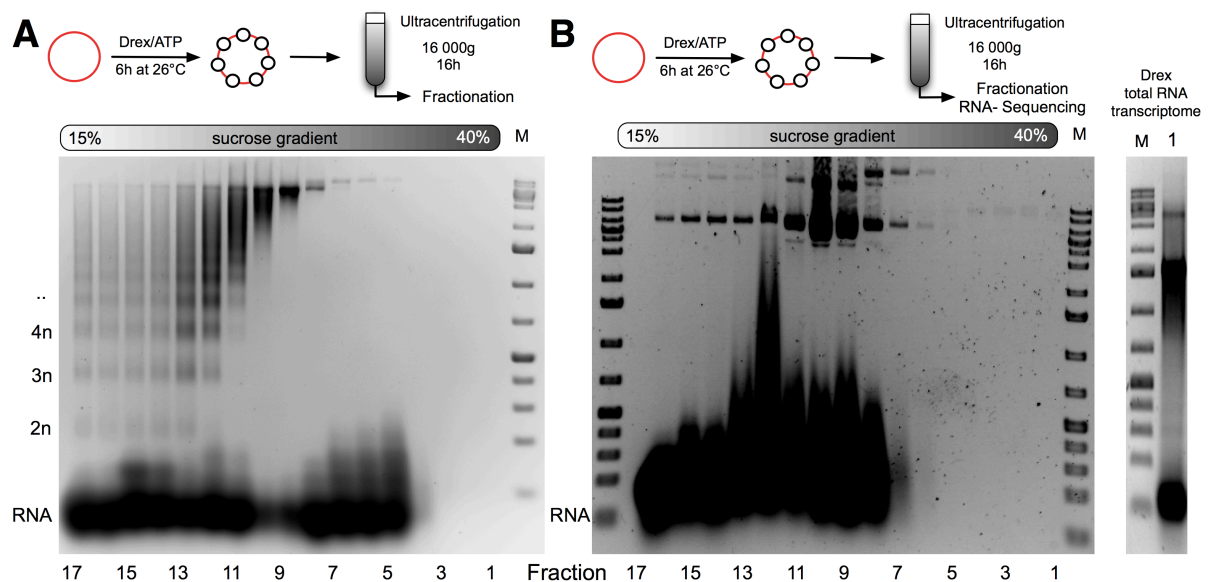


Figure 4.20: Characterization of the caRNA-chromatin interaction.

(A) Reconstituted chromatin was partially digested with MNase and the reaction was stopped by the addition of EDTA. Chromatin fragments were analyzed by sucrose gradient centrifugation (5 to 30% sucrose) at high salt conditions (600 mM NaCl), as indicated. Individual fractions (500 µl)

were isolated, proteins were digested with proteinase K and the remaining nucleic acids were analyzed by agarose gel electrophoresis. The locations of RNA and nucleosomes (1n, 2n, ...) are depicted. **(B)** Isolation of caRNA. Reconstituted chromatin was applied to sucrose density gradient centrifugation (15 to 40% sucrose). Individual fractions (500 µl) were isolated, proteins were digested with proteinase K and the remaining nucleic acids were analyzed by agarose gel electrophoresis. Fractions 7 to 10 were selected for the isolation of caRNAs. Total RNA from Drex was isolated and used as transcriptome sample. The samples were used for library preparation and illumina high throughput sequencing, performed by Sarah Diermeier.

Annotation and quantification of the transcripts revealed that caRNA consists of a small but highly enriched subset of the total RNA (Figure 4.21A and B). In general, non-coding RNA species were enriched approximately 3-fold in caRNA fractions whereas the number of protein-coding transcripts was strongly reduced. A detailed analysis of the biotype of the enriched non-coding transcripts revealed a striking accumulation of snoRNAs in the caRNA fractions. Mature snoRNAs as well as snoRNA precursors exhibit the highest enrichment in chromatin, with up to a several hundred-fold enrichment of the Me28S-U2134b, Me-RA, Me28S-G980 and others (Figure 4.21B).

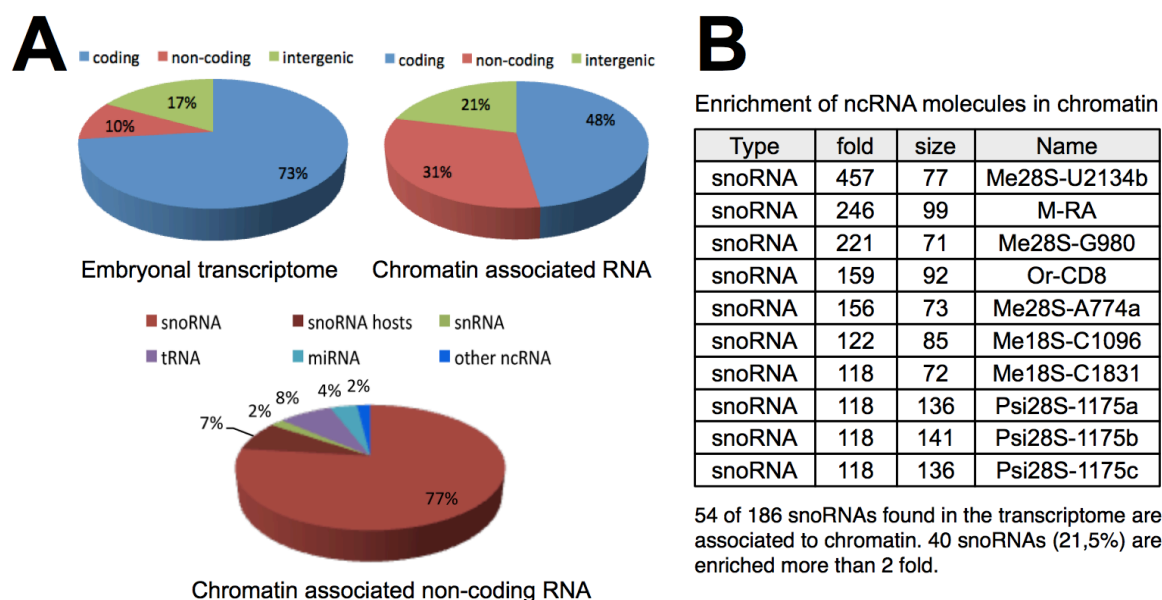


Figure 4.21: snoRNAs are highly enriched in caRNAs.

(A) Analysis of RNA deep sequencing data. The charts on top show the percentage of coding (blue), non-coding (red) and intergenic RNAs (green) identified in the early embryo extract and within the chromatin associated RNAs. The lower chart shows a detailed analysis of the non-coding RNAs present within the caRNA pool. **(B)** Table showing a list of the 10 non-coding RNAs exhibiting the highest enrichment within the dataset of caRNAs.

In order to test if these snoRNAs play an opening role in chromatin structure Me28S-U2134b and Me28S-G980 RNAs were prepared by *in vitro* transcription (Figure 4.22A) and tested in sucrose gradient sedimentation experiments as described above (compare Figure 4.9). The re-addition of snoRNA molecules to RNaseA treated, compacted chromatin, results in a shift of the chromatin to lighter fractions (Figure 4.22B), whereas tRNA showed no effect on chromatin sedimentation.

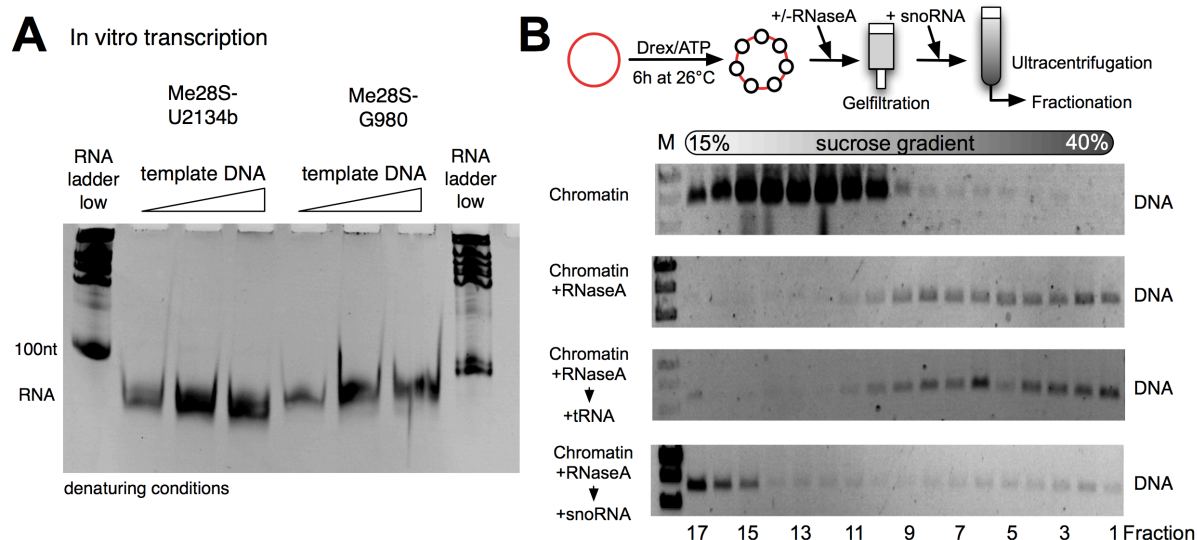


Figure 4.22: Chromatin associated snoRNAs open up chromatin.

(A) *in vitro* transcription of snoRNAs Me28-U2134b and Me28-G980. A titration series of template DNA for *in vitro* transcription of the snoRNAs is analyzed by gelelectrophoresis under denaturing conditions in a Urea/TBE gel. The snoRNAs show the estimated size of 77 respectively 71nt for Me28-U2134b and -G980. **(B)** The scheme describes the experimental setup. Chromatin was incubated with or without RNaseA as indicated and purified by gel filtration. The remaining RNaseA activity was inhibited by the addition of RNasin. Chromatin fractions were subsequently incubated with *in vitro* transcribed snoRNAs Me28-U2134b, Me28S-G980 and a passive carrier tRNA for 15 min as indicated. Chromatin conformation was analysed by density gradient centrifugation on a linear sucrose gradient (15 to 40%). Individual fractions were collected, proteins were digested, and DNA was analysed on a 1.3% agarose gel.

The data suggests that snoRNA molecules are specifically tethered to chromatin and involved in maintaining an open chromatin structure.

4.8. Df31 specifically interacts with snoRNAs

Based on these results, it is of high interest whether snoRNAs do specifically bind to the Df31 protein.

The snoRNAs Me28S-U2134b and Me28S-G980, were selected from the list and synthesized with fluorescent labels for interaction studies. Both molecules were split in two “halves”, retaining the predicted snoRNA structures and the predicted base pairing (Figure 4.23A, B).

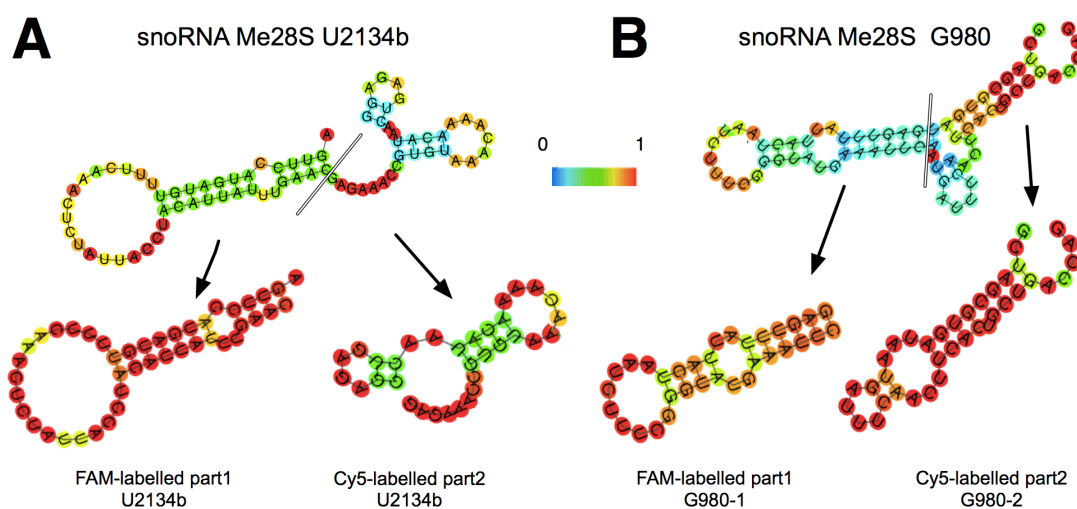


Figure 4.23: RNA secondary structure prediction

The scheme represents the MFE RNA secondary structure of Me28S-U2134b (A) and Me28S-G980 (B) predicted with the program RNAFold. The snoRNA was synthesised as two differently labelled RNA fragments (G980 part1 and G980 part2) that retained the overall secondary structures. The structure below is colored by base-pairing probabilities. For unpaired regions the colour denotes the probability of being unpaired.

The labelled RNA molecules were used in microscale thermophoresis experiments with recombinant Df31 protein. Df31 binds with higher affinity to the part2 of the G980 snoRNA, exhibiting a K_D of 7 μM (+/-0.4), whereas two non-specific RNAs and the other half of the snoRNA were bound with affinities between 20 and 40 μM (Figure 4.23A). Competitive binding assays with equimolar concentrations of the specific and non-specific RNA shows that Df31 has a more than 100-fold preference for the snoRNA (Figure 4.24B).

Testing the snoRNA U2134b, Df31 binds with higher affinity to the part1 of the U2134b snoRNA, exhibiting a K_D of 14.5 μM (± 1.3), whereas two non-specific RNAs and the other half of the snoRNA were bound with affinities between 20 and 52 μM (Figure 4.24C). Competitive binding assays using equimolar concentrations of snoRNA U2134b part1 and part2 show that Df31 preferentially binds to snoRNA U2134b part1 (Figure 4.24D).

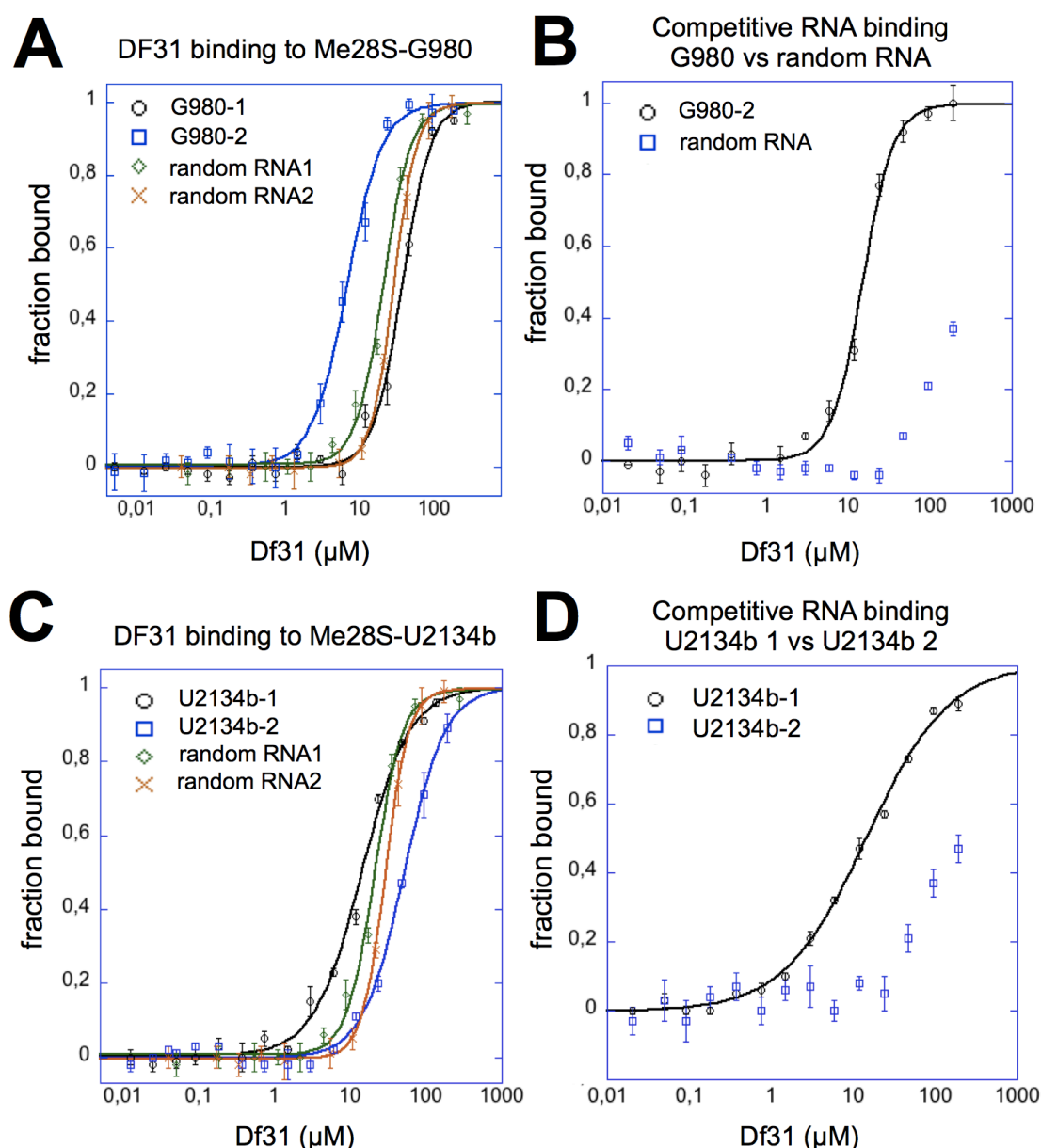


Figure 4.24: Df31 specifically interacts with snoRNAs

(A) Quantification of Df31-Me28S-G980 interactions by microscale thermophoresis.

Fluorescently labelled Me28S-G980 RNA fragments and non-specific RNA molecules (each 50 nM) were incubated with increasing concentrations of recombinant Df31. Specific interactions were quantified by microscale thermophoresis. snoRNA binding was plotted using the Hill equation. Under these experimental conditions K_d is the peptide concentration where half of the

oligonucleotides are bound. **(B)** Competitive binding assays comparing the affinity of the two Me28S-G980 RNA fragments to Df31. Differently labelled snoRNA fragments (each 50 nM) were mixed and incubated with increasing concentrations of Df31. Specific interactions were quantified by microscale thermophoresis as described in (A). **(C)** Quantification of Df31-Me28S-U2134b interactions by microscale thermophoresis. Fluorescently labelled Me28S-U2134b RNA fragments and non-specific RNA molecules (each 50 nM) were incubated with increasing concentrations of recombinant Df31. Specific interactions were quantified as described in (A). **(D)** Competitive binding assays comparing the affinity of the two Me28S-U2134b RNA fragments to Df31. Fluorescently labelled Me28S-U2134b RNA fragments (part1 and part2 each 50 nM) were mixed and incubated with increasing concentrations of recombinant Df31. Specific interactions were quantified by microscale thermophoresis as described in (A).

To verify the snoRNA binding property of Df31, electromobility shift assays were performed. Cy5-labeled G980 snoRNA part 2 was incubated with increasing amounts of Df31 and analysed on a native polyacrylamid gel.

Correlating with increasing amounts of Df31, increasing amounts of free RNA were bound and a specific Df31-RNA band appeared (Figure 4.25A).

As shown before, the re-addition of snoRNA molecules to compacted RNase A treated chromatin, resulted in decondensation of the chromatin template (Figure 4.22). Df31 and snoRNAs as RNP complex are thought to mediate this decondensation. However, as prerequisite to form this effector complex, Df31 has to be present in adequate amounts in the chromatin sample after size exclusion, necessary to deplete RNase A. To test this, the presence of Df31-his, included in the Drex chromatin assembly, was monitored after RNase A treatment and the size exclusion by western blot specific for the Df31-his-epitope. H3 served here as loading control. After RNase A treatment and the subsequent size exclusion, Df31 is still present in the chromatin, however in slightly reduced amounts, estimated by comparing the western blot signals of the untreated (Figure 4.25B left) and RNase A treated (Figure 4.25B right) chromatin sample. However, the amount of Df31 is still adequate to form a RNP complex with snoRNAs and open up chromatin structures *in vitro*.

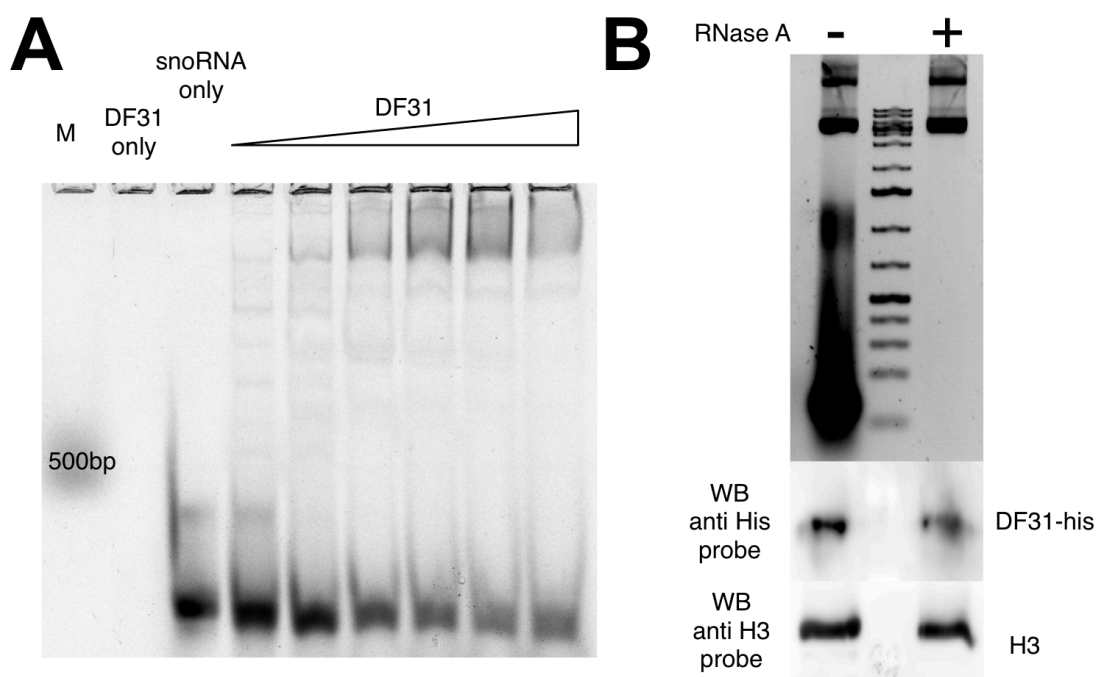


Figure 4.25: Df31 snoRNA binding *in vitro*

(A) The RNA binding ability of Df31 is shown by EMSA. 2,5nM Cy5 labelled G980 snoRNA was incubated with increasing amounts of Df31-his (250-5000pM). The interaction is monitored in a native polyacrylamid gel. **(B)** Monitoring Df31 presence in the chromatin conformation analysis *in vitro*, as prerequisite for RNP complex formation. Df31-his was included in the assembly process. After RNase A treatment the size exclusion was performed and the resulting chromatin was further analysed. The nucleic acid content was monitored by agarose gelelectrophoresis, whereas Df31-his and H3 were visualized by western blot with specific antibodies.

The experiments suggest that Df31 binds to the snoRNA molecules and is able to recruit the RNA molecules to chromatin.

4.9. Characterisation of the RNA binding domain of Df31

As mentioned before the prediction of RNA binding domains in the Df31 protein failed due to the undefined structure of the protein. However, RNA binding prediction using primary sequence showed overlapping results for predicted RNA binding residues. Four possible RNA binding regions could be identified (Figure 4.26).

Df31 and deletion variants

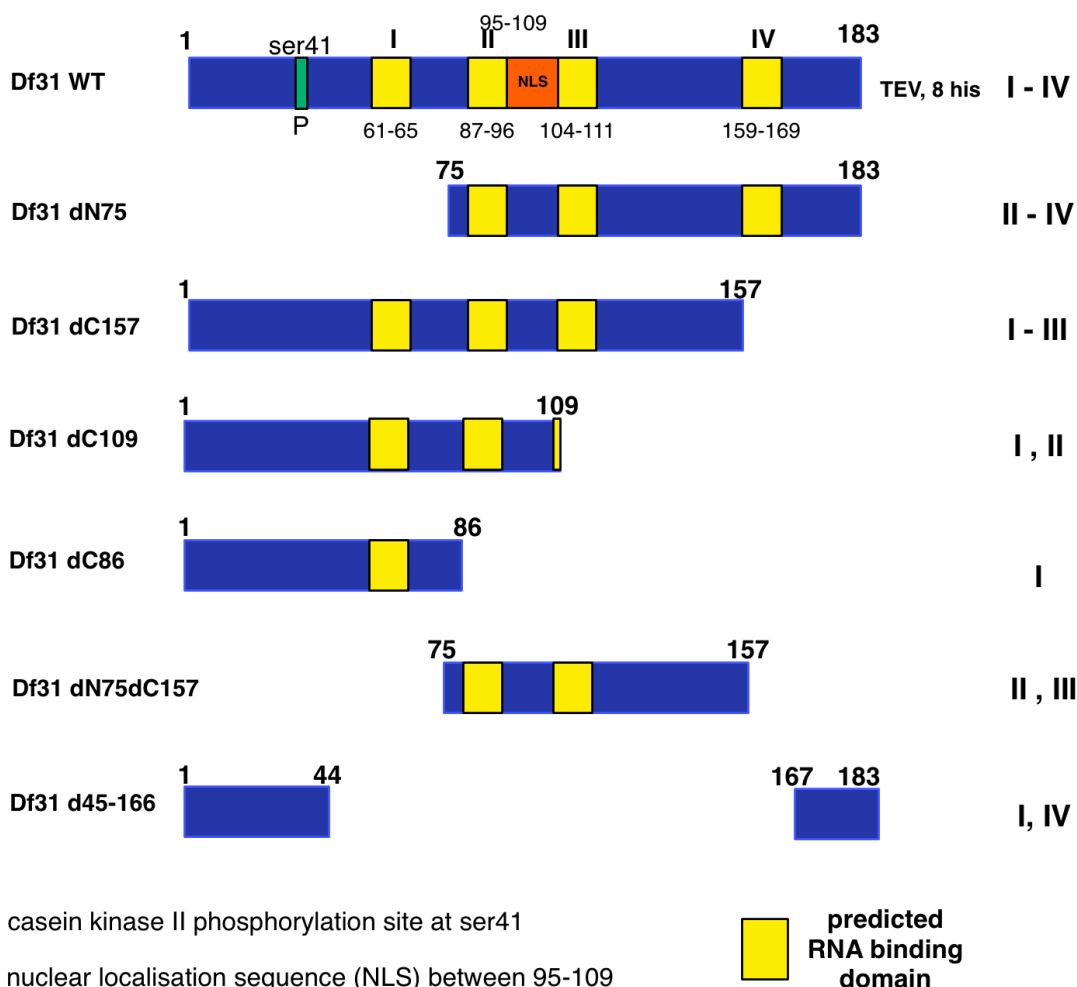


Figure 4.26: RNA binding prediction of Df31 and overview of Df31 deletion mutants

RNA binding sequences in the Df31 protein was predicted with BindN and RNAbindR.

Overlapping sequences are shown in the scheme. The different deletion mutants expressed are indicated in the scheme.

To localize the RNA binding region, deletion mutants of Df31 were designed and cloned. The deletion mutants were expressed in different *E.coli* strains (BL21 plac I, Rosetta plac I), the proteins were purified via the his-Tag. The purity and length of the mutants was checked in SDS PAGE (Figure 4.27).

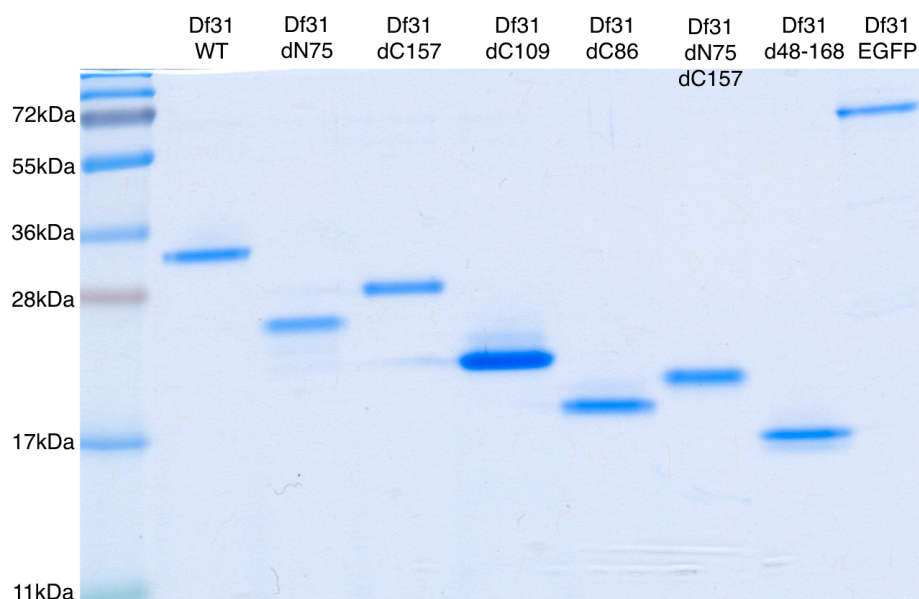


Figure 4.27: purification of Df31 deletion mutants

Df31 variants were expressed in E.coli and purified via Ni NTA beads. The length and purity of the proteins was checked in SDS PAGE. The protein marker page ruler plus is indicated.

The truncation mutants will subsequently be used to identify and localize RNA binding domains of Df31.

4.10. Generation and characterisation of Df31 antibodies

In collaboration with Axel Imhof's group and Elisabeth Kremer's group in Munich, antibodies against Df31 were created. To immunize the host animals Df31-Wt was recombinantly expressed and purified (Thomas Schubert) and injected into rats (Kremer group). The serum of different animals was initially used to screen for specific antibodies (Miriam Pusch, Imhof Group). Two antibodies were selected and produced in larger amounts. One antibody (1A10-11/VR-G1) showed suitable efficiency in immunoprecipitation. (Miriam Pusch, Imhof group). To identify the antibody binding regions in Df31, western blot analysis with the truncation mutants of Df31 were performed (Figure 4.28).

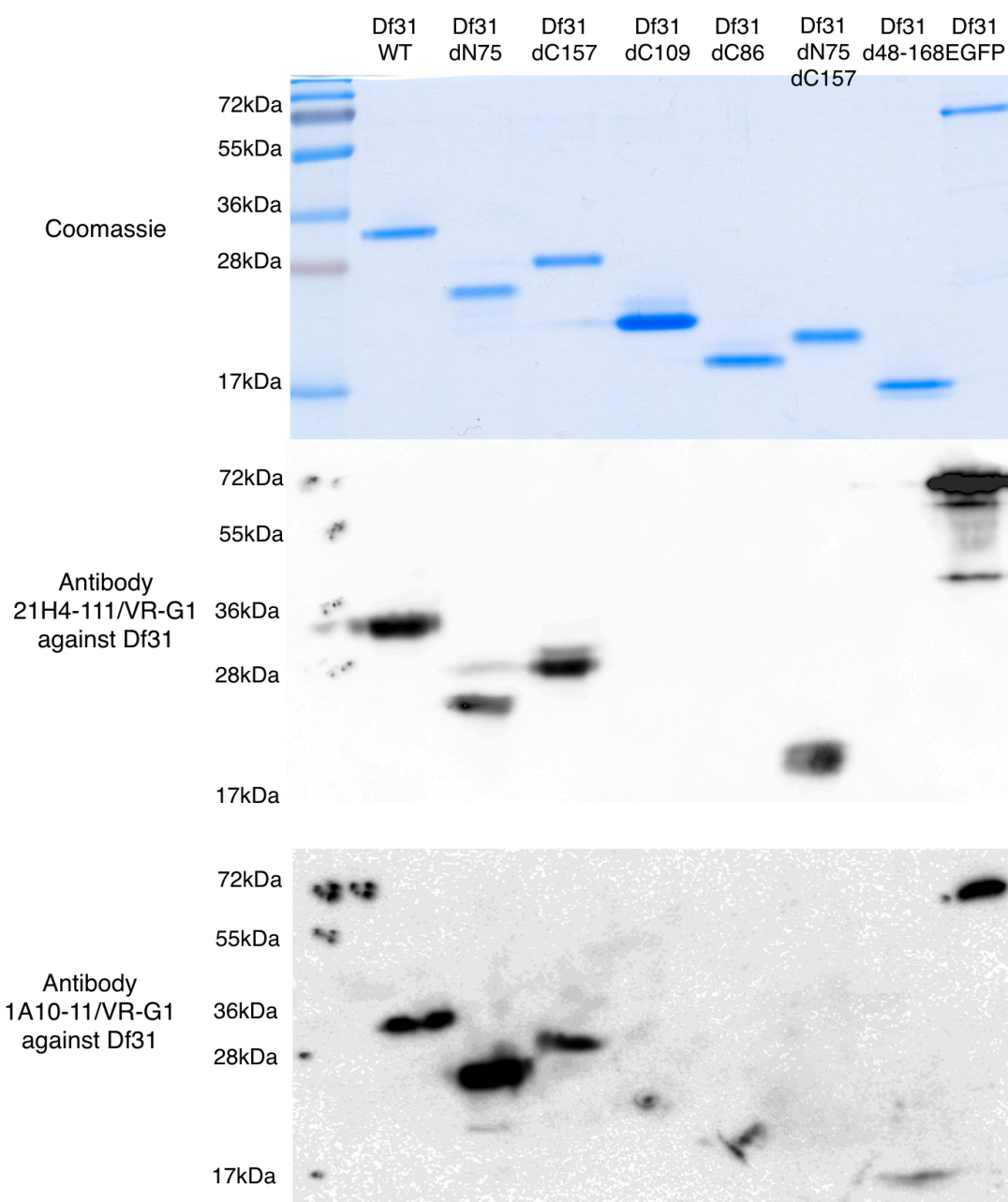


Figure 4.28: Identification of the binding regions of the Df31 antibodies

1µg of each Df31 truncation mutant was analysed in SDS PAGE followed by western blot with the Df31 specific antibodies. The dilution of the primary antibody was 1:50, whereas the secondary antibody against rat was diluted 1:5000 in PBST +5% milk powder. The upper panel shows the SDS PAGE stained with coomassie. The middle panel represents the western blot pattern produced by the antibody 21H4-111/VR-G1. The lower panel represents the western blot pattern produced by the antibody 1A10-11/VR-G1.

Df31 truncation mutants were separated by SDS PAGE (Figure 4.27) and used for western blot analysis. Df31 proteins possessing c-terminal more than c-terminal 157 amino acids of the proteins could be detected by western blot analysis with

the antibody 21H4-111/VR-G1 (Figure 4.28 middle panel). This experiment pinpoints to a binding region between 109 and 157aa of the protein for this specific antibody.

Furthermore, mapping the binding region of the antibody 1A10-11/VR-G1 was inconsistent (Figure 4.28 lower panel). WT Df31 and only minor deletions gave strong signals, whereas longer deletions impaired the antibody binding. Df31 dC86, dC109, dN75dC157 and Df31 d48-168 could not or only weakly be detected. For subsequent western blot analyses, the antibody 21H4-111/VR-G1 was used.

4.11. snoRNAs are enriched in the caRNA fraction of human chromatin

As purified human nuclear RNA was capable to re-open the condensed chromatin structure in our assay system (Figure 4.9), two recent high throughput analyses of chromatin associated RNAs in human fibroblasts (Mondal et al., 2010) and HeLa cells (Caudron-Herger et al., 2011) were analysed (performed by Sarah Diermeier). Analysis of the non-coding RNA and quantification of the snoRNA pool present in the human fibroblast transcriptome compared to the snoRNAs associated with chromatin revealed a strong enrichment of a fraction of these molecules in chromatin (Figure 4.29A). Out of 231 snoRNA found in these cells, 23 were enriched at chromatin, whereas 19 (8.2%) were enriched more than 2 fold compared to the transcriptome. Similarly, an accumulation of snoRNAs that are associated with the fraction of chromatin was detected in HeLa cells (Figure 4.29B). 248 snoRNA were found in the nuclear transcriptome. 92 (37%) of the 148 chromatin-associated snoRNAs were enriched more than 2 fold compared to the nuclear transcriptome.

A

chr	start	stop	enrichment	strand	gene ID	description
chr16	2012980	2013091	102,71	-	SNORA64	small nucleolar RNA, H/ACA box 64 [Source:HGNC Symbol;Acc:10221]
chr2	232320576	232320626	101,9	-	SNORA75	small nucleolar RNA, H/ACA box 75 [Source:HGNC Symbol;Acc:32661]
chr1	28906910	28907006	78,92	-	SNORA44	small nucleolar RNA, H/ACA box 44 [Source:HGNC Symbol;Acc:32637]
chr11	10823015	10823105	70,67	-	SNORD97	small nucleolar RNA, C/D box 97 [Source:HGNC Symbol;Acc:32760]
chr1	28835084	28835266	28,16	+	SNORA73B	small nucleolar RNA, H/ACA box 73B [Source:HGNC Symbol;Acc:10116]
chr11	8705786	8705851	18,18	+	SNORA3	small nucleolar RNA, H/ACA box 3 [Source:HGNC Symbol;Acc:32586]
chr9	139620568	139620688	14,94	-	SNORA43	small nucleolar RNA, H/ACA box 43 [Source:HGNC Symbol;Acc:32636]
chr1	28833876	28834075	13,97	+	SNORA73A	small nucleolar RNA, H/ACA box 73A [Source:HGNC Symbol;Acc:10115]
chr11	93468288	93468385	13,27	-	SNORA40	small nucleolar RNA, H/ACA box 40 [Source:HGNC Symbol;Acc:32633]
chr3	186504319	186504692	11,97	+	SNORA81	small nucleolar RNA, H/ACA box 81 [Source:HGNC Symbol;Acc:32667]
chr11	75111451	75111561	11,87	+	SNORD15A	small nucleolar RNA, C/D box 15A [Source:HGNC Symbol;Acc:10114]
chr19	10220453	10220496	10,52	+	SNORD105B	small nucleolar RNA, C/D box 105B [Source:HGNC Symbol;Acc:33572]
chr1	155895803	155895867	10,22	-	SCARNA4	small Cajal body-specific RNA 4 [Source:HGNC Symbol;Acc:32560]
chr11	75115480	75115594	10,01	+	SNORD15B	small nucleolar RNA, C/D box 15B [Source:HGNC Symbol;Acc:16649]
chr11	9450328	9450488	6,98	+	SNORA23	small nucleolar RNA, H/ACA box 23 [Source:HGNC Symbol;Acc:32613]
chr1	93306291	93306347	5,21	+	SNORA66	small nucleolar RNA, H/ACA box 66 [Source:HGNC Symbol;Acc:10223]
chrX	54835751	54840963	3,4	+	SNORA11	small nucleolar RNA, H/ACA box 11 [Source:HGNC Symbol;Acc:32599]
chr16	58582467	58582522	2,55	-	SNORA46	small nucleolar RNA, H/ACA box 46 [Source:HGNC Symbol;Acc:32639]
chr3	186505102	186505210	2,09	+	SNORA63	small nucleolar RNA, H/ACA box 63 [Source:HGNC Symbol;Acc:10106]
chr15	66795157	66795230	2,01	-	SNORD16	small nucleolar RNA, C/D box 16 [Source:HGNC Symbol;Acc:32712]

B

chr	start	stop	enrichment	strand	gene ID	description
chr5	138613694	138614985	39,8	+	SNORA74A	small nucleolar RNA, H/ACA box 74A [Source:HGNC Symbol;Acc:10119]
chr8	99054349	99054423	22,6	-	SNORA72	small nucleolar RNA, H/ACA box 72 [Source:HGNC Symbol;Acc:10234]
chr6	31590878	31590968	14,2	+	SNORA38	small nucleolar RNA, H/ACA box 38 [Source:HGNC Symbol;Acc:32631]
chr3	39451773	39453268	14,2	+	SNORA62	Small nucleolar RNA SNORA62/SNORA6 family [Source:RFAM;Acc:RF00091]
chr1	113195149	113196467	14,0	+	snoU13	Small nucleolar RNA U13 [Source:RFAM;Acc:RF01210]
chr6	86387039	86388417	13,9	-	SNORD50B	small nucleolar RNA, C/D box 50B [Source:HGNC Symbol;Acc:32722]
chr6	86387039	86388417	13,9	-	SNORD50A	small nucleolar RNA, C/D box 50A [Source:HGNC Symbol;Acc:10200]
chr1	155895731	155895849	12,4	-	SCARNA4	small Cajal body-specific RNA 4 [Source:HGNC Symbol;Acc:32560]
chr5	138611457	138612222	11,3	+	SNORA74	Small nucleolar RNA SNORA74 [Source:RFAM;Acc:RF00090]
chr11	75110563	75111993	9,4	+	SNORD15A	small nucleolar RNA, C/D box 15A [Source:HGNC Symbol;Acc:10114]

Figure 4.29: snoRNA molecules are highly enriched in human chromatin

(A) Deep sequencing results of chromatin-associated RNAs isolated from chromatin derived from human fibroblasts. The table shows the 10 highest enriched snoRNAs in chromatin of human fibroblasts compared to the transcriptome. **(B)** Deep sequencing results of chromatin-associated RNAs isolated from chromatin derived from HeLa cells. The table shows the 10 highest enriched snoRNAs in chromatin of HeLa cells compared to the nuclear transcriptome.

As snoRNAs are highly enriched in human and *Drosophila* chromatin and human total RNA has the potential to open up *Drosophila* chromatin, an evolutionary conserved mechanism is suggested wherein the binding of these molecules to chromatin results in an opening of the condensed higher order structures of chromatin.

To validate this hypothesis of a conserved RNA dependent mechanism, a study about the influence of RNA on the accessibility of human chromatin was performed in HeLa cells.

4.12. RNA maintains chromatin accessible *in vivo* human HeLa cells

To investigate whether RNA affects chromatin structure *in vivo* human HeLa cells, cellular RNA was hydrolysed and chromatin structure was probed by its accessibility to the endonuclease micrococcal nuclease (MNase) as performed in *Drosophila*.

As described above limited MNase digestion typically creates a ladder of DNA fragments, where the number of observed nucleosomal fragments is highly dependent on the MNase concentration and incubation time. Digestion of the cellular chromatin with 10 U of MNase for 2 minutes gives rise to a DNA ladder, reaching from mononucleosome to also larger DNA fragments (Figure 4.29A, lane 3). The addition of increasing amounts of RNaseA for 5 minutes, prior to MNase digestion, resulted in decreased sensitivity of chromatin towards MNase (Figure 4.29A, panel 4). The accessibility of cellular chromatin correlates with the depletion of RNA, as shown by visualisation of RNA and DNA after the MNase accessibility assay (Figure 4.30 A lanes 6 and 7). Here, nucleic acid purification was performed in the absence (lanes 1 to 5) or in the presence of RNaseA (lanes 7 to 11) in the stop buffer, revealing the levels of RNA remaining in the chromatin fraction. Moreover, higher concentrations of MNase are again capable of generating a nucleosomal ladder, suggesting that in the absence of RNA, chromatin forms a more compact structure (Figure 4.30A, lanes 10 and 11). In line with that, permeabilised HeLa cells were incubated with RNaseA (150 µg/ml) for increasing time (0 to 10 min) and subsequently monitored for changes in chromatin accessibility by MNase digestion, revealing decreased accessibility after 6min of RNaseA incubation (Figure 4.30B). The permeabilisation buffer and the EDTA concentration used while the RNase treatment do not influence the MNase activity (Figure 4.30C).

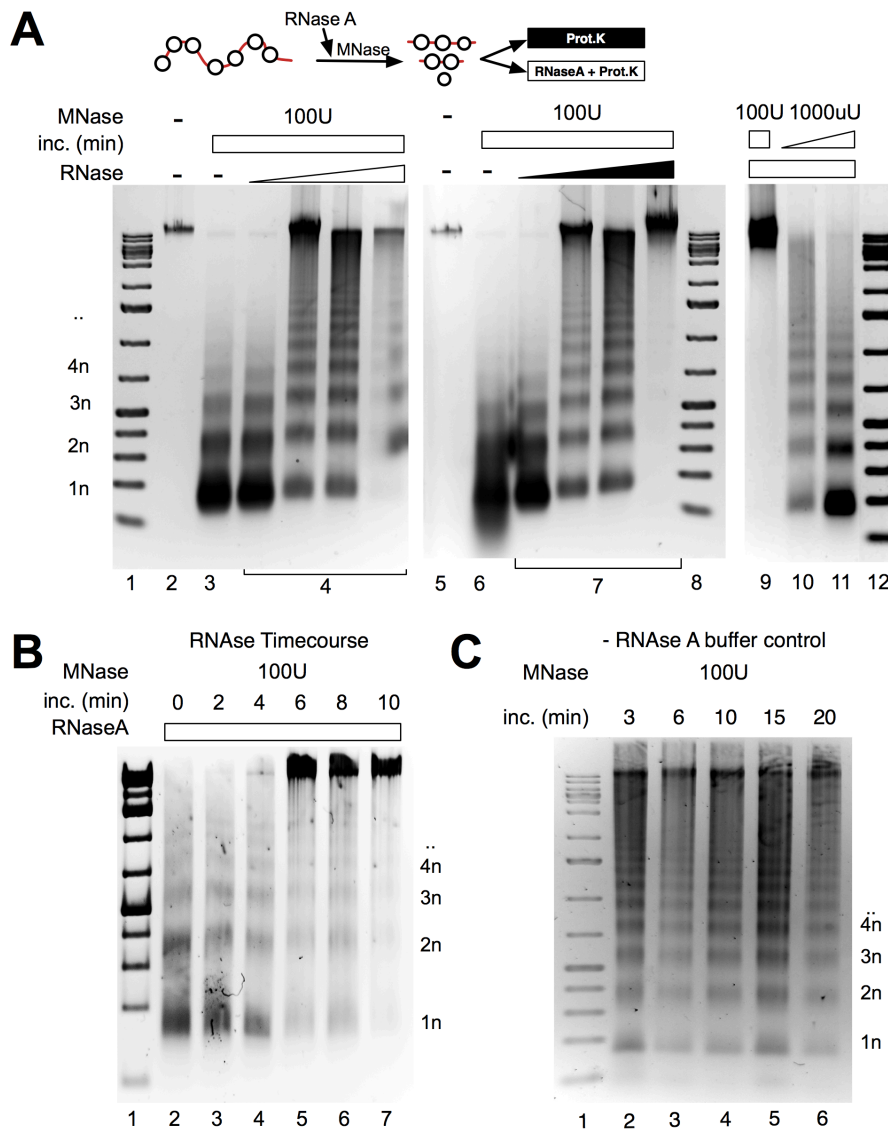


Figure 4.30: RNA maintains accessible chromatin structures *in vivo* HeLa cells

(A) RNaseA treatment of permeabilised HeLa cells prior to MNase accessibility analysis.

Permeabilised HeLa cells were incubated for 5 minutes without (lanes 3 and 6) or with RNaseA (panels 4 and 7, lanes 9-11), MNase accessibility was analysed with 10U MNase. Reactions were stopped, either proteins (black boxes) or proteins and RNA (white boxes) were digested, and the nucleic acids were visualised by agarose gel electrophoresis. The positions of the monomers and multimers of the nucleosomal DNA (1n, 2n,...) and the DNA marker (lanes 1,8,12) are indicated.

(B) Monitoring the RNaseA dependent kinetics of chromatin accessibility *in vivo*. Permeabilised HeLa cells were treated with 150 µg/ml RNaseA for 0 to 10 min (lanes 2 to 7) and then incubated with 10 U MNase for 2 min. The reaction was stopped, nucleic acids were purified and analyzed by agarose gel-electrophoresis. The DNA marker is shown in lane 1. **(D)** Permeabilisation buffer and the EDTA concentrations of the RNase A reaction buffer do not influence MNase activity.

Permeabilised HeLa cells were incubated with EDTA in the same concentration used in the RNase A reaction buffer and probed for MNase accessibility as described in (B) with longer incubation times. The DNA marker is shown in lane 1

To test whether Polymerase II transcribes the RNA involved in chromatin opening, HeLa cells were untreated or treated with α -amanitin for 6 h and assayed for MNase accessibility (Figure 4.31A; compare lanes 1 and 2). The chromatin of alpha amanitin treated cells is shown in the profile analysis to be less accessible to the nuclease than the chromatin of untreated cells. Furthermore, structural changes of nuclear chromatin were visualised by DAPI staining of the DNA in HeLa cells and fluorescence microscopy (Figure 4.31B). Whereas DNA staining in non-treated cells appears homogenous, increasing incubation time with α -amanitin results in a rough, compacted DNA staining pattern correlating with chromatin condensation. The compaction of cellular chromatin correlates with the disappearance of RNA. Newly transcribed RNA is monitored by the incorporation of 5-ethenyl-Uridine (EU, Invitrogen), which can be modified and visualised by CLICK-chemistry. In the non-treated HeLa cells newly transcribed RNA is detected in large amounts, whereas in the α -amanitin treated cells RNA transcription is highly reduced (performed by Maiwen Cauldron-Herger and Helen Hofmeister).

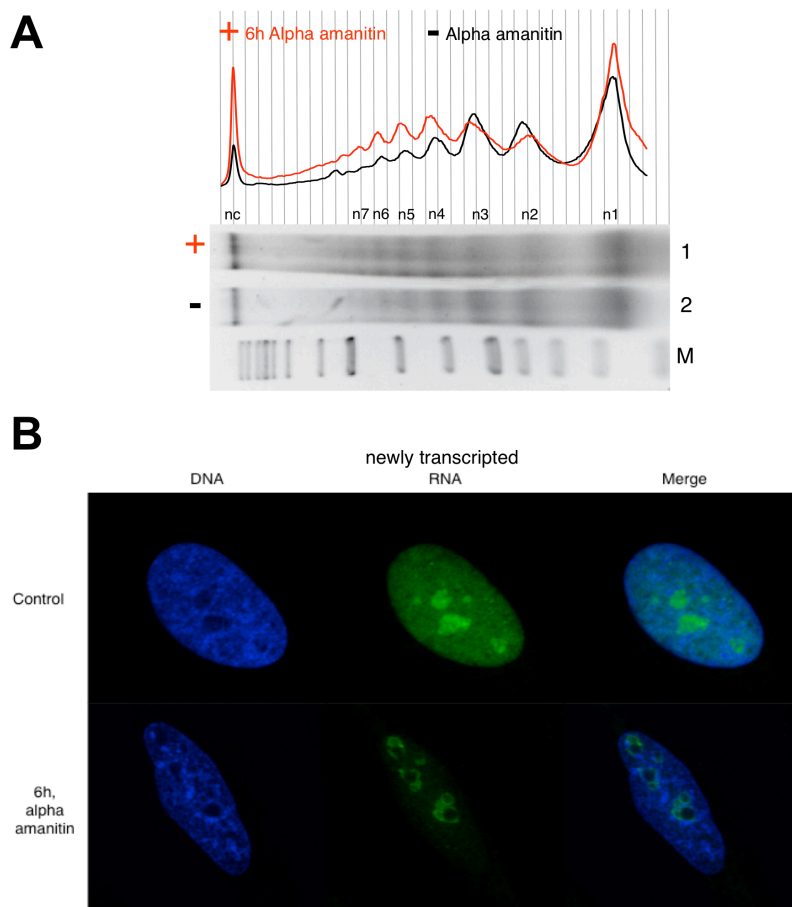


Figure 4.31: Pol II transcribed RNA maintains accessible chromatin structures *in vivo* HeLa

(A) HeLa cells were incubated with α -amanitin (50 $\mu\text{g/ml}$) for 6h (red, lane 1) or without (black, lane 2). Cells were harvested and counted. Chromatin accessibility was monitored by MNase accessibility with an identical number of cells. The DNA marker (M) and the positions of the nucleosomes are indicated. In addition a profile is shown, whereas the analysis of untreated chromatin is shown in black and the alpha amanitin treated chromatin in red. **(B)** HeLa cells were incubated with α -amanitin (50 $\mu\text{g/ml}$) for 6 h. The right panel shows the DNA and RNA staining of α -amanitin treated *Drosophila* cells by fluorescence microscopy. DNA was monitored by DAPI and newly transcribed RNA was visualized by monitoring incorporated 5-ethenyl-Uridine by CLICK-chemistry.

The accessibility analysis and the fluorescence microscopy pictures suggest that a RNA fraction synthesized by RNA Pol II is required to maintain chromatin structures in an accessible form.

Taken together the *in vivo* studies clearly show that depletion of cellular RNA influences the accessibility of chromatin. The accessibility of chromatin correlates with the RNA content, whereas the RNA seems to be transcribed by RNA Polymerase II.

4.13. The influence of RNA on the accessibility of the human ribosomal DNA locus

The ribosomal DNA locus was chosen as a model locus to determine the influence of cellular RNA on the accessibility of a specific genomic region. To examine how RNA affects the chromatin structure of this locus, cellular RNA was hydrolysed and chromatin structure of this locus was probed by its accessibility to MNase followed by southern blot visualisation (Figure 4.32). Permeabilised HeLa cells were treated with RNaseA and the accessibility was monitored by the MNase sensitivity assay. RNA and proteins were digested and the global influence of RNA depletion on the chromatin accessibility was monitored by agarose gelelectrophoresis followed by ethidium bromide staining. A southern blot with an rDNA specific probe was used to get information about the chromatin structure of the locus.

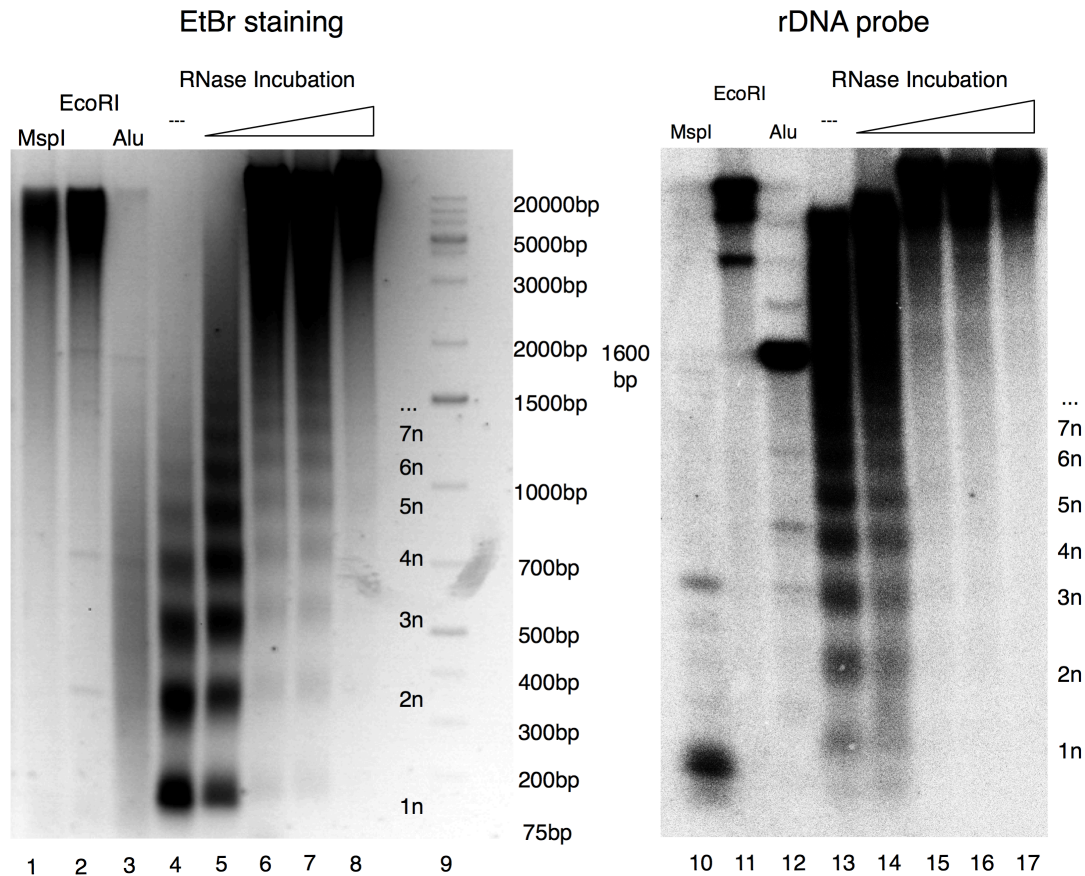


Figure 4.32: RNA maintains the accessibility of the ribosomal DNA locus.

Permeabilised HeLa cells were incubated for 5 minutes without (lanes 4 and 13) or with RNaseA (lanes 5-8, 14-17), MNase accessibility was analysed with 10U MNase. Reactions were stopped, proteins and RNA were digested, and the nucleic acids were visualised by agarose gel electrophoresis followed by ethidium bromide staining (left panel). The positions of the monomers and multimers of the nucleosomal DNA (1n, 2n,...), the DNA marker (lanes 9) and control genomic DNA digests (lanes 1-3, 10-12) are indicated. The right panel shows the chromatin accessibility of the rDNA locus visualised by locus specific southern blot hybridisation of the left panel. The positions of the monomers and multimers of the nucleosomal DNA (1n, 2n,...), the DNA marker (lanes 1) and control genomic DNA digests (lanes 1-3, 10-12) are indicated.

To get more insights into the influence of cellular RNA on the rDNA locus, RNA transcription was blocked and chromatin structure of this locus was probed by its accessibility to MNase followed by southern blot visualisation (Figure 4.33). HeLa cells were untreated or treated 3h or 6h with 50µg/ml alpha amanitin and the accessibility was monitored by the MNase sensitivity assay of the same number of cells. RNA and proteins were digested and the global influence of RNA

depletion on the chromatin accessibility was monitored by agarose gelelectrophoresis followed by ethidium bromide staining. A southern blot with an rDNA specific probe (-500/+85) was used to get information about the chromatin structure of the locus.

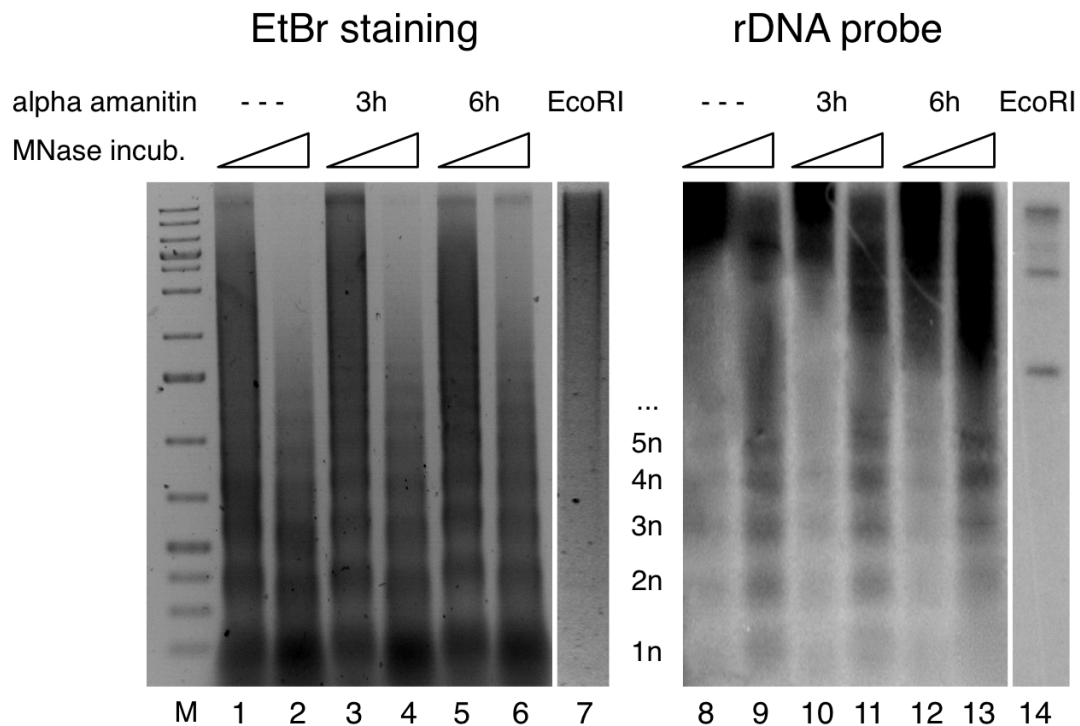


Figure 4.33: Polymerase II inhibition decreases the accessibility of the ribosomal DNA locus. HeLa cells were incubated without (lanes 1,2 and 8,9) or with alpha amanitin (50µg/ml; 3h incubation lanes 3,4 and 10,11; 6h incubation lanes 5,6 and 12,13), MNase accessibility was analysed with 10U MNase. Reactions were stopped, proteins and RNA were digested, and the nucleic acids were visualised by agarose gel electrophoresis followed by ethidium bromide staining (left panel). The positions of the monomers and multimers of the nucleosomal DNA (1n, 2n,...), the DNA marker (M) and control genomic DNA EcoRI digest (lanes 7) are indicated. The right panel shows the chromatin accessibility of the rDNA locus visualised by locus specific southern blot hybridisation of the left panel. The positions of the monomers and multimers of the nucleosomal DNA (1n, 2n,...) and control genomic DNA EcoRI digest (lane 14) are indicated.

These experiments show that the accessibility of the rDNA locus is highly influenced by cellular RNA. RNaseA treatment as well as Polymerase inhibition resulted in decreased nuclease accessibility of the rDNA locus.

Hence the rDNA locus is a suitable model system to further study the RNA-dependent higher order structures of chromatin in HeLa cells.

4.14. Human homologues of Df31

The RNP complex built of Df31 and snoRNAs is shown to influence higher order structures of *Drosophila* chromatin and maintain its accessibility. To identify proteins fulfilling this role in HeLa cells, it was checked for human homologues of Df31 by sequence and function.

Different human homologues of Df31 were found by comparing the amino acid sequence (Table 4.14). Several already known chromatin proteins were identified, which localize to the nucleus. HMGN5 as one of the top hits was shown to decondense chromatin by interference to H1 binding. NASP is shown to be a H1 binding protein involved in transport of H1 molecules into the nucleus. Prothymosin and Parathymosin are both remodelling enzymes influencing chromatin structure and accessibility. SRCAP, also called Swr1 represents a histone chaperone, mainly functioning in H2AZ exchange.

Homologue prediction by functional aspects in combination with secondary structure prediction remained without convenient result. The software HHpred could not detect functional Df31 homologues in human and other organisms with a higher probability than 5% (Soding et al., 2005) (Wass and Sternberg, 2008).

Protein name	E Value	Identical	aa	location
Cylicin 2	5e-06	27.8%	348	Nucleus, sperm head
HMGN5	7e-06	30.1%	282	Nucleus, Nucleolus
NASP	2e-04	27.9%	724	Nucleus, cytoplasm
Prothymosin alpha	2e-04	31.2%	101	Nucleus
Eukaryotic translation initiation factor 4 gamma	4e-04	29.6%	1143	Nucleus, Cytoplasma
HIV TAT specific factor 1 variant	4e-04	29.2%	758	Nucleus
Nucleophosmin	4e-04	21.5%	294	Nucleus, Nucleolus
SRCAP	9e-04	25.1%	3230	Nucleus
Paf1	1e-03	27.3%	531	Nucleus
parathymosin	1e-03	30.2%	102	Nucleus
Acidic nuclear phosphoprotein family 32	2e-03	28.2%	250	Nucleus
scaffold attachment factor B	0,0097	22.2%	915	Nucleus

table 4.14: structural homologues of Df31 in human

Paralign was used to find human homologues of Df31 by comparative alignment. The name, the E-value, the conservation to Df31, the amino acid length and the localisation of the proteins are indicated.

4.15. Bioinformatic analysis of HMGN5, a possible Df31 homologue

Based on comparative sequence alignment HMGN5 was one of the top hits for human homologues of Df31. The 31kDa HMGN5 possesses not just a high overall conservation, it furthermore shares 30% total sequence identity with Df31 (Figure 4.34).

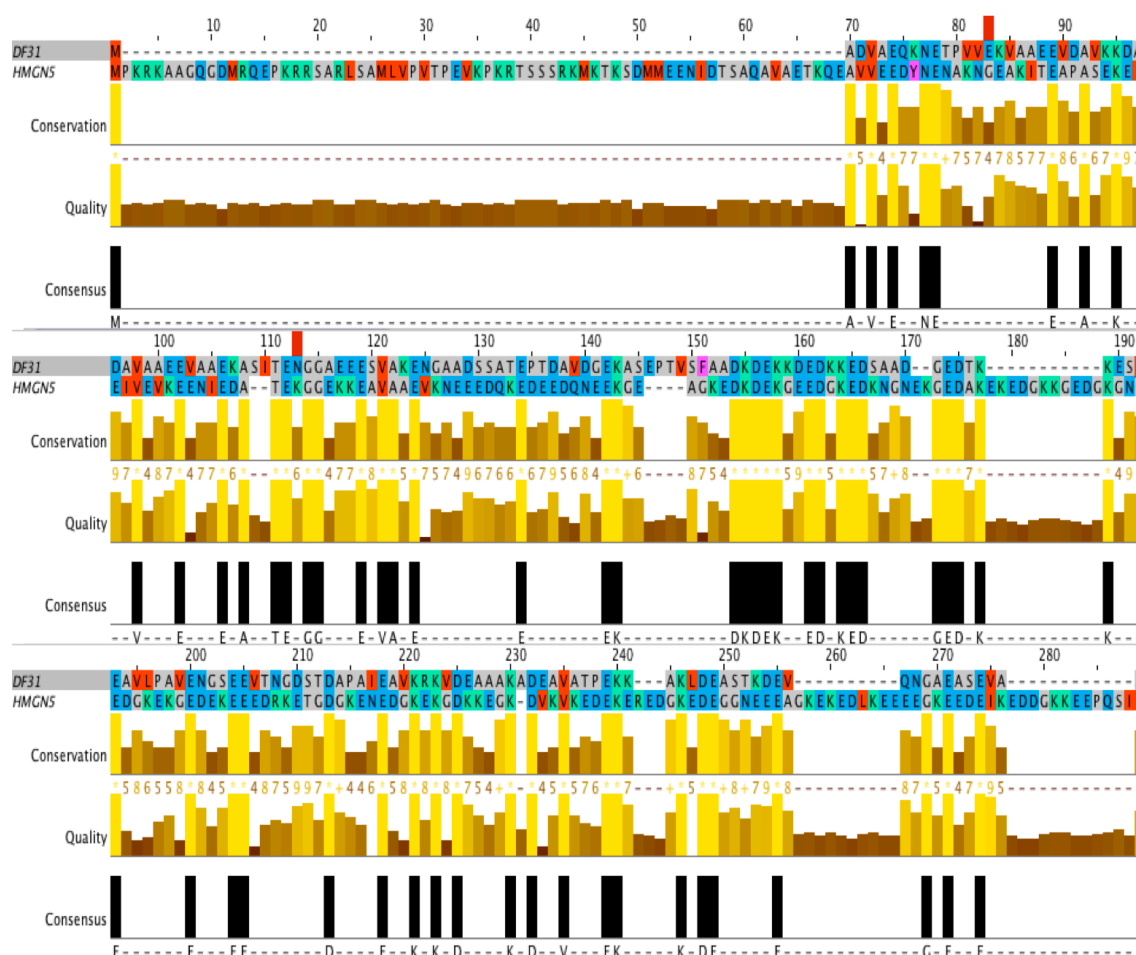


Figure 4.34: Sequence alignment between Df31 and HMGN5

Paralign was used to search for human homologues of Df31. The alignment is shown as jalview picture. HMGN5 one of the top hits shows high overall conservation to Df31 indicated by the yellow/brown bars and shares 30% identical consensus sequence with Df31 (black bars).

HMGN5 represents a highly abundant protein in human as indicated by analysis of the human peptide atlas (Desiere et al., 2005) performed with the web based PaxDb software at the university of Zurich (<http://pax-db.org/#!/home>) (Figure 4.35). The proteome atlas of homo sapiens comprises more than 12500 proteins, whereas HMGN5 is found at position 4203. Comparatively, H3 is found in position 2727 and H1 in position 223 of the protein abundance ranking.

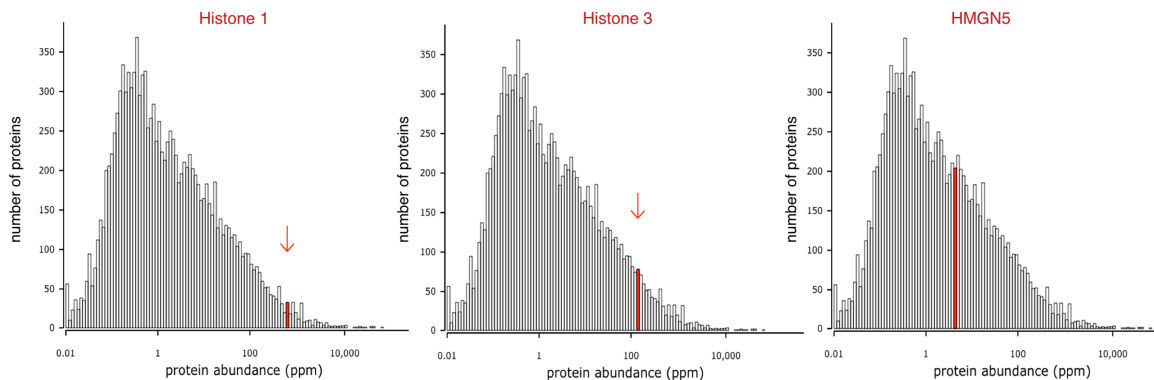


Figure 4.35: Abundance of HMGN5 in *homo sapiens*

The graphs indicate the abundance of H1, H3 and HMGN5 (red) in human according to the human peptide atlas. The analysis was performed with the web based software PaxDb provided by the university of Zurich. The number of proteins is plotted on the y-axis, whereas the protein abundance is plotted on the x-axis whereas the abundance increases to the right.

In addition to the sequence conservation, Df31 and HMGN5 share biochemical features. Reminiscent to Df31, the 283 aa HMGN5 possesses a high content of charged amino acids (Arg + Lys = 60aa, Asp + Glu = 102) and a theoretical pI of 4.5 as evaluated by ProtParam (Wilkins et al., 1999). Furthermore HMGN5 also exhibits a highly unfolded and disordered structure as the folding prediction algorithm FoldIndex suggests (Figure 4.36) (Prilusky et al., 2005).

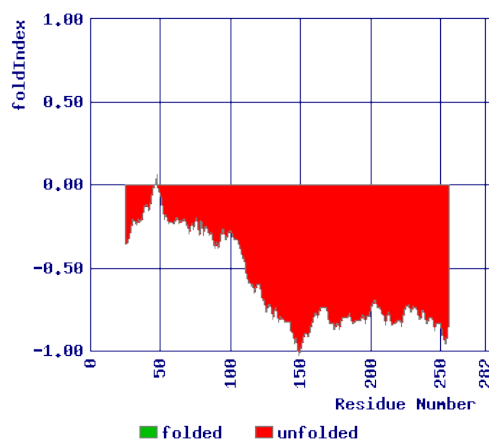


Figure 4.36: Folding prediction of HMGN5. The graph shows the folding prediction (red) based on the FoldIndex algorithm. The x-axis represents the 282 aa residues of HMGN5, whereas at the y-axis the FoldIndex is plotted. The negative Index (red) suggests that the protein is unfolded and disordered at certain residues.

Disordered structure is a common feature of high mobility group proteins like HMGN5, resulting in differences in electromobility in SDS PAGE, reminiscent to Df31.

GO-term prediction using the CombFunc software indicates HMGN5 being a chromatin binding protein with a probability of 48% and a positive regulator of transcription with a probability of 44%. Furthermore HMGN5 possesses a nucleoside-triphosphatase activity with a probability of 39% (Wass and Sternberg, 2008). Recently, HMGN5 was shown to interfere H1 dependent chromatin compaction thereby promoting decondensation of chromatin (Rochman et al., 2010; Rochman et al., 2009). Hence, HMGN5 influences chromatin higher order structures and maintains chromatin accessibility, implying functional conservation between Df31 and HMGN5. These functional similarities between Df31 and HMGN5 are underlined by similar localisation of the proteins at euchromatic regions in their respective organisms.

Prediction of HMGN5 functional homologues in human and other organisms performed with HHpred resulted in a partial homology to Drosophila regulator of chromatin structure (RCC1), however the overall probability to be functional homologous is only 9.8% (Soding et al., 2005).

In order to determine the localisation of HMGN5 in HeLa cell nuclei, immunofluorescence of the endogenous protein was performed (Figure 4.37). HeLa cells were grown on cover slips and after fixation and permeabilisation hybridized with antibodies against HMGN5 and B23 (nucleophosmin) as a marker for the nucleolus. In addition the DNA was stained with DAPI. Standard fluorescence microscope analysis and confocal microscopy were used to localize

HMGN5 in the cell. Signals originated from the nucleus and the nucleolus can be detected in both microscopic approaches, implying that HMGN5 may influence also the chromatin higher order structures of the ribosomal DNA loci.

A Fluorescence microscope:

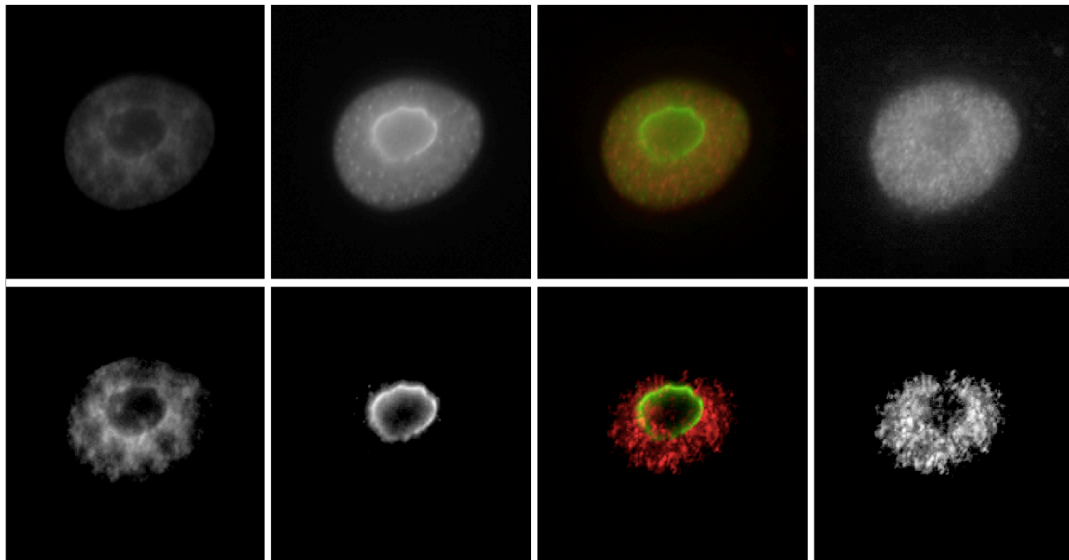
Dapi

B23

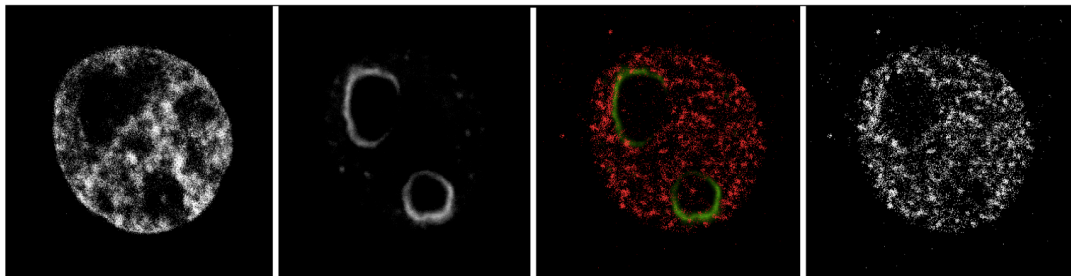
Merge

B23
HMGN5

HMG5



B Confocal microscope:



200nm stack

Figure 4.37: Nuclear and nucleolar localisation of HMGN5

(A) Immunofluorescence of endogenous HMGN5 in HeLa cells visualized by standard fluorescence microscopy. DAPI stained DNA is depicted in the left panels. B23, a nucleolar marker in the middle as well as the merge between B23 and HMGN5, which is shown in the right panels. To upper panels represent the original fluorescence pictures, whereas in the lower panels the max. polarized pictures are shown. **(B)** Immunofluorescence of endogenous HMGN5 in HeLa cells visualized by confocal microscopy. DNA, B23 and HMGN5 are shown as described above.

4.16. HMGN5 interacts with RNA

Based on primary sequence, besides the known nuclear localisation sequence and the phosphorylation site, four possible RNA binding sequences were detected (Figure 4.38A). HMGN5 was expressed in *E. coli* and purified via the his-Tag. The purity was checked in SDS PAGE. In addition a western blot analysis of the protein was performed (Figure 4.38B).

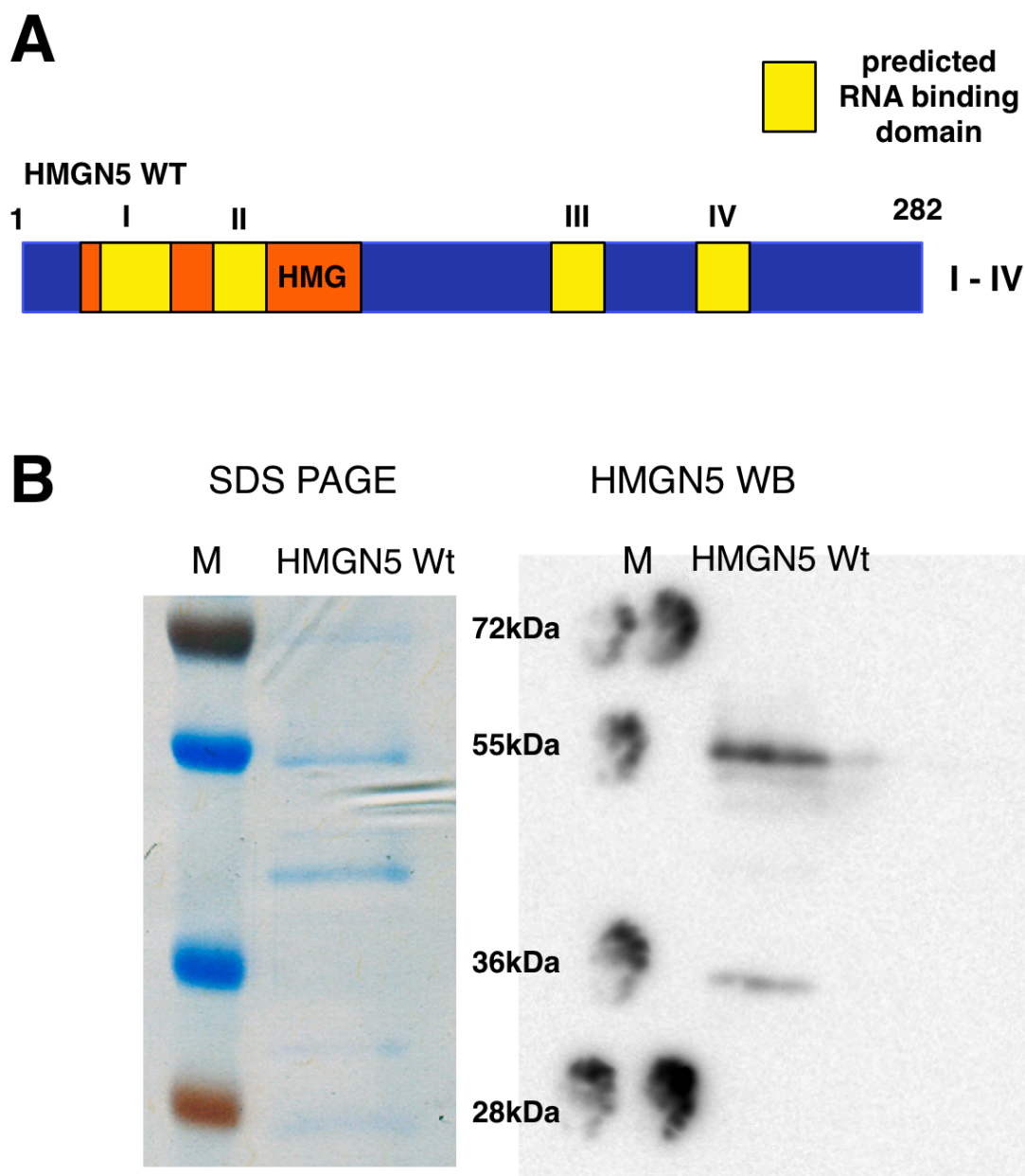


Figure 4.38: RNA binding sequence prediction of HMGN5 and purification

(A) Based on primary sequence the RNA binding regions of HMGN5 were predicted with BindN and RNAbindR. Predicted, in both algorithms detected regions are shown in the scheme (red boxes) as well as the high mobility group protein sequence (orange box). **(B)** HMGN5 was

expressed in *E. coli* and purified with Ni-Nti beads. The purity is checked in SDS PAGE (left panel) and western blot analysis (right panel).

Microscale thermophoresis was used to determine the RNA binding properties of HMGN5 (Figure 4.39). Therefore fluorescently labelled, unspecific RNA molecules (en3 RNA-FAM) were incubated with increasing amounts of HMGN5 and analysed with MST. HMGN5-RNA binding has a K_D value of $6\mu\text{M}$ ($\pm 0.8\mu\text{M}$) for the interaction with non-specific RNA (en3-RNA).

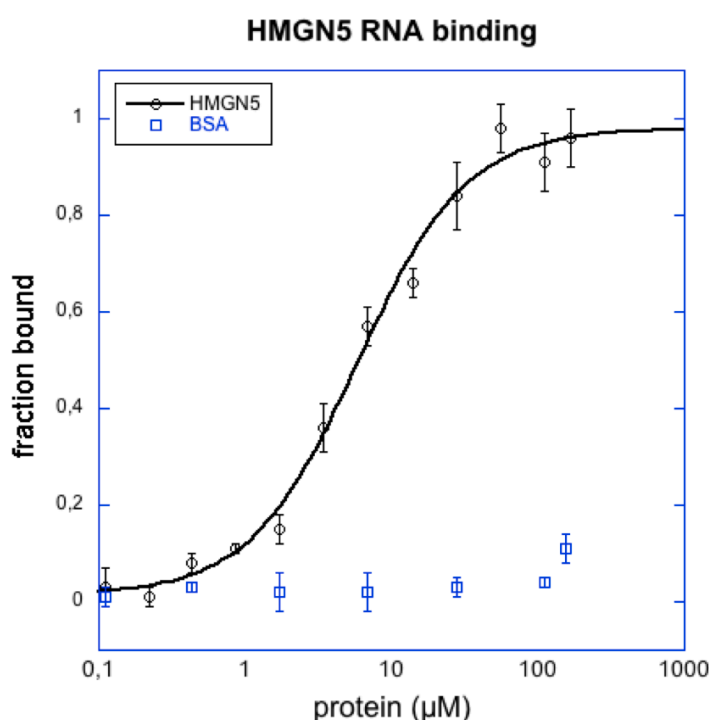


Figure 4.39: RNA binding study of HMGN5.

50nM fluorescently labelled RNA (en3 RNA) was incubated with increasing amounts of HMGN5. The binding was analysed by microscale thermophoresis.

These experiments clearly show that HMGN5 possesses the ability to bind RNA.

4.17. Characterisation of the RNA binding domain of HMGN5

In order to find and characterize RNA binding domains in the HMGN5 protein webbased search algorithms were used. Complementarity to known RNA binding domains could not be detected, so RNA binding prediction using primary sequence were performed. The web based algorithms BindN and RNAbindR

showed overlapping results. Four possible RNA binding regions could be identified by these algorithms (Figure 4.40). Truncation mutants were designed to delete the different predicted sites of RNA interaction.

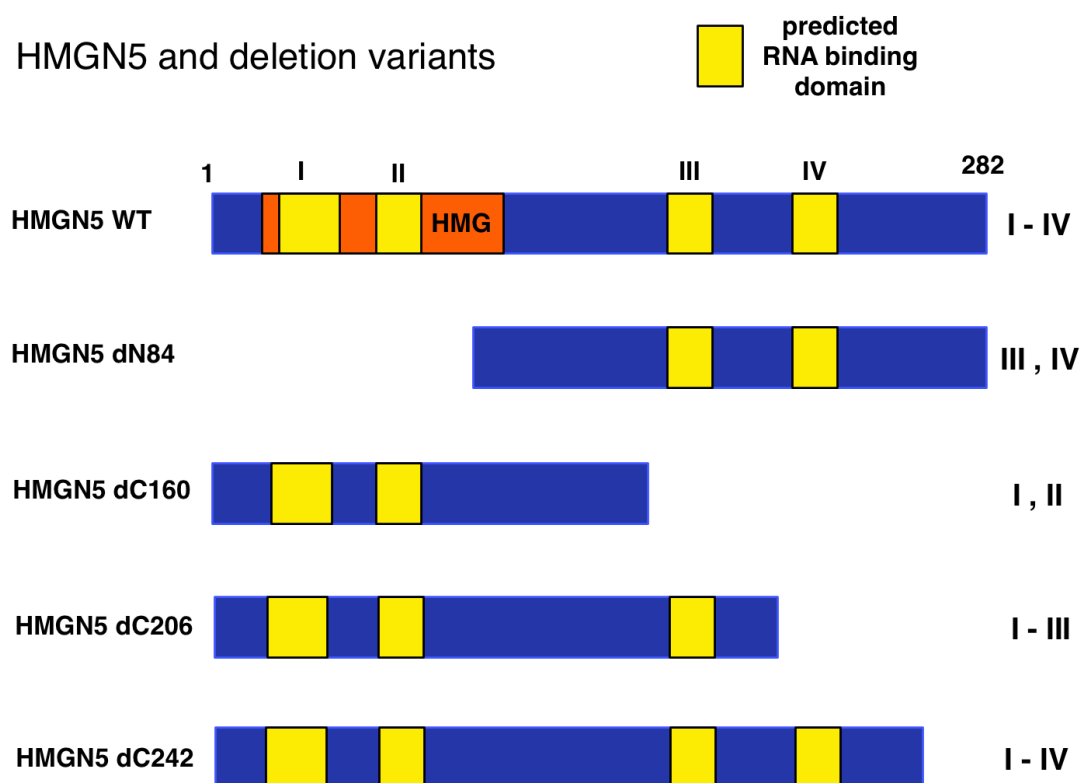


Figure 4.40: RNA binding prediction of HMGN5 and overview of HMGN5 deletion mutants

RNA binding sequences in the HMGN5 protein was predicted with BindN and RNAbindR. Detected overlapping sequences are shown in the scheme. The different deletion mutants expressed are indicated in the scheme.

In order to identify and localize the RNA binding domains of HMGN5 these truncation mutants will be subsequently used in RNA binding assays.

5. Discussion

5.1. RNA maintains chromatin accessible in *Drosophila* cells.

The presented study was performed in order to determine the influence of RNA on chromatin structure and organisation. It suggests that RNA plays a key role as integral component of chromatin, maintaining accessible higher order structures.

Depletion of RNA, either by RNaseA or Polymerase II inhibition by alpha amanitin treatment, resulted in a genome wide decrease of chromatin accessibility *in vivo* (section 4.1.). Strikingly, the accessibility correlated with the amount of RNA *in vivo*, which seems to be transcribed by polymerase II. In support of this, microscopic and EM studies in human HeLa cells observed a similar compaction of chromatin after RNA depletion (Bouvier et al., 1985) or transcriptional inhibition (Nickerson et al., 1989). The presented results are furthermore strengthened by a recent publication, showing that depletion of cellular RNA leads to condensation and compaction of human chromatin analysed by fluorescence microscopy (Caudron-Herger et al., 2011). Altogether, these observations imply that RNA maintains chromatin accessible.

Reminiscent to the effect of RNA on the accessibility of cellular chromatin, the accessibility of reconstituted chromatin clearly depended on the presence of RNA (section 4.2.). Moreover, a correlation between the amount of RNA and the accessibility of chromatin could be revealed *in vitro*, confirming the *in vivo* observations. Interestingly, only RNase enzymes cutting single stranded RNAs affected the chromatin accessibility, whereas RNase H, cutting DNA-RNA hybrids did not impair the nuclease sensitivity. The results point out that single stranded polymerase II transcripts play vital roles in the maintenance of an accessible chromatin state.

5.2. Chromatin associated RNAs decondense and open up higher order structures of chromatin

Sucrose gradient sedimentation experiments indicated that RNA affects chromatin accessibility by influencing higher order chromatin folding (section 4.3.). A proportion of RNA was found in these experiments being tightly bound to *in vitro* reconstituted chromatin even under high salt conditions (600mM KCl). Depletion of these associated RNAs resulted in a shift of chromatin from light into dense regions of the sucrose gradient. This points to a conformational change of chromatin from the open, accessible to the condensed, inaccessible conformation. After re-addition of RNA, it was again detected to be associated to chromatin. Moreover, the presence of caRNAs correlated with a shift back to lighter regions of the gradient, suggesting a reversible chromatin conformation change induced by caRNAs. However, yeast tRNA and oligonucleotides were not capable to open up chromatin higher order structures, underlining the specificity of chromatin associated RNAs. Interestingly, human nuclear RNA interacted with *Drosophila* chromatin and could re-open and maintain its decondensed conformation, implying a conserved role of RNA in chromatin organisation. Noteworthy, the decondensating effect of caRNA on *in vitro* reconstituted chromatin seems to be independent of transcription as the DNA template used for chromatin reconstitution is transcriptionally impotent due to the lack of suitable promoters.

Isolation of caRNA revealed that mainly short RNA molecules interact with chromatin. High throughput sequencing of these RNAs showed strong enrichment of ncRNA molecules at *Drosophila* chromatin (section 4.7.). Interestingly, also the analysis of caRNAs derived from human chromatin indicates ncRNAs to be highly prominent at chromatin (Mondal et al., 2010)(section 4.11.). Noteworthy, the caRNAs isolated in the study of Mondal et al. seem to be bound to human euchromatin as well as heterochromatin as the sucrose gradient analyses supposes. Furthermore, the caRNAs of *Drosophila* identified in this study were isolated independent of the eu- or heterochromatic origin. This argues for a general role of caRNAs in maintenance of chromatin accessibility.

Interestingly, snoRNAs were the highest enriched ncRNA molecules at chromatin compared to the transcriptome in human and *Drosophila*. The *Drosophila* C/D snoRNAs U2134b and G980 were enriched 457 and 221 fold at chromatin. In chromatin conformation analyses performed by sucrose gradient sedimentation, *in vitro* transcribed snoRNAs G980 and U2134b exhibited the potential to open up chromatin higher order structures (section 4.7.). The presented results clearly show an involvement of caRNAs not only in the maintenance of open euchromatin, but also in keeping the heterochromatin fraction more or less accessible.

So far the highly abundant and well structured snoRNA molecules were implied to play a role in RNA editing and ribosome biogenesis (Bachellerie et al., 2002). In eukaryotes, two specific modifications, 2'-*O*-methylation and pseudouridination, are directed by two large families of snoRNAs, which are named box C/D and H/ACA snoRNAs after the presence of short consensus sequence motifs, respectively. Molecular targets for 2'-*O*-methylation and pseudo-uridination are tRNAs, snRNAs and rRNAs. Both types of guide snoRNAs function as small ribonucleoprotein particles (snoRNPs), consisting of a site-specific snoRNA associated with a small set of proteins common to each guide family. Recently, a number of snoRNAs, mostly C/D box snoRNAs, with tissue-specific expression and no obvious sequence complementarity to rRNA or snRNAs have been identified. As part of a still poorly understood gene regulatory mechanism, these orphan snoRNAs are thought to direct mRNA modifications (Vitali et al., 2005) and to play a role in hnRNA splicing (Bratkovic and Rogelj, 2011). Growing evidence suggests that many snoRNAs can give rise to other regulatory RNA species, such as microRNA (miRNA)-like and piwi-interacting RNA (piRNA)-like short RNAs, in a wide variety of organisms. Components of an RNA interference pathway produce these sno-derived RNAs (sdRNAs) from double-stranded snoRNA structures, indicating a link between snoRNAs and RNA silencing (Ender et al., 2008).

Interestingly, several protein components of C/D snoRNPs, are linked with chromatin remodelling and transcription complexes. The yeast homologues of the human snoRNP proteins p55 and p50 (also called Rvb1 and Rvb2), Rvb1p

and Rvb2p in, have been described to form a dimer with ATPase activity *in vitro* and chromatin remodelling activity *in vivo*, affecting the transcription of 5% of the yeast genome (Jonsson et al., 2001; King et al., 2001). In addition, Rvb1p and Rvb2p were found in the yeast INO80 remodeling complex, which stimulates transcription by chromatin remodelling (Shen et al., 2000). Human p50 and p55 were found to interact with the histone acetylase TIP60, which acetylates nucleosomes *in vitro* and possesses ATPase and DNA helicase activity (Ikura et al., 2000). Furthermore, the well described snoRNA binding proteins Nop56p/Nop58p interact with matrix-attached regions (MARs) in plants, which are thought to organize chromatin higher order structures by establishing of the nuclear matrix (Hatton and Gray, 1999). Moreover, human and rat p55 was enriched in the nuclear matrix fraction suggesting general function(s) of the snoRNA binding protein in chromatin organisation (Holzmann et al., 1998). Furthermore, rat p55 was described being tightly bound to TBP and Polymerase II in immunoprecipitation experiments, suggesting p55 to influence transcription (Kanemaki et al., 1997; Qiu et al., 1998).

These observations support the findings of the presented study, suggesting that a subpopulation of snoRNAs is stably associated with chromatin in different organisms, thereby influencing chromatin structure and function.

Moreover, it could be speculated that the snoRNAs possibly have to be modified for full functionality. RNA editing has the potential to dynamically alter and diversify snoRNAs, thereby redirecting their functions (Sie and Kuchka, 2011). Furthermore, 2'-O methylation of nucleotides may protect the snoRNA from hydrolytic degradation, increase hydrophobic surfaces for interaction, or stabilize snoRNA structures. Pseudouridines possess increased flexibility in their C-C glycosyl bonds, which may influence snoRNA tertiary structure (Bachellerie et al., 2002). Altogether RNA editing mechanisms could increase diversity of snoRNAs and fulfill roles in snoRNA folding and recruiting of interaction partners.

5.3. Df31 is involved in an RNA dependent mechanism opening up chromatin

To determine the nature of these potential RNA binding proteins, chromatin-bound proteins in the presence or absence of RNA were analysed (performed by Miriam Pusch, Imhof group)(section 4.4.). Among the factors that showed reduced affinity to chromatin after removal of RNA, was the chromatin decondensation factor 31. Bioinformatic analysis demonstrated Df31 being a highly abundant protein in *Drosophila*, expressed all over the life cycle (section 4.5.). Furthermore, it showed that Df31 features an unfolded and disordered structure (section 4.5.). This flexible structure was described to serve as interaction platform and to favour molecular interaction with proteins or nucleic acids (Dunker et al., 2001). A recent study investigating the proteome network in *Drosophila* revealed that Df31 indeed possesses various protein binding-partners (Guruharsha et al., 2011). Pull-down experiments with over-expressed Df31 in *Drosophila* S2R+ cells point to more than 100 binding partners of Df31.

Interestingly, Df31 interacts with other chromatin modifiers like the remodelling complex Iswi, the suppressor of variegation Su(var3-9), topoisomerase I or the dodeca satellite binding protein 1. Worth mentioning, the pull-down experiments demonstrated, that the tagged version of Df31 interacted also with endogenous of Df31, implying oligomerisation of the protein. In addition, Df31 was found to bind various RNA binding proteins, like ribosomal proteins, spliceosomal components and RNA helicases.

In addition to the suggested RNA binding of Df31 seen in the proteomic assay (section 4.4.), bioinformatic analyses indicated Df31 to be an RNA binding protein due to its flexible structure and charge distribution (section 4.5.). These predictions were proven by further experiments. Microscale thermophoresis experiments exhibited Df31 binding preferentially to ssRNA, whereas ssDNA and dsDNA are discriminated. This implies that Df31 and RNA form a stable complex *in vitro* (section 4.6.). Pull-down experiments demonstrated that Df31 is bound to histones and chromatin in an RNA dependent manner, which supports the quantitative proteome analysis (section 4.4.). Microscale thermophoresis experiments exposed H3 to be the anchor point for Df31-chromatin interaction.

These results are strengthened by a study of Guillebault, showing Df31 binding to the H3 tail (Guillebault and Cotterill, 2007).

Genome-wide mapping studies show that Df31 is localized preferentially in euchromatic regions of the *Drosophila* genome (Filion et al., 2010). In this study Filion and co-workers defined five distinct chromatin types, denominated as Green, Blue, Black, Yellow and Green chromatin. Df31 was shown to localize with Red and Yellow chromatin that form two distinct types of euchromatin. Yellow chromatin contains widely expressed genes, whereas Red chromatin is restricted to more tissue specific regulated genes (Filion et al., 2010). The localisation at euchromatin supposes Df31 to act in the organisation of these open chromatin structures.

However, the mechanism by which Df31 is targeted to the euchromatic domains remains unclear. Possibly, Df31 recognizes a specific histone H3 modification pattern that is common to the RED and YELLOW chromatin types, or the protein could be co-recruited with other factors common to both chromatin types.

Furthermore, RNA could possibly target and recruit Df31 to the specific loci, as it is shown for other chromatin architectural proteins without sequence specificity. Recently, the RITS complex, which is involved in heterochromatin formation, was shown to be recruited to its target site via its bound, heterochromatin derived RNA. The RNA recognizes the binding sites and anchors the protein at the specific site via DNA-RNA hybrid formation (Nakama et al., 2012). Furthermore, the *de novo* methyltransferase DNMT3b was described being recruited to its targets via interaction with a promoter associated RNA (pRNA), forming a triple helix structure with the rDNA promoter region (Schmitz et al., 2010). Future experiments will address the mechanism of Df31 recruitment to euchromatic chromatin regions (perspectives).

The specific recruitment of Df31 to euchromatin argues against a global function of this protein in chromatin, but suggests the specific regulation of the accessibility of Red and Yellow chromatin. The knock down of Df31 resulted in a similar effect on chromatin accessibility as RNA depletion. But in contrast, only a twofold increase of cells containing compacted chromatin and only a minor fraction of the genome was rendered inaccessible towards MNase digestion (Figure 4.19). Possibly, the knock down of Df31 was not sufficient to reveal the

global functions of the protein. However, it is more likely that Df31, as its chromatin localisation indicates, is required to maintain specific euchromatic regions accessible. As only a subpopulation of the genome represents these types of chromatin, it is not surprising that MNase digestion kinetics revealed only a fraction of MNase resistant chromatin fragments in Df31 depleted cells. In summary, these findings indicate that Df31 and RNA act together in an RNP complex, playing a role in the organisation of euchromatic higher order structures.

5.4. Df31 specifically interacts with chromatin-associated snoRNAs

As Df31 and chromatin associated snoRNAs are both shown in this study to affect chromatin organisation, a possible interaction between the molecules was analysed. Microscale thermophoresis assays and electro mobility shift assays clearly showed that Df31 interacts with two highly enriched chromatin-associated snoRNAs (section 4.8.). Interestingly, competition assays with random RNAs demonstrated that Df31 preferentially binds to the chromatin associated snoRNAs, thereby discriminating random RNAs. Nevertheless, the existence of this RNP complex *in vivo* has to be clarified in further experiments in detail (see perspectives).

The experiments emphasize that Df31 and snoRNAs form RNP complexes *in vitro* and may regulate chromatin accessibility of specific genomic regions as RNP complex *in vivo*.

5.5. snoRNP mediated chromatin opening

This study identified and characterized a novel role for snoRNA molecules, showing that they stably interact with chromatin and mediate the opening of higher order structures of chromatin. snoRNA molecules are targeted to chromatin by specific RNA and histone binding proteins, like *Drosophila* Df31 identified in this study. It is proposed that these non-coding RNAs bind to larger genomic domains, targeted by Df31 that specifically recognizes euchromatic, genomic regions in order to maintain these regions accessible and active. It is

suggested that snoRNAs play an important role in nuclear architecture, being involved in opening and maintaining accessible higher order structures of chromatin.

However, the exact mechanism how snoRNAs and mediator proteins, as RNP complexes, regulate chromatin higher order structures remains elusive and needs further analyses (perspectives).

5.6. Potential snoRNP dependent mechanisms to maintain accessible chromatin

In general, six potential models can explain and contribute to the observations of snoRNAs and Df31 playing a role in maintaining specific chromatin regions accessible.

(i) The 30 nm fibre is stabilized by internucleosomal interaction, mainly the contact of histone H4 N-terminal domain (NTD) with a 'charge patch' on the surface of H2A, requiring direct interactions between the nucleosome (Dorigo et al., 2003; Dorigo et al., 2004). This study shows that Df31 interacts only weakly with H4 and may not directly bind to the H4 NTD. However, Df31 was shown to bind to the H3 tail in pull down experiments (Guillebault and Cotterill, 2007). As the H3 and H4 NTD are only separated by 3 superhelical turns on the nucleosome (Gordon et al., 2005), an interaction of Df31 and the H3 tail could disturb the H4 NTD interaction with the neighbouring nucleosome by steric hindrance and indirectly impair higher order folding of chromatin. In addition, the binding of the snoRNA through Df31 could also result in retargeting of the basic H4 NTD from the acidic H2A surface to the negatively charged backbone of the RNA molecule, thereby disturbing the stability by internucleosomal interactions. Such a mechanism could be envisioned as the basic Df31-snoRNA mechanism, since it was shown that histone NTDs do specifically bind to the sugar-phosphate backbone of DNA (Arya et al., 2006).

(ii) In addition, recent studies indicate that the H3 tail directly contributes to higher order structures of chromatin by stabilising of the 30nm fibre through interarray interactions (Kan et al., 2007; Zheng et al., 2005). These interarray interactions could be disturbed by either the direct binding of Df31 to the H3 tail

or the Df31 mediated interaction of the negatively charged snoRNA with the positively charged H3 tail. Both would lead to the loss of interarray interactions, resulting in disturbed higher order folding and decondensation of chromatin.

(iii) The linker histone H1 has a nearly stoichiometric abundance with the nucleosomes of eukaryotic genomes and stabilizes the intrinsic secondary chromatin structures formed by nucleosomal arrays (Gordon et al., 2005). Df31 also represents a highly abundant protein, displaying 0,1% of the total protein content in *Drosophila* embryos, which is comparable to H1 levels (Crevel et al., 2001). A competitive influence of Df31 on H1 chromatin binding sites, like HMG-box proteins (Catez et al., 2004), could explain the influence of Df31 on chromatin accessibility. Though, Df31 does not interfere with binding of this building block of compacted chromatin, as it does not displace H1 from *in vitro* reconstituted nucleosomal arrays (Guillebault and Cotterill, 2007).

(iv) Higher order structures of chromatin are influenced by histone modifications and ATP-dependent remodelling complexes. Df31 was shown to interact with Su(var3-9), which acts as H3K9 methyltransferase in heterochromatin formation. On the one hand, Df31 could bind Su(var3-9) and prevent histone H3K9 methylation, which is necessary for the HP1 mediated chromatin compaction (Schotta et al., 2003). On the other hand, the highly abundant Df31 may compete with Su(var3-9) for histone binding, as both proteins target the H3 tail.

The *Drosophila* ATP-dependent remodelling complex Iswi highly influences H1 dependent chromatin compaction. *Drosophila* Iswi is described to promote H1 assembly *in vivo*, resulting in heterochromatin formation (Corona et al., 2007) (Siriaco et al., 2009). Df31 may compete with H1 for Iswi binding and impair the assembly of H1 containing heterochromatin.

Both mechanisms would result in impaired heterochromatin formation and decondensation of the chromatin fibres.

(v) Two additional features of Df31 could contribute to its chromatin opening activity. First, it was shown that the protein contains histone chaperoning activity and second, the protein is capable to mediate interstrand bridging (Worby et al., 2001). Both activities could serve to generate irregularities in the chromatin, i.e. nucleosome free regions or

distorted fibres by folding and cross-linking of the fibre. These effects would disfavour the formation of regular higher order structures that are generally marked by regularly spaced nucleosomes, whereas euchromatin exhibits nucleosome free regions at regulatory sites and irregularly spaced nucleosomes (Mavrich et al., 2008). The histone chaperone function of Df31 would only affect the displacement or relocation of a small number of nucleosomes, as supercoiling assays and MNase assay did not reveal changes in histone loading and the quality of the nucleosomal array (section 4.2.).

(vi) Df31 dependent chromatin interstrand bridging comprises a possible mechanism explaining both snoRNA and Df31 controlled chromatin accessibility. This potential mechanism involves a RNP network, in which Df31 as basis may bind to more than a single snoRNA molecule. These stable RNA/protein complexes can crosslink different strands of chromatin by interacting with H3 tails on these strands. This net like structure may stabilize chromatin domains, leaving them open and accessible (Figure 5.1).

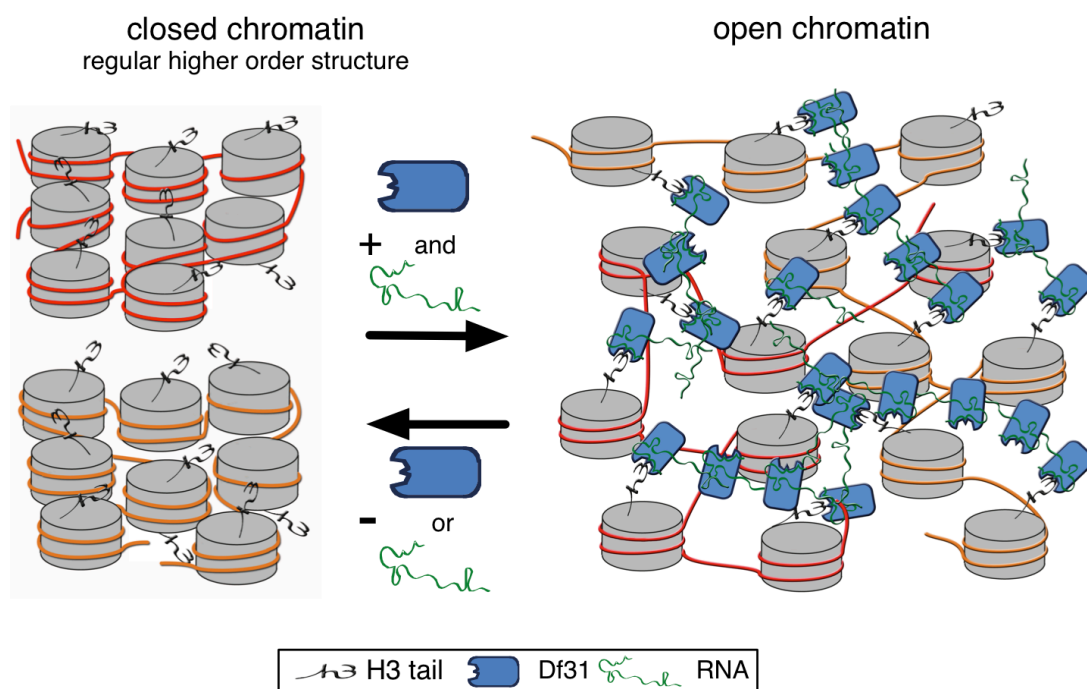


Figure 5.1: Working model how snoRNPs maintain accessible higher order structures of chromatin. The Df31-RNA complexes form a net-like structure, criss-crossing chromatin fibres, which is necessary to open up chromatin higher order structures.

In general the snoRNA could increase the local concentration of Df31. Possibly Df31 could oligomerize in presence of RNA and in this manner the interaction with chromatin is strengthened. Stable attached Df31 could then mediate chromatin accessibility by the aforementioned mechanisms, whereas all six mechanisms may contribute more or less to the maintenance of accessible chromatin. Future experiments need to address the mechanism in more detail (perspectives).

5.7. A conserved RNA-dependent mechanism regulates accessibility of chromatin domains

Several studies indicated that RNAs affect the chromatin structure in human cells lines, however the influence of RNA on chromatin accessibility remained unclear (Belgrader et al., 1991; Bouvier et al., 1985; Caudron-Herger et al., 2011; Ma et al., 1999; Nickerson et al., 1989).

The presented study investigated the role of RNA in the maintenance of chromatin accessibility in human HeLa cells (section 4.12.). Reminiscent to *Drosophila*, RNA depletion led to compacted, inaccessible chromatin structures. Furthermore, the same correlation between RNA amount and chromatin accessibility could be detected in HeLa cells. Interestingly, the accessibility of the ribosomal DNA locus, used as model system, was more affected by the depletion of RNA than the global chromatin (section 4.13.). In addition, polymerase II inhibition clearly decreased the accessibility of the global chromatin and of the rDNA locus. Again, the rRNA genes seem to be especially sensitive to alpha amanitin treatment, as compared to the general compaction of genomic DNA. Analysing the chromatin associated RNAs of different human cell lines revealed a high population of ncRNAs at human chromatin (section 4.11.). Reminiscent to *Drosophila*, snoRNAs were highest enriched at human chromatin compared to the transcriptome. In *Drosophila*, 40 out of 186 snoRNAs in the transcriptome exhibited an enrichment of over two fold compared to the transcriptome. This represents 21.5% of the snoRNA population, whereas in human fibroblast 8.2% of all snoRNAs in the transcriptome and in HeLa cells 37% of the snoRNAs in the nuclear transcriptome were found to interact with chromatin. Noteworthy, HeLa

nuclear RNA showed the potential to open *Drosophila* chromatin, implying a conserved mechanism to maintain accessible higher order structures of chromatin (section 4.7.).

In search for human homologues of Df31, bioinformatic analyses revealed the high mobility group protein HMGN5 as most promising candidate (section 4.14.). HMGN5 possesses high overall sequence identity to Df31, similar biochemical characteristics and both proteins are highly abundant in their respective organisms (section 4.15.). Reminiscent to Df31, HMGN5 is highly unstructured and disordered. Moreover, RNA binding predictions indicated HMGN5 to interact with RNA. Further experiments, performed in this study, including microscale thermophoresis identified HMGN5 to interact with RNA (section 4.16.).

Interestingly, HMGN5, as revealed by confocal microscopy, localizes to the nucleus and the nucleolus, the seat of rDNA transcription (section 4.15.). HMGN5, also known as nucleosome binding protein 1 (NSBP1), is described to localize to euchromatic regions. It is assumed that HMGN5 plays a role in maintaining these regions decondensed, thereby influencing transcription of several genes (Rochman et al., 2010; Shirakawa et al., 2009). A recent publication described the mechanism how HMGN5 maintains euchromatic regions (Rochman et al., 2009). HMGN5 is thought to interfere with H1 mediated chromatin compaction by binding to H1 and competing with H1 for chromatin binding sites. This mechanism impairs condensation of the chromatin fibre and supports open, accessible chromatin structures. Though, the targeting mechanism of HMGN5 to euchromatin remains unclear. Either HMGN5 recognizes active histone tail modifications or the task of recruitment is assigned to the RNA. HMGN5 could be targeted to euchromatin by chromatin associated RNA, being specific to these euchromatin regions.

To sum up, HMGN5 and Df31 are both present as RNP complex *in vitro* and may act together with chromatin-associated snoRNAs to maintain accessible higher order structures of chromatin *in vivo*.

This implies a highly conserved mechanism to regulate higher order structures of chromatin mediated by RNP complexes. Redundant with the RNP complexes characterized in this study, other caRNAs in complex with different binding/anchor proteins could influence chromatin structures of the genome.

This could create a great variety and diversity of RNP complexes, that potentially influence different parts of the genome and play major roles in the regulation of DNA-dependent processes in eukaryotic cells.

5.8. Perspectives

The presented study clearly demonstrated that chromatin associated RNAs play a key role in higher order structures of chromatin. snoRNAs were found being highly enriched at *in vitro* reconstituted chromatin compared to the transcriptome. However, further experiments have to proof this chromatin interaction *in vivo*. In this regard, cellular chromatin could be released by DNaseI treatment or sonication of isolated S2 cell nuclei. Chromatin associated RNAs, which are separated from free RNAs by sucrose gradient centrifugation, may be isolated and identified using high throughput sequencing. This experiment would provide important information about the *in vivo* association of snoRNAs to chromatin.

Df31 was shown in this study to influence chromatin structure as RNP complex. *In vitro* RNA binding studies indicated Df31 to bind to chromatin associated snoRNAs. However, the RNAs that are bound to Df31 *in vivo* are not detected by the *in vitro* approaches. Furthermore, RNAs with even higher affinity to Df31 could not be detected by these methods. A stable cell line, expressing Df31, (established in Axel Imhof's lab in Munich) could be used to pull-down and isolate Df31-bound RNAs. Moreover, ChIP assays using the novel Df31 antibodies, generated in this study, could help to isolate Df31-bound RNAs. These RNAs could be identified by RNA sequencing and the snoRNA/chromatin interaction could be proven. Further bioinformatic analyses would be able to reveal common motifs. In addition, bioinformatic approaches could expose evolutionary conservation of these RNAs across species. Moreover, the influence of these Df31 bound RNAs on chromatin higher order structures could be further characterized *in vitro*.

The knock-down of Df31 decreased the accessibility of chromatin *in vivo* as shown in this study (section 4.6). However the physiological relevance of the protein has to be shown. In this regard, gene expression of the stable cell line,

overexpressing Df31 and of Df31 knockdown cells could be compared to the gene expression of untreated S2 cells. This analysis will provide important insights into the influence of Df31 on gene expression.

A genome wide mapping study indicated Df31 being exclusively located to euchromatic regions (Filion et al., 2010). However, the mechanism, how Df31 is recruited to the euchromatic regions remained unclear. Either the Df31 bound RNA recruits the protein to the specific regions or Df31 recognizes H3 tail modifications that mark active chromatic regions.

With regard to an RNA-dependent recruitment of Df31 to euchromatin, previously identified Df31 bound RNAs could be transcribed *in vitro* and tested in pull-down experiments whether they target and recruit Df31 to reconstituted chromatin .

A possible mechanism dependent on histone tail modifications could be verified by a histone tail array. Differently modified histone tails are spotted on a microarray, which could recruit Df31 by high affinity binding. This experiment will expose putative Df31 recruiting histone modifications and reveal the mechanism of selective targeting of Df31 to chromatin regions.

The presented study suggests that the RNP complex, composed of Df31 and chromatin associated RNAs, maintains chromatin accessible. However, the exact mechanism how, the RNP complex acts, has to be characterized in more detail. The current working model supposes that Df31 binds to several snoRNAs and H3 tails simultaneously, thereby oligomerizing. This creates a net-like structure by crosslinking of chromatin fibres, which maintains chromatin accessible. A recent biochemical characterisation of Df31 suggested that Df31 acts as monomer (Szollosi et al., 2008). However, this *in vitro* study did not determine an RNA-dependent oligomerisation of the protein. The native blue gelelectrophoresis technique could exhibit an RNA-dependent oligomerisation of Df31.

Furthermore, analytical ultracentrifugation could reveal oligomeres of Df31, which correlate with the presence of RNA.

In addition, RNA may influence Df31 structure and function. Df31, as a disordered protein, could possibly adopt an ordered structure after binding to RNA. CD-spectroscopy could illustrate this RNA dependent conformational

change of Df31. Comparative *in vitro* histone and chromatin binding studies could further uncover if RNA is able to modulate Df31 binding properties. In order to characterize the domain structure of Df31, the RNA and histone binding regions should be identified. *In vitro* microscale thermophoresis binding approaches using the aforementioned truncation mutants could provide important information about the domain organisation of Df31.

To characterize the RNA mediated effect on chromatin structure in human, Df31 homologues have to be subsequently analysed in more detail. Bioinformatic analyses based on primary sequence, were performed to determine possible Df31 homologues. It resulted in a list of 10 potent structural homologues of Df31 in human. However, functional homology could not be revealed by bioinformatic analysis. However, the functional homology to Df31 may be depicted by knockdown experiments of the candidate homologues. In this regard, fluorescence microscopy and accessibility experiments could demonstrate possible influence of the homologues on chromatin structure, reminiscent to Df31. Furthermore the influence of these homologues on the accessibility of the model locus rDNA could be investigated.

HMGN5, the top candidate of Df31 homology, was shown in this study to interact with RNA. Yet, the specifically bound RNA could not be resolved, so far. In order to identify these specific RNAs, pull-down experiments using specific HMGN5 antibodies could be carried out to isolate the RNAs. High throughput sequencing would then expose the identity of the HMGN5 interacting RNAs.

As revealed by RNA high throughput analyses in *Drosophila* and human, snoRNAs are highly enriched at chromatin compared to the transcriptome. The direct functional analysis of these snoRNAs by knock-down experiments is complex, yet. A recent study demonstrated that conventional knock down techniques are not suitable for snoRNAs (Ploner et al., 2009). Due to RNP complex formation and the highly structured conformation of snoRNAs, the knock-down efficiencies of these techniques are limited. In addition, snoRNAs are frequently processed out of precursors, containing several snoRNAs, which renders knockdown of a single snoRNA impossible. Noteworthy, a novel

technique for small ncRNA knock-down, with possible impact on snoRNAs, was described recently (Liang et al., 2011). This novel technique could allow to specific knockdown of a single snoRNA, making a direct functional analysis of snoRNA molecules in chromatin structure possible. Finally, the described, novel functions of snoRNAs in the organisation of higher order structures of chromatin could be studied in detail with the help of this technique.

6. Materials and Methods

6.1. Materials

Unless otherwise stated, all common chemicals and materials were purchased from GE Healthcare (Freiburg), Merck (Darmstadt), Invitrogen (Karlsruhe), Fermentas (St. Leon-Rot), New England Biolab (Frankfurt am Main), Promega (Mannheim), Roche (Mannheim), Roth (Karlsruhe), Serva (Heidelberg), Bio-Rad (Munich), Stratagene/Agilent (Waldbronn) and Sigma-Aldrich (Munich). Radioactively labelled nucleotides were ordered at Hartmann Analytic (Brunswick).

6.1.1. technical devices

description	supplier
Gel dryer	Drystar
Agarosegel UV imaging system	GelMax, Intas
Sonifier 250	Branson
Chemiluminescence – Image Reader LAS-3000	Fujifilm
Centrifuge Centrikon T-324	Kontron Instruments
PCR machine	Peqlab
PCR machine veriti	Applied biosystems
PCR machine (old)	Perkin Elmer
Peristaltic– Pump LKB – P1	GE Healthcare
Real TIME PCR machine	Corbett Research, Rotor Gene ,RG-3000
Table top centrifuge	Eppendorf
Trans – Blot® SD Semi-dry transfer cell	BioRad
Thermomixer Compact	Eppendorf
Ultracentrifuge Centrikon T-1170,	Kontron Instruments
Optima™ L-80 XP	Beckman Coulter
Ultrospec 3100 pro	Amersham Biosciences

Uvikon Spectrophotometer 922	Kontron Instruments
Gradient Master™	BioComp
Monolith NT.115	Nanotemper technologies
Monolith NT.015T	Nanotemper technologies
Axiovert 200M + ApoTome 2	Zeiss
Qubit® 2.0 Fluorometer	Invitrogen
Nanodrop® ND – 1000 Spectrophotometer	peQLabBiotechnologie GmbH

6.1.2. Software tools

software	application	Supplier
Geneious	<i>in silico</i> cloning tool, organization software	Biomatters Ltd.
LabLife	lab organization tool	LabLife Software (www.lablife.org)
Multigauge V3.1	LAS reader viewer software	FujiFilm
Netprimer	primer design tool	Premiersoft (www.premierbiosoft.com)
OligoPerfect Designer	primer design tool	(http://tools.invitrogen.com)
Invitrogen		
Kaleidograph 4.1	graphical analysis software	Synergy software
RNAfold	RNA secondary prediction tool	(http://rna.tbi.univie.ac.at/cgi-bin/RNAfold.cgi)
RNApred	RNA secondary prediction tool	(http://www.imtech.res.in/raghava/rnapred/help.html)
RNABindR v2.0	RNA and protein parameter prediction tool	(http://einstein.cs.iastate.edu/RNABindR/)
Galaxy	high throughput sequencing analysis tool	(http://galaxy.psu.edu/)
Axiovision	Zeiss microscope software	Zeiss

UCSC Genome Browser	genome viewer	(http://genome.ucsc.edu/ENCODE)
VectorNTI V10	<i>in silico</i> cloning tool, organization software	Invitrogen
NEB double digest finder	restriction digest organization tool	New England Biolabs (www.neb.com)
Reverse Complement	nucleic acid reverse complement tool	Reverse Complement (www.Bioinformatics.org)
SMART	modular protein domain prediction tool	http://smart.embl-heidelberg.de/smart/change_mode.pl
Paralign	aa alignment tool	http://www.paralign.org/
Functional RNA project, Centroid fold	function database, RNA secondary prediction tool	http://www.ncrna.org/
Blast	comparative alignment and search tool	http://blast.ncbi.nlm.nih.gov/Blast.cgi
BindN	RNA/DNA binding residue prediction tool	http://bioinfo.ggc.org/bindn/
Protparam	protein parameter analysis tool	http://web.expasy.org/protparam/
MAFFT	aa alignment viewer	http://mafft.cbrc.jp/alignment/server/
RPISeq	protein-RNA interaction prediction tool	http://pridb.gdcb.iastate.edu/RPISeq/
PiRaNhA	RNA binding residue prediction tool	http://www.bioinformatics.sussex.ac.uk/PIRANHA/

6.1.3. Chemicals and consumables

Description	Supplier
1.5 ml and 2 ml micro centrifuge tubes	Eppendorf
15 ml and 50ml tubes	Sarstedt
Agarose (ME, LE GP and low melting)	Biozym
Ammonium acetate	Merck
ATP	Sigma
α - ³² P-ATP (300Ci/mmol)	Hartmann Analytic
γ - ³² P-ATP(300Ci/mmol)	Hartmann Analytic
Bacto Agar	BD
Bacto Peptone	BD
Bacto Tryptone	BD
Barrier food wrap	Saran
Blue Gal	Invitrogen
Boric acid	Merck
Bradford Reagent	BioRad
Bromphenolblue	Serva
BSA 98%	Sigma
BSA purified	NEB
β -Mercaptoethanol	Sigma
Chloroform solution	Merck
Cellculture flasks	Greiner
Concentration tubes Microsep 10K,30K	Omega
Coomassie G250	Serva
Cryovials	Roth
dCTP, dGTP, bio dATP, bio dUTP	Invitrogen
Dialysis membrane	Spectra/Por, Roth
DMSO	Sigma
dNTP mix	NEB
DTT	Roth
Dynabeads M280-Straptavidin	Dynal, Invitrogen
EDTA	Sigma

EGTA	Sigma
Ethidium bromide	Sigma
ETOH tech., p.a.	Merck
FCS dialyzed	Sigma
Filter paper Whatman 3MM	Whatman
Filter tips	Roth
Filter unit	Nalgene, 0.2 µm filter holes
Glass pipettes 5 ml and 10 ml	Hirschmann®
Glassware	Schott
Glycerin	Merck
Glycogen	Roche
HEPES	Roth
Hiload 16/60 Superdex 200 gel filtration column	GE Healthcare
IPTG	Roche
Isopropanol p.a.	Merck
Laboratory film	Parafilm®
Magnesium chloride	Merck
Methanol p. a.	Merck
Nickel-NTA-agarose (Ni ²⁺ -beads)	Quiagen
Nitrocellulose membrane (GSWP, 0,22µM)	Millipore
NP40	Sigma
Orange G	Sigma
Pasteur pipettes	Brand
PCR-reaction tubes 0.2 ml	Biozym
Petridishes and tissue culture plates	Greiner, Sarstedt
Phenol solution	Merck
Pipette tips	Gilson, Brand
PMSF	Sigma
Potassium chloride	Merck
Propidium iodide	Sigma
Protein gel cassettes (disposable)	Invitrogen

Quick spin columns (Sephadex 50)	Roche
Random primer	Promega
Rotiphorese Acrylamid- Bisacrylamidmix	Roth
SDS	Serva
β-Mercaptoethanol	Sigma
Sephacryl 300HR	Sigma
Siliconized 1,5ml reaction tubes	BioRad
Sodium chloride	VWR
Sodium dodecyl sulfate (SDS)	Roth
Sybr Safe	Invitrogen
Syringes and accessories	Roth
TEMED	Roth
Thymidine	Sigma
Tris	Invitrogen
Triton X-100	Sigma
Trypsin/EDTA (TC)	PAA
Tween 20	Sigma
Ultracentrifugation tubes for SW40 rotor	Beckman Coulter
Yeast extract	BD

6.1.4. Standard Solutions

Stock solutions and buffers were made according to standard protocols [Sambrook and Russell, 2000; LabFAQS, 2010]. Protease Inhibitors (Leupeptin 0.5 µg/ml, Pepstatin 1 µg/ml, Aprotinin 1 µg/ml and PMSF 0.5mM) were freshly added. Common solutions are listed below.

Buffer	Composition
AE buffer	50mM NaAC pH 5.3 10mM EDTA
EX-X buffers	20mM Tris-HCl pH 7.6

	1.5mM MgCl ₂
	0.5mM EGTA
	10% glycerol
	XmM KCl
	pH adjusted to 7.6 with HCl
Phosphate Buffered Saline (PBS)	140mM NaCl
	2.7mM KCl
	8.1mM Na ₂ HPO ₄
	1.5mM KH ₂ PO ₄
	pH adjusted to 7.4 with HCl
TBE-buffer	90mM Tris
	90mM Boric acid
	2mM EDTA
Southern blot denaturation solution	0.5M NaOH
	1.5M NaCl
Southern blot ammonium acetate solution	1 M NH ₄ Ac
TE buffer	10mM Tris-HCl pH 7.6
	1mM EDTA
DNA sample buffer (10x)	50% glycerol
	50mM Tris-HCl pH 7.6
	10mM EDTA
	0.05% (w/v) bromophenol blue, xylene cyanol and Orange G
Orange G loading dye (10x)	50% 129glycerine
	10mM EDTA
	0.05% (w/v) Orange G
SDS-protein sample buffer (5x)	300mM Tris-HCl pH 6.8
	10% (w/v) SDS
	50% glycerol
	5% β-Mercaptoethanol
	0.2% (w/v) bromphenol blue
SDS-PAGE stacking buffer (4x)	0.5 M Tris-HCl

	0.4% SDS, pH 6.8 with HCl
SDS-PAGE separating buffer (4x)	1.5M Tris-HCl 0.4% SDS, adjust to pH 8.8 with HCl
SDS-PAGE running buffer	192mM glycine 25mM Tris 0.1% (w/v) SDS
HU buffer	5% SDS 200 mM Tris pH 6,8 1 mM EDTA 8 M urea bromphenolblue 5% β -Mercaptoethanol
Coomassie staining solution	45% water 45% methanol 10% acetate acid
Silver staining fixing solution	50% methanol 12% acetate acid 0.05% formaldehyde 37%
Silver staining wash solution	50% ethanol p.A.
Silver staining pre-incubation solution	20% (w/v) Na ₂ S ₂ O ₃
Silver staining stain solution	0.2% (w/v) AgNO ₃ 0.075% formaldehyde 37%
Silver staining developing solution	6% (w/v) Na ₂ CO ₃ 0.05% formaldehyde 37% 0.5% (w/v) Na ₂ S ₂ O ₃
Silver staining stop solution	1% acetate acid
High salt buffer for chromatin assembly	10mM Tris/HCl pH 7.6 2M NaCl 1mM EDTA 0.05% NP40 1mM β -mercaptoethanol

Low salt buffer for chromatin assembly	10mM Tris/HCl pH 7.6 50mM NaCl 1mM EDTA 0.05% NP40 1mM β -mercaptoethanol
McNap buffer	30mM ATP 300mM Creatin Phosphate 30mM MgCl ₂ 100ng/ μ l Creatin Kinase 10mM DTT
Nuclease sensitivity permeabilisation buffer	15mM Tris/HCl 300mM Sucrose 60mM KCl 15mM NaCl 3mM CaCl ₂ 1,5mM MgCl ₂ 0,5mM EGTA 0,2% (v/v) NP40 0,5mM β -ME
Nuclease sensitivity stop buffer	50mM Tris/HCl 20mM EDTA 1% SDS 2,5 μ l RNase A (10mg/ml), 1h incub 37°C 2,5 μ l PK (10mg/ml)
TFBI	30mM KAc50mM MnCl ₂ 100mM KCl 15% Glycerine Fill up to 500ml with water Adjust pH to 5,8 with acetic acid (0,2M)
TFBII	10mM MOPS 75mM CaCl ₂ 10mM KCl

	15% Glycerine
	Fill up to 100ml
	Adjust pH to 7,0 with NaOH
Lysis buffer His purification	EX300
	Protease inhibitor Mix (PI) (Lev 1:2000, 1:1000 Apro, 1:1000 Pep, 1:500 PB)
Wash buffer His purification	Ex300
	20mM Imidazol
	Protease inhibitor Mix
Elution buffer His purification	Ex300
	250mM Imidazol
	Protease inhibitor Mix
Lysis buffer GST purification	PBS
	1mM TCEP
	0,5% TritonX – 1000
	Protease inhibitor Mix
Wash buffer GST purification	PBS
	1mM TCEP
	0,5% Triton X – 1000
	Protease inhibitor Mix
Elution buffer GST purification	20mM Tris, pH 8.0
	20mM Glutathione
	Protease inhibitor Mix

6.1.5. Enzymes

Enzyme	Supplier
Antarctic Phosphatase	New England Biolabs
iProof DNA polymerase	Bio-Rad
Klenow enzyme	New England Biolabs
Micrococcus Nuclease (MNase)	Roche, Invitrogen
Proteinase K	Sigma

PfuUltra II Fusion DNA Polymerase	Agilent
Restriction endonucleases	New England Biolabs
Rnase A	Roche, Invitrogen
Rnase H	Roche
Rnase T1	Invitrogen
T7 RNA Polymerase	New England Biolabs
DNase I	Roche, Worthington

6.1.6 Kits

Kit	Supplier
Plasmid purification Kit	Qiagen
Plasmid isolation Kit	Qiagen
QIAquick PCR purification Kit	Qiagen
Pure Link™ QUICK Plasmid Miniprep Kit	Invitrogen
Pure Link™ HiPure Plasmid Maxiprep Kit	Invitrogen
QIAEX® Gel Extraction Kit	Qiagen
Super signal WEST Dura WB Kit	Pierce

6.1.7. Standard DNA, RNA and protein marker

2log DNA ladder	NEB
100 bp DNA ladder	NEB
10bp ladder	Invitrogen (10821-015)
Gene Ruler, ultra low range	Fermentas (SM1211)
Gene Ruler 1kb plus DNA ladder	Fermentas (SM1333)
Pre-stained Protein – Marker IV	Peqlab
Pre-stained protein marker page ruler	Fermentas
RiboRuler low range	Fermentas

6.1.8. Protease inhibitors, RNase inhibitors and antibiotics

Substance	supplier
Aprotinin bovine	Genaxxon
Ampicillin	Sigma
Leupeptin hemisulfate	Genaxxon
Pepstatin A	Genaxxon
Chloramphenicol	Roth
RNasin	Promega
Penicillin/Streptomycin	Invitrogen/ Gibco
Protease Inhibitor Cocktail	Roche

6.1.9. Bacterial cell lines and media

strain	description	resistance	genotype
DH5alpha	general DNA plasmid propagation	none	F- ϕ 80lacZ Δ M15 Δ (lacZYA-argF) U169 endA1 recA1 hsdR17 (rk-,mk+) supE44 thi-1 gyrA96 relA1 phoA
TOP10	general DNA plasmid propagation	streptomycin	F- mcrA Δ (mrr-hsdRMS- mcrBC) ϕ 80lacZ Δ M15 Δ lacX74 nupGrecA1 araD139 Δ (ara- leu)7697galE15 galK16rpsL(StrR) endA1 λ -
XL1 Blue	F' episome, general DNA plasmid propagation, blue/ white screening	tetracycline	recA1 endA1 gyrA96 thi-1 hsdR17 supE44 relA1 lac [F'proAB lacIqZDM15 Tn10 (Tetr)]

BL21 (DE3) placI	Protein expression	none	F-ompT gal hsdSB (rB- mB-) dcm lon λDE3
GM2929	general DNA plasmid propagation, methylation negative	none	araC14, leuB6(Am), fhuA13, lacY1, tsx-78, glnV44(AS), galK2(Oc), galT22, λ ⁻ , mcrA0, dcm- 6, hisG4(Oc), rfbC1, rpsL136(strR), dam- 13::Tn9, xylA5, mtl-1, recF143, thi-1, mcrB9999, hsdR2

Luria-Bertani (LB) medium

1.0% (w/v) Bacto-Tryptone

1.0% (w/v) NaCl

0.5% (w/v) Bacto-Yeast extract

→ Adjust the pH to 7.0 with 10 M NaOH

The medium was autoclaved for 20 min at 120°C and after cooling down to 60°C the appropriate antibiotics was added. For preparing plates the LB medium was mixed with 1.5% agar.

SOB medium

2% (w/v) Bacto-Tryptone

10 mM NaCl

0.5% (w/v) Bacto-Yeast extract

2.5 mM KCl

10 mM MgCl₂*

→ Adjust the pH to 7.0 with 10 M NaOH

* add before use

The medium was sterilized in an autoclave for 20 min at 120°C.

6.1.10. Eukaryotic cell lines and media

name	description	source	growth conditions	remarks
HeLa cells	Human cervix carcinoma	DSZM No: ACC 57; from A. Nemeth	37°C, 5% CO ₂ ; DMEM + glutamax, 10% FBS	human hypertriploid/ hypotetraploid karyotype with 15% polyploidy; epithelial-like cells growing in monolayers; 25- 30h doubling time
Schneider S2 cells	<i>Drosophila</i> Primary cell line late embryo, macrophage like cell line	Prof. Dr. Axel Imhof, LMU Munich	26-27°C, Schneider Medium, +10%FCS +1%Pen/Strep +15% Glutamine	Doubling time 20-25h, confluent growth
Schneider S2R+ cells	<i>Drosophila</i> Primary cell line late embryo, macrophage like cell line	Prof Dr. Frank Sprenger, University of Regensburg	26-27°C, Schneider Medium, +10%FCS +1%Pen/Strep +15% Glutamine	Doubling time 20-25h, wnt knock out → adherent growth

HeLa medium

450ml	DMEM
50ml	FBS (aliquoted in -20, 10% total)
5ml	1:100 Penicillin-Streptomycin (aliquoted in -20, 1% total)

Aliquot into 50ml falcons

Store at 4°C - do not freeze

S2, S2R+ Cell medium

420 ml	Schneider's medium
50 ml	Fetal Bovine Serum (aliquoted in -20)
5 ml	1:100 Penicillin-Streptomycin (aliquoted in -20)
33.3ml	l-Glutamine (200mM stock) (aliquoted in -20)
500ml	

Aliquot into 50ml falcons

Store at 4°C - do not freeze

6.1.11. Antibodies

antibody	source	species	application	comment
B23	Sigma	mouse	IF 1:500	Monoclonal
HMG5	Abcam	rabbit	IF 1:500	polyclonal
(NSBP1)				
Anti His-HRP india	Pierce	---	WB 1:5000	Use BSA instead of milk powder for blocking Nr. 86
anti His	Qiagen	mouse	WB, use at 1:3000 dilution	monoclonal Nr. 101
Goat anti	Jackson	Goat	IF	

rabbit Cy3			1:200	
F(ab') ₂				
Goat anti	Molecular	Goat	IF	Nr. 95
mouse	probes		1:500	
Alexa488				
F(ab') ₂				

6.1.12. Oligonucleotides

Unmodified Oligonucleotides:

List of all oligonucleotides used in this study, purchased from Eurofins MWG Operon and diluted with MilliQ-water to a final 100µM solution. Oligonucleotides for PCR amplification and sequencing reactions were designed to show a minimum of secondary structure, primer dimerization and with a melting temperature T_m of 60°C with the freely available *netprimer* software provided by *premierbiosoft*. Oligonucleotides used for cloning, sequencing and colony PCRs are deposited on the Längst account on addgene (www.lablife.org) and named TSP (number).

name	application	use in application	sequence
	snoRNA in vitro		GTGTGTATTAGAATATG
TSP_46	txn	snoRNA M rev	GTGTATCTAT
	snoRNA in vitro		TAATACGACTCACTATA
TSP_45	txn	snoRNA M for	GGAATTCAATGATTTC
	snoRNA in vitro		ACTTCAC
TSP_44	txn	snoRNA g980 for, rev = TSP_30	TAATACGACTCACTATA
	snoRNA in vitro		GGGCTAGCGTGATGAGT
	txn		TTATTAC
TSP_43	txn	snoRNA U2134b for, rev = TSP_28	TAATACGACTCACTATA
	snoRNA in vitro		GGAGTTCCATGATGTTT
	txn		TCAAACCTCT

TSP_42	cloning	H4 tail EGFP rev NdeI into pt7 blue EGFP	TATCCATATGACGGCGA ATCGC
TSP_41	cloning	H4 tail EGFP for HindIII into pt7 blue EGFP	CGCGAAGCTTCCATGGA TTCTGGGCGAGGTAAG
TSP_40	cloning	H3 tail EGFP rev NdeI into pt7 blue EGFP	TATCCATATGCTTCACA CCTCCGGTGGCT
TSP_39	cloning	H3 tail EGFP for HindIII into pt7 blue EGFP	CGCGAAGCTTCCATGGA GGCTCGTACCAAGCAA GTATCTCAAAGATACAA
TSP_38	qPCR	CG42238 RA as control rev	TGAACACAG
TSP_37	qPCR	CG42238 RA as control for	GATCGACAGCAGGCAGG CTGCTCCTGGGGATCCA
TSP_36	qPCR	mRNA tophit CG15550 rev 2	T CAGGCTAAGCCCTCCGT
TSP_35	qPCR	mRNA tophit CG15550 for 2	TT GATGGCGATTGGCCATG
TSP_34	qPCR	mRNA tophit CG15550 rev	AAGT TCACTGGAATCCATACC
TSP_33	qPCR	mRNA tophit CG15550 for	CACC GCGATTCCCACGGCCAG
TSP_32	qPCR	snoRNA host CG13900 rev	GTA GTACC AGTGTGCCGCTCACCCA
TSP_31	qPCR	snoRNA host CG13900 for	AAA CGA CTGGTCAGCAGTGAAGT
TSP_30	qPCR, snoRNA in vitro txn	snoRNA MeS28 G980 rev	TGA GCTAGCGTGATGAGTTT
TSP_29	qPCR	snoRNA MeS28 G980 for	ATTAC CCTCTCAGTTATGTTTT
TSP_28	qPCR, snoRNA in vitro txn	snoRNA MeS28 U2134b rev	GTT AGTTCCATGATGTTTTTC
TSP_27	qPCR	snoRNA MeS28 U2134b For	AAACTCT CCGGGGTCGACGGCGGC
TSP_26	cloning	N-Flag DF31 SalI rev into pET11 NsiI MF1	CACTTCGCTAG

			GATAAGGGTACCGAAA
TSP_25	cloning	N-Flag TEV DF31 KpnI for into pET11 NsiI MF1	ACCTGTATTTTCAGGGC GCTGATGTGGCTGAGCA AAAAAGATCGATTTAG GCGGCCACTTCGCTAGC
TSP_24	cloning	his-DF31 ClaI rev into pTriEx	CTCGG ATATACCATGGCACACC ACCATCACCATCACCAT CACGCTGATGTGGCTGA
TSP_23	cloning	his-DF31 NcoI for into pTriEx	GCAAAAG TCGACGCTCGAGGCCCT GAAAATACAGGTTTTCA GCATCTGTTGAGTCACC
TSP_22	cloning	DF31 dC133 rev / + SDP -71	GTTGGT TAGCAGTCGACTTACTT
TSP_21	cloning	GST H3 rev, amplify on MF81	CACACCTCCGGT AGCCTGGATCCGCTCGT
TSP_20	cloning	GST H3 for, amplify on MF81	ACCAAGCAAAC CTCGAGGCCCTGAAAAT ACAGGTTTTCTCTTTT
TSP_19	cloning	DF31 dC109 his rev / +SDP- 71	TTGGTGTCTCCCCTCT AAC CTCGAGGCCCTGAAAAT ACAGGTTTTTCATCGGCG GCAAAAGAAACAGTGG
TSP_18	cloning	DF31 dC86 his rev / +SDP71	GCT
TSP_17	cloning	EGFP n-Tag BsrGI for HMGN5 n-term	AGCTGTACAAGGAAGTA AAAGAAGAAAATA
TSP_16	cloning	EGFP n-Tag BsrGI for HMGN5 WT and c-term	AGCTGTACAAGCCCCAAA AGAAAGGCTGCA
TSP_15	cloning	EGFP n-Tag BsrGI for DF31 n-term	GCTGTACAAGAAGGCGT CTGAGCCCAC
TSP_14	cloning	EGFP n-Tag BsrGI for DF31	GCTGTACAAGGCTGATG

		WT and c-term	TGGCTGAGCAA
			CATGCCATGGTCTTGTA
TSP_13	cloning	EGFP n-Tag NcoI rev	CAGCTCGT
			CATGCCATGGTGAGCAA
TSP_12	cloning	EGFP n-Tag NcoI for	GGGCGA
			ACCATGGTGAGCAAGGG
TSP_11	cloning	EGFP-his protein NcoI for	CGA
			AGATCGATTTAGTGATG
			GTGA
		EGFP c-Tag ClaI rev, +his-Tag	TGGTGATGGTGGTGCTT
TSP_10	cloning	/ EGFP-his protein ClaI rev	GTAC AGCTCGTC
			ATACTCGAGGTGAGCAA
TSP_9	cloning	EGFP c-Tag ClaI rev, -his-Tag	GGGC GA
			AGATCGATTTACTTGTA
TSP_8	cloning	EGFP c-Tag XhoI for	CAGC TCGTCC
	sequencing		GAGTGAGAGACACAAA
TSP_7	pTriEx, cloning	sequencing	AA ATT CCA
			CTCGAGTTCATCTTCTT
TSP_6	cloning	HMGN5 dC243 XhoI rev	TTCC ATCTT
			CTCGAGTCCTGTTTCTT
TSP_5	cloning	HMGN5 dC206 XhoI rev	TTCT GTCTT
			CTCGAGCTCTTTTCCAT
TSP_4	cloning	HMGN5 dC160 XhoI rev	CTTC TTCC
			CATGGAAGTAAAAGAA
TSP_3	cloning	HMGN5 dN84 FatI for	GAAAA TATTG
			CTCGAGAACAATACTCT
TSP_2	cloning	HMGN5 Wt// dN84 XhoI rev	GTGGC
			CATGCCCAAAGAAAGG
TSP_1	cloning	HMGN5 WT//dC160 FatI for	CTGCA
			GAGCTGCATGTGTCAGA
LP5	Sequencing pGex	pGEX rev standard	GGTTT
	Sequencing	T7 promoter/lac Operator	AATACGACTCACTATAG
LP9	pTriEx	for	GGGAATTGT

	Sequencing pT7		GTTTTCCCAGTCACGAC
LP15	blue	M13 for(-40)	GTTG
	Sequencing		CTAGTTATTGCTCAGCG
LP21	pTriEx	T7 terminator rev	G
	Sequencing pT7		CAAGCTCTAATACGACT
LP26	blue	T7 Promoter long	CACTATAGGG
DF31_			ACTGTTTCTTTTGCCGC
qPCR for 1	qPCR DF31		C
DF31_			CTTCGCTGCTCTCTTTT
qPCR rev 1	qPCR DF31		TTG
DF31_			TGACTCAACAGATGCTC
qPCR for 2	qPCR DF31		CC
DF31_			CCCCATTCTGAACCTCA
qPCR rev 2	qPCR DF31		TCC

Modified Oligonucleotides:

name	application	Modification	sequence
snoRNA U2134b			AGUUCCAUGAUGUUUUCAAACUCUAU
part1	MST	5'FAM	UACCUACAUAUUUUGAAC
snoRNA U2134b			GAGAAACCGUGUAAACAAAACUAACU
part2	MST	5'Cy5	GAGAGG
			GAGUUUAUUACUAAUCUUUCGGGUUAU
snoRNA G980 part1	MST	5'FAM	GAAAUUC
			GCUAGCGUGAUAAUGAUUUCAACUUC
snoRNA G980 part2	MST, EMSA	5'Cy5	ACUGCUGACCAG
			CCUCCUUUUUUCUUUUUUUUUUUUU
En3	MST	5'FAM	UUUCU
			UUGUCAGGGUCGACCAGUUGUUC
Sal box	MST	5'Cy5	UUUGAG
			AAAAAAAAAAAAAAAAAAAAAAAAA
Poly A	MST	5'Cy5	AAAAA
			CGGAGGCCCAACCTCTCCGACGACAGGT
5'ETS rDNA probe	Southern blot	radioactive	CGCCAGAGGACAGCGTGTGACG

6.1.13. plasmids

Name	application	number	Created by
pRSet DNMT1 human aa 530-830 BamH1	<i>in vitro</i> chromatin assembly		Max Felle
pTriEx DF31 WT	protein production		Geneart
pMK-T DF31 WT	subcloning		Geneart
pTriEx DF31 1 times ATG WT	protein production		Sarah Diermeier
pMT-Hygro DF31 N-Flag	Stable cell line creation		Sarah Diermeier
pMT-Hygro DF31 N-Myc	Stable cell line creation		Sarah Diermeier
pTriEx DF31 Δ N86	protein production		Sarah Diermeier
pTriEx DF31 Δ C109	protein production		Thomas Schubert
pTriEx DF31 Δ C 157	protein production		Sarah Diermeier
pTriEx DF31 Δ N75 Δ C157	protein production		Sarah Diermeier
pTriEx DF31 Δ 46-168	protein production		Sarah Diermeier Thomas Schubert
pTriEx DF31-EGFP	protein production		Thomas Schubert

pTriEx EGFP	protein production	Thomas Schubert
pGEX-4T3 H3 1-36aa	protein production	Thomas Schubert
pGEX H4 1-41	protein production	Thomas Schubert
pTriEx HMGN5 WT	protein production	Thomas Schubert
pTriEx HMGN5 Δ N84	protein production	Thomas Schubert
pTriEx HMGN5 Δ C160	protein production	Thomas Schubert
pTriEx HMGN5 Δ C206	protein production	Thomas Schubert
pTriEx HMGN5 Δ C242	protein production	Thomas Schubert
pT7 blue U2134b	snoRNA <i>in vitro</i> txn	Thomas Schubert
pT7 blue G980	snoRNA <i>in vitro</i> txn	Thomas Schubert

6.2. Methods

Preparation and transformation of chemically-competent bacteria with DNA, amplification of plasmid DNA in *E. coli* bacteria, purification, concentration determination, restriction enzyme digestion, ligation of DNA fragments, analysis of DNA on agarose and polyacrylamide gels, and amplification of the DNA by the polymerase chain reaction (PCR) was performed according to the standard protocols [Sambrook and Russell, 2000]. Bacteria were cultured in Luria-Bertani

medium [Bertani, 1951] and selective antibiotics were added corresponding to the plasmid encoded resistance. Plasmid DNA was isolated with plasmid purification kits (Invitrogen/Qiagen). Isolation of DNA fragments from agarose gels was performed using the Qiagen Gel Extraction kit.

6.2.1. Working with DNA

6.2.1.1. Determination of RNA and DNA quality and quantity

The DNA concentration of single and double stranded DNA was determined by absorption measurement at 260nm using a NanoDrop ND1000 spectrophotometer (Pecolab). Protein impurities could be determined by absorption measurement at 280nm and the ratio A₂₆₀/A₂₈₀. DNA impurities were determined by electrophoretically separation of DNA fragments using 0.8 - 2.0% (w/v) agarose gels in 1x TBE supplemented with 0.01% SybrSafe. Qbit measurements were also used to measure DNA, RNA amounts. The technique is based on the use of specific dye that emit light only when bound to their specific partner.

6.2.1.2. DNA precipitation with ammonium acetate

DNA fragments were precipitated from the supernatant by adding 1/3 volumes of 7.5 M ammonium-acetate (pH 7.7) and 2.5 volumes of 100% ethanol, vortexed briefly and incubated on ice (10min). Precipitates were pelleted (4°C, 13000g, 15-30min.), washed with 70% ethanol and dissolved in an appropriate volume in either MilliQ or TE-buffer. For visualization glycogen can be added (2µl of a 20mg/ml solution). The ammonium acetate precipitation reduces the co-precipitation of dNTP's and oligonucleotides. It is not suitable for subsequent polynucleotide kinase (PNK) reactions.

6.2.1.3. Polyacrylamide and agarose gel electrophoresis

Agarose gel electrophoresis was generally performed with gels containing 0.8 - 1.2% agarose in 1X TBE buffer, 1:10000 SYBR Safe (Invitrogen), in 1x TBE running buffer at a constant voltage of 100-120V. DNA standard marker and samples were supplemented with 10x DNA loading dye. In contrast to agarose gel electrophoresis, DNA was separated by polyacrylamide gel electrophoresis

(PAGE) in 0.4 X TBE at 4°C at 100V. In order to remove unpolymerized acrylamide the gel was prerun for 1 hour at 80V. For visualization the gel was stained after the gel run in 0,4x TBE containing ethidiumbromide (0,5mg/ml) for 15min and washed twice with water for 10min each.

6.2.1.4. Radioactive body labelling of DNA

For radioactive labelling of longer DNA sequences radioactive γ -32P-dATP was added to a standard PCR reaction. 50 μ l reaction volume contained 100 ng template DNA and of 500nM of each primer, 100 μ M of dCTP, dGTP and dTTP, 20 μ M dATP and 16.7nM γ -32P-dATP. Random amplification using Prime-a-gene Labelling System (Promega) with Klenow Fragment and random primer was used according to manufacturer's protocol. In general non-incorporated nucleotides were separated from labelled DNA using spin columns prepacked with Sephadex G-50 (GE Healthcare). Labelling efficiency was measured by scintillation counter.

6.2.1.5. Radioactive end labelling of DNA

Short DNA sequences, especially oligonucleotide probes for southern blotting, were radioactively labelled with T4 polynucleotide kinase. A standard reaction in 1x T4-PNK buffer contained 0.66pM oligonucleotide, 10 units enzyme (NEB) and 90 μ M α -32P-dATP in 15 μ l total volume. After 45 min incubation at 37°C reaction was stopped by adding 5 μ l 0.2M EDTA and 50 μ l H₂O. Non-incorporated nucleotides were separated from labelled DNA using spin columns prepacked with Sephadex G-50 (GE Healthcare). Labelling efficiency was measured by scintillation counter.

6.2.1.6. Restriction digest

Restriction enzymes were used at reaction conditions according to the manufacturer's recommendations concerning buffer, addition of BSA and temperature (see www.neb.com). For the analytical digest 0.1 - 1 μ g DNA was incubated with 5 units of the respective restriction endonuclease in a total volume of 20 μ l. The preparative restriction digest was done with 15 μ g DNA using 60 units restriction endonuclease in a total volume of 60 μ l. The large scale

digest, especially for nucleosome assembly, was done with 300 µg DNA using 150 units restriction endonuclease in a total volume of 150 µl. To check the completion of the digest, DNA was electrophoretically separated using 0.8 - 2.0% TBE-agarose gels supplemented with SYBR Safe (Invitrogen).

6.2.1.7. DNA ligation

DNA – fragments with sticky or blunt ends can be ligated with the T4 DNA ligase (NEB). The molar insert to vector ratio was usually between 3 and 5. The ATP containing 2x ligase buffer was stored in aliquots at -20°C. The ligation reaction was performed in a styrofoam box at 4°C overnight.

6.2.1.8. Polymerase Chain Reaction

50 µl		1 x (µl)
Primer for	10µM	1
Primer rev	10µM	1
dNTP's	10 mM	1
Taq-Puffer	10x	5
Taq-Polymerase		1
template		50-100ng
H2O		fill up to 50
Total volume		50

cycle step	temperature	time	number of cycles
initial denaturation	94	4min	1
denaturation	94	30sec	

annealing	55-58	30sec	30-32
extension	72	1min/1kb	
final extension	72	5min	1

It is recommended to include a “water” and “positive” control.

6.2.1.9. Colony PCR

Colony PCR is a fast and quick method to screen for positive clones after DNA ligation. A pipette tip was dipped into a bacterial colony on an agar plate that was to be tested for the presence of the insert. The adhering cells were resuspended in 25µl water in a 0,2ml PCR tube and subsequently gridded on fresh LB plates containing the necessary antibiotics. All tubes were placed in the PCR cyclor and cells lysed by heating to 100°C for 10min. Then, 25µl of colony PCR master mix were added to each tube in the PCR cyclor, and the thermocyclor program for colony PCR was started. Afterwards, the PCR reactions were analysed on an agarose gel for presence of the amplicon.

50 µl		1 x (µl)
Primer for	10µM	0,5
Primer rev	10µM	0,5
dNTP's	10 mM	1
Taq-Puffer	10x	5
Taq-Polymerase		1
H2O + colony		25
H2O		17
Total volume		50

cycle step	temperature	time	number of cycles
initial denaturation	94	5min	1
denaturation	94	40sec	
annealing	55-57	40sec	35
extension	72	1min/1kb	
final extension	72	5min	1

It is recommended to include a “water” and “positive” control.

6.2.1.10. Southern blotting

Partially MNase digested chromatin from HeLa cells was purified and DNA fragments were electrophoretically separated on a 14 x 21 cm 1% agarose gel in 1x TBE supplemented with 0.01% SYBR Safe stain. Typically 5 µg DNA were mixed with loading dye and loaded per lane. As a size marker 5µl 1 kb GeneRuler (Fermentas) and as positive control 5 µg genomic DNA digested with specific restriction endonucleases (EcoRI, MspI, AluI) were run in parallel. After separation of the fragments for 5 h at 100V the gel was documented using the FLA3000 (FujiFilm) and subsequently incubated for 12 min in 0.25 M HCl to partially hydrolyze DNA. This step was followed by denaturation of double stranded DNA in denaturation solution (0.5M NaOH, 1.5M NaCl) for 2x 15min. The gel was incubated for 2x 15 min in 1M ammonium acetate for neutralization. DNA was transferred to nitrocellulose membrane by semi dry blotting using a stack of 2x Whatman paper rinsed in NH₄Ac, 2 parafilm stripes paced at the edges for isolation (0.5 cm). The inverted gel was placed onto the Whatman paper and wet with NH₄Ac. Then the nitrocellulose membrane was rinsed in NH₄Ac and placed onto gel. 3x Whatman rinsed in NH₄Ac, 1 packet paper towels and a weigh were placed on top of this stack. After transfer over night DNA was cross linked by UV light (30 J/cm²). Before radioactively labelled DNA probes were hybridized to the DNA fragments nitrocellulose membrane was pre-incubated for 60 - 90 min in 0.5M sodium phosphate pH 7.2, 7% SDS and 1mM

EDTA at 60°C in a rotating wheel. To generate probes for rDNA 5'ETS detection DNA was body labelled with γ -P₃₂-dATP by RadPrime Labelling (Invitrogen). All probes were added to pre-hybridization solution with a final activity of 10⁶ - 10⁷ cpm/ml and incubated over night at 60°C in a rotating wheel. Not bound probe was washed of 2x 30 s with 40mM sodium phosphate pH 7.2, 0.1% SDS. Finally dried membrane was placed on an IP plate until significant radioactive signals were detectable with FLA3000 laser reader (FujiFilm).

6.2.2. Working with RNA

In general working with RNA needs to be done performed under RNase free conditions. RNase Zap was used to decontaminate surfaces and RNA containing reactions were supplied with RNasin (Promega). For pipetting filter tips were used and buffers were set up with Milipore water.

6.2.2.1. RNA isolation, Phenol/Chloroform

Several steps of this protocol have to be performed with very high attention (Phenol is very toxic!)

The RNA containing starting sample is filled up to 500µl with AE-buffer and supplied with 1%SDS. After addition of 500µl Phenol solution the samples were vortexed and shaken at max. intensity at 65°C for 4min. The samples were cooled down in ice for 2min and the resulting phases were separated by centrifugation in a table top centrifuge for 5min, max speed. The upper phase was used for further purification avoiding the other phases. After adding another 500µl Phenol and separation of the phases by centrifugation the upper phase was used and supplied with 500µl Chloroform solution. A vortexing step was followed by a centrifugation step. The final upper phase was precipitated by Ammonium acetate/Ethanol supplied with Glycogen. The RNA was resolved in RNasin containing TE and used for further applications.

6.2.2.2. *In vitro* transcription

T7 Standard reaction:

Substance	Quantity
Template DNA (with T7 promoter)	100ng (12-17nM, 10ng/100bp)
ATP, UTP, GTP and UTP	2mM final concentration each
RNA pol buffer (NEB)	1 times
RNasin	10-20U (0,5µl)
T7 RNA Polymerase (NEB)	75U (250ng, 126 nM, 1,5µl)
RNase free water	To 20µl

The reaction was incubated for 2h at 37°C and heat inactivated at 65°C for 15min. 1-2U DNase I was added to deplete the DNA template. Proteins were digested with proteinase K in 1%SDS total at 55°C for 1h. RNA was precipitated with Ammoniumacetat/Ethanol supplied with Glycogen.

RNA was checked under denaturing conditions (0,5g/ml Urea, TBE) and also under native conditions in a TBE gel. The gel was pre-run for 45min at 120V, max A and later stained in Ethidium bromide.

6.2.3. Protein biochemical methods

Protein analysis was performed according to the standard protocols (Sambrook et al., 1989; Sambrook and Russell, 2001). Generally, proteins were kept on ice (4°C), in the presence of protease inhibitors (either complete® (Roche), or a mix of Leupeptin, Pepstatin, Aprotinin (all 1 µg/ml), PMSF (0.2 to 1 mM)) and reducing agents (DTT 1mM, or β- mercaptoethanol 5mM).

6.2.3.1. Determination of protein concentrations

Protein concentrations were determined using the colorimetric assay described by Bradford (Bradford, 1976). Qbit measurements based on fluorescently labelled dyes, emitting light only bound to protein (Invitrogen) were also used to

determine protein concentration. In addition the concentration of purified proteins was estimated according to protein standards with a known concentration (e.g. BSA) in SDS-PAGE followed by Coomassie Blue staining.

6.2.3.2. Denaturing SDS-polyacrylamide gel electrophoresis (SDS-PAGE)

Protein separation according to the molecular weight using discontinuous SDS polyacrylamide gel electrophoresis (SDS-PAGE) was performed according to the method of Laemmli (1970). Quantity and quality of recombinant proteins was initially analyzed by this method. Separating and stacking gels were prepared according to standard protocols using ready-to-use polyacrylamide solutions from Roth (Rotigel, 30 %, 49:1). For electrophoresis, protein samples were mixed with Laemmli SDS-PAGE sample buffer, heat-denatured for 5 min at 95°C and directly loaded onto the gel. Proteins were separated at 35mA (4 mA/cm), until the dye front reached the bottom of the gel. The molecular weight of proteins was estimated by running pre-stained marker proteins (PAGE ruler, Fermentas) in parallel. Following electrophoresis, proteins were stained with either Coomassie Brilliant Blue or Silver.

6.2.3.3. Native polyacrylamide gel electrophoresis (Native Blue PAGE)

Based on the method described by Schagger and von Jagow proteins were analyzed under native conditions [Schagger and von Jagow, 1991]. Therefore protein-protein interactions could be detected and size of the complexes was estimated by comparison to unstained marker proteins. According to manufacture's protocol for NativePAGE (Invitrogen) 1.5-3 µg BSA, DF31, HMG5 and 5 µl NativeMark unstained protein standard (Invitrogen) were loaded on a 4 - 16% NativePAGE Novex Bis-Tris gel (Invitrogen). Separation of proteins was done at 4°C with 150 volts for 60 min, then voltage was increased to 250V proteins for 90 min. Proteins were fixed in 40% methanol, 10% acetic acid and subsequently silver stained as described below. After documentation, the gels were dried onto a Whatman paper at 80°C for 2 h on a gel dryer (BioRad).

6.2.3.4. Coomassie blue staining of protein gels

Polyacrylamide gels were stained for approximately 15 min on a slowly rocking

platform with Coomassie staining solution (0.1% Coomassie Blue R in 10% acetic acid, 45% methanol). Gels were destained in 10% acetic acid and 45% methanol until protein band became clearly visible. After documentation, the gels were dried onto a Whatman paper at 80°C for 2 h on a gel dryer (BioRad).

6.2.3.5. Silverstaining of protein gels

The staining of protein gels with silver nitrate solution was carried out according to the protocol of Blum [Blum et al., 1987]. The gel was incubated for 6 min in fixing solution (50% methanol, 12% acetic acid and 0.05% formaldehyde 37 %) and washed once in 50% ethanol for 20 min. Before staining gel was preincubated for 1 min in preincubation solution (5% Na₂S₂O₃), washed two times with water (ddH₂O, 20 sec) and subsequently staining solution was added for 20 min (0.2% AgNO₃, 0.075% formaldehyde 37 %). Afterwards the gel was washed with water (2 times, 20 sec each) and developed with the developing solution (6% Na₂CO₃, 0.05% formaldehyde 37 %, 0.5% Na₂S₂O₃) until the protein bands of interest were visible (typically, after 2 to 5 min). The staining reaction was stopped by incubating the gel in 1% acetic acid stop solution (more than 5 min). The gel was documented and dried onto a Whatman paper at 80°C for 2 h on a gel dryer (BioRad).

6.2.3.6. Semi dry Western Blot and immunodetection

Proteins were separated by SDS-PAGE and transferred to nitrocellulose filters or PVDF membranes using the Bio-Rad 'Trans-Blot SD Apparatus' for 1h at 24V. If more than one mini-gel is used the transfer was prolonged (up to 2 h). For protein transfer, the PVDF membrane was activated in 100% methanol and then incubated together with the gel in transfer buffer (Towbin buffer: 192mM glycine, 25mM Tris, 20% methanol, 0.05% SDS) for 5- 10min. After incubation the gel was sandwiched between 3 gel-sized Whatman papers soaked in transfer buffer at the bottom, the PVDF membrane and 3 gel-sized Whatman papers soaked in transfer buffer on top (3MM Whatman pieces each). After transfer, the PVDF membrane was incubated for 15min -1h in blocking solution (1x PBS, containing 5% dried milk and 0.1% Tween-20) in order to reduce non-specific background. Filters were sealed in a plastic bag and incubated for 1h with an

appropriate dilution of the primary antibody (PBST+milk) directed against the protein of interest. Filters were washed three times in PBS-Tween (15 -20min each) and incubated for one additional hour with horseradish peroxidase-coupled secondary antibody (PBST+milk), which is directed against the Fc part of the primary antibody. After 3 washes (10min each, in PBS-Tween) antigen-antibody complexes were detected using Super signal WEST Dura WB Kit (Pierce) and detection with the Image Reader LAS-3000 (Fujifilm) according to the instructions given. All steps were performed at room temperature. The initial blocking step or the incubation with the primary antibody were alternatively performed at 4°C overnight. Most primary antibodies were frozen in PBST+milk solution and used up to five times.

6.2.3.7. TCA precipitation

Samples with a low protein content can be TCA precipitated following resuspension in a smaller volume of loading dye. In general 10% of 100% TCA solution and 1µl of 2% deoxycholate solution are added to the protein sample. After vigorous vortexing, proteins are precipitated by centrifugation (13000g, 30min, 4°C), washed once with ice-cold 100% acetone and resuspended in 1/10th of the original volume in 2x Lämmli dye.

6.2.3.8. Chloroform/Methanol precipitation

This protocol is adapted from Wessel and Flügge 1984. The volume of the sample is adjusted to 150µl with H₂O, followed by the addition of four volumes (600µl) methanol, one volume /150µl) chloroform and 3 volumes (450µl) H₂O. After each of the addition steps the sample was mixed well by vortexing. The resulting phases were separated by centrifugation in a table top centrifuge for 5min, max speed. The upper phase was discarded carefully avoiding the loss of protein containing interphase. Upon addition of 3 volume (450µl) methanol and vortexing, the proteins were pelleted by centrifugation 5min at max speed. After resolubilisation in protein loading buffer the proteins were visualized in SDS page.

6.2.4. *E. coli* culture and methods

6.2.4.1. Liquid culture

For plasmid preparations a single colony is picked from a agar plate with a sterile tip and inoculated into LB or SOB medium supplemented with the respective antibiotic and shaken overnight at 37°C at 180 rpm. For standard Mini-prep (Invitrogen) preparations, 5ml are used. For expression cultures an appropriate culture volume is inoculated, that after overnight incubation at 37°C, 180 rpm (OD₆₀₀: 3-5), the expression medium can be inoculated with an OD₆₀₀ of 0,3-0,5.

6.2.4.2. Glycerol stock

For long term storage of bacterial cultures and convenient handling of frequently used strains, 850µl of a stationary liquid culture are mixed with 400µl of 50% sterile glycerol and frozen at -80°C.

6.2.4.3. Preparation of competent cells

E. coli bacteria from glycerol stocks were streaked out on LB plates and incubated o/n at 37°C. From this plate one colony was used to grow a 3 ml LB preculture o/n at 37°C. The next day 1 ml of the preculture was transferred into 200 ml LB medium and grown to an OD at 600 nm of 0.6. The culture was cooled on ice for 10 min and then centrifuged (15 min, 4000 rpm, 4°C, Heraeus Cryofuge 6000i). After centrifugation the supernatant was discarded and the cell pellet was carefully resuspended in 15ml ice cold TFBII. Cells were incubated on ice for 5 min and afterwards the centrifugation step was repeated. The pelleted cells were then gently resuspended in 2 ml ice cold TFBII. Aliquots of 50 µl were snap frozen in liquid nitrogen, and stored at -80°C. An efficiency of 10⁷ cfu/µg was achieved using this preparation.

6.2.4.4. Transformation of chemically competent bacteria

50µl of chemically competent cells were thawed on ice and 40ng of purified plasmid DNA or 10µl of ligation reaction were added. The suspension was mixed by gently tapping the tube and incubated on ice for 5min. Cells were transformed

by exposing them to a heat-shock of 42°C for 45 seconds, then cooled down on ice for 5 min. 250µl of LB or SOB medium without antibiotics was added and the bacteria culture was incubated at 37°C on an orbital shaker rotating at 350rpm for a time depending on the resistance genes to be expressed. For ampicillin, cells were incubated for 30 min, for chloramphenicol, kanamycin and tetracyclin, one hour of incubation was performed. After the bacteria were given time to express the resistance genes, 50µl and 200µl of the mixture were plated on agar plates containing the appropriate antibiotics. Plates were incubated at 37°C overnight.

6.2.5. Expression and purification of recombinant proteins from *E. coli*

6.2.5.1. Protein expression

BL21/BL21 *placI* cells were transformed with the respective plasmids (pTriEx/pGex vectors).

The evening before an inoculation culture (20 – 30ml) was prepared. This was added into 200ml LB_{Amp} – medium. The cells were induced when OD₆₀₀ was about 0.3 – 0.6 with 1mM IPTG. Then the cells were cultivated until the OD₆₀₀ is 1.3 – 1.5. The culture was centrifuged for 10min at 4000rpm at 4°C, supernatant was removed and the pellet was dissolved in 10ml 1xPBS pH 7.4. Then the solution was transferred into a 50ml falcon tube and again centrifuged for 10min at 4000rpm at 4°C. The pellet was frozen in liquid N₂.

6.2.5.2. Preparation of bacterial cell lysate

For purification 50ml of lysis buffer supplemented with protease inhibitors was added to the frozen cells. The was then cooled using a freezing mixture and sonified using a Branson digital sonifier 250D (big tip) 5 times for 30 seconds at 50% amplitude and 50% duty cycle with 30 seconds pause in between. 20µl cell lysate were collected for SDS – PAGE **(CL)**. Afterwards, the insoluble fraction was removed by centrifugation for 30min at 4500 g and 4°C. The resulting supernatant was then used for further purification. The pellet was resuspended in 0.5ml lysis buffer and 50µl of the solution were collected for SDS – PAGE **(P)**.

6.2.5.3. His purification of recombinantly expressed protein

2ml of 50% Ni – NTA slurry were washed twice in 10ml lysis buffer and the beads were spinned down at 2000g for 2min at 4°C. 2ml of the 50% Ni – NTA slurry were added to the sample which was shaken gently for 90min at 4°C. Beads were spinned down at 2000g for 5min at 4°C and 50µl of the supernatant were collected for SDS – Page **(NB)**, the flow trough was discarded. It was again washed twice with 15ml wash buffer. 50µl of the solution were collected for SDS – PAGE **(W1/W2)**. After a further washing with 10ml wash buffer, 50µl of the solution were collected for SDS – PAGE **(W3)** and the solution was transferred into a 15ml falcon. The protein was eluted with 2ml elution buffer for 60min in an overhead wheel. The solution was spinned down at 2000g for 10min at 4°C. 20µl of the solution were collected for SDS – PAGE **(E1)**. E1 was split up in 10µl aliquots and frozen in liquid N₂. The beads were resuspended with 1ml elution buffer and 100µl of the supernatant was collected for SDS – PAGE **(B)**. To test protein size and purity a SDS page was used

6.2.5.4. GST purification of recombinantly expressed protein

2ml of GST – Sepharose – beads were washed three times in 10ml 1xPBS and the beads were spinned down in the desktop centrifuge. 2ml of GST – Sepharose – beads were added to the sample which was shaken gently for 60min at 4°C. Beads were spinned down at 2000g for 5min at 4°C and 50µl of the supernatant were collected for SDS – Page **(NB)**, the flow trough was discarded. It was washed four times with 10ml wash buffer. 50µl of the solution were collected for SDS – PAGE **(W1 – W4)**. The protein was eluted with 2ml elution buffer for 60min in an overhead wheel. The solution was spinned down at 2000g for 10min at 4°C. 20µl of the solution were collected for SDS – PAGE **(E1)**. E1 was split up in 10µl aliquots and frozen in liquid N₂. The beads were resuspended with 1ml elution buffer and 100µl of the supernatant was collected for SDS – PAGE **(B)**. To test protein size and purity a SDS page was used

6.2.6. Eukaryotic cell culture and methods

General

All work with mammalian tissue cultures was performed according to standard protocols with standard precautions. All work was carried out under a sterile hood in laminar flow, all solutions were either purchased sterile or sterilised by autoclaving. Working space, gloves and devices were thoroughly wiped with 70% ethanol before use. Expendable accessories were opened directly before use and it was taken care not to handle anything above opened culture flasks. Bottlenecks of tissue culture flasks, media and other solutions were passed through the flame after opening and before closing.

6.2.6.1. *Drosophila* Schneider S2R+ cell culture:

Maintenance:

The adherent S2R+ cells grow at 25-27°C without CO₂ in S2, S2R+ cell medium:

450 ml	Schneider's medium
50 ml	Fetal Bovine Serum (aliquoted in -20)
5 ml	1:100 Penicillin-Streptomycin (aliquoted in -20)
33.3ml	l-Glutamine (200mM stock) (aliquoted in -20)
500ml	

Harvesting and splitting:

The cells were split at an estimated confluence of 95-100% with visible cell aggregations and cell layers, typically after 3-4 days. For splitting, the medium was removed using a pump and a sterile pasteur pipette. Then prewarmed trypsin/EDTA solution was added to the cells (3ml per 75cm² flask) and the flask was incubated for 3-4min at RT°C. The process of detachment was monitored under the microscope and when cells began to look round and come loose, the cells were further detached by tapping the dish and pipetting the suspension up and down. The reaction was stopped by adding culture medium at three times the volume as EDTA/Trypsin. After determination of cell density, an appropriate volume of cells was transferred to a new flask and filled with medium to the final

volume.

Freezing

Drosophila cell cultures can be cryo preserved and stored over long periods of time at -80°C. This procedure allows to discontinue a cell culture and to repeatedly work with cells of low passage, as a cell line may change properties and loose viability at high passages due to ageing, selection and, in the worst case, contamination. Cells were grown to subconfluency - approximately $1-2 \times 10^7$ cells/ml. Harvest cells were resuspended in freezing medium (FBS + 10% DMSO, filtered **OR** Complete medium + 10% DMSO, filtered). 1ml cell suspension per cryovial was aliquoted and frozen in a foam box, tape closed at -80°C. After a few days the vials were transferred to LN₂ for long term storage.

Thawing

A 75cm² cell culture flask with 15ml medium was prepared and the cells were thawed in the meanwhile quickly in water bath. Just before cells are completely thawed, decontaminate the outside of the tube with 70% EtOH. Transfer the cells to the flask and grow them at 27°C.

6.2.6.2. Mammalian cell culture:

Maintenance

Mammalian cells in culture were propagated in DMEM containing 10% FCS and penicillin/streptomycin. The medium was warmed to 37°C before used, but stored at 4°C. The medium of the cultures was changed every 2-3 days depending of the confluence of the cells.

Harvesting and splitting

The cells were split at an estimated confluence of 80%. For splitting, the medium was removed using a pump and a sterile pasteur pipette. Then trypsin/EDTA solution was added to the cells (3ml per P15 dish) and the dish incubated for 3-4min at 37°C. The process of detachment was monitored under the microscope and when cells began to look round and come loose, the cells were further

detached by tapping the dish and pipetting the suspension up and down. The reaction was stopped by adding culture medium at three times the volume as EDTA/Trypsin. After determination of cell density, an appropriate volume of cells was transferred to a new flask and filled with medium to the final volume. Cells were incubated in a humidified incubator reserved for mammalian tissue culture at 37°C and 5% CO₂.

Freezing.

For cryopreservation, a cell culture of as low a passage number as possible was expanded to one or several cell culture flasks. At approximately 90% confluence, cells were detached from the dishes as for splitting. The cell density and viability were determined and the cells were spun down at 500rpm for 5min. The supernatant was removed and cells were gently resuspended in a volume of FCS containing 5% DMSO to make a final cell density of 1×10^7 cells/ml. The suspension was thereafter aliquoted to 1ml in sterile cryo-tubes precooled to -20°C. The closed tubes were transferred to the -80°C freezer and for long-term preservation stored in liquid nitrogen.

Thawing

A P15 cell culture dish with 15ml medium was prepared and the cells were thawed in the meanwhile quickly in water bath. Just before cells are completely thawed, decontaminate the outside of the tube with 70% EtOH. Transfer the cells to the flask and grow them at 27°C.

6.2.7. Chromatin methods

6.2.7.1. Isolation of genomic DNA from HeLa cells

For preparation genomic HeLa DNA confluent 15 cm dishes (diameter) with approximately 2×10^7 cells were once washed with PBS. Then 3 ml permeabilization buffer (15mM Tris/HCl pH 7.6, 300mM sucrose, 60mM KCl, 15mM NaCl, 3mM CaCl₂, 0.5mM EGTA, 0.2% (v/v) NP40) was added and cells were incubated for 2 min at 37°C. Cellular RNA was digested by addition of 250 µg RNase A in 3 ml 50mM Tris/HCl pH 8, 20mM EDTA and 1% SDS. After 2 hours

of digestion at 37°C 250 µg proteinase K was added to subsequently degrade all cellular proteins. This reaction was performed over night at 37°C. The next day the highly viscous DNA containing cell lysate was aspirated and vortex for 5 - 10 min to shear genomic DNA and increase solubility. Addition of 0.5 volumes of 7.5M ammonium acetate and 2 volumes of 100% ice-cold ethanol to the lysate precipitated DNA. This mixture was incubated for 10 min on ice and then centrifuged for 30 min at 4°C at 20,000 *g*. The DNA pellet was washed once with 70% ethanol. Before dissolving DNA all ethanol had to be carefully removed and drying of the pellet had to be avoided, since this would highly reduce DNA solubility. Then the pellet was resuspended in 2 ml prewarmed ddH₂O and over night incubated at 45°C in thermo shaker to dissolve genomic DNA.

6.2.7.2. MNase digestion of HeLa chromatin

Chromatin of HeLa cells was analyzed by partial digestion of nucleosomal linker DNA. Confluent 6 well plates or 15 cm dishes were once washed with 1-5 ml PBS. Prior to use micrococcal nuclease (MNase) from *Staphylococcus aureus* was added to the permeabilization buffer (15mM Tris/HCl pH 7.6, 300mM sucrose, 60mM KCl, 15mM NaCl, 4mM CaCl₂, 0.5mM EGTA, 0.2% (v/v) NP40 and fresh 0.5mM 2-mercaptoethanol). Per well 300µl and per dish 3 ml permeabilization buffer supplemented with, depending on the experiment, 100 - 2000 units MNase was added and cells were incubated for 2 min at 37°C. The nuclease reaction was stopped by addition of 300µl - 3 ml stop buffer (50mM Tris/HCl pH 8, 20mM EDTA and 1% SDS) and RNA was digested by addition of 25-250 µg RNase A. After 2 hours of incubation at 37°C 25-250 µg proteinase K was added to subsequently degrade all cellular proteins. This reaction was performed over night at 37°C. The next day the viscous DNA containing cell lysate was aspirated and non-digested nucleosomal DNA was isolated as described below.

Chromatin in vitro assembly:

For all in vitro assembly techniques (pRSet DNMT1 human aa 530-830 BamH1) was used as template. The in vitro reconstituted chromatin was used for RNase and MNase digests as well as for sucrose gradient centrifugation assays.

6.2.7.2. Drex assembly

Nucleosomes were assembled from DNA and *Drosophila* embryonic extract by the technique according to Becker and Wu (Becker and Wu 1992). Preparation of cytoplasmic extracts from 0–90 min *Drosophila* embryos and chromatin reconstitution were essentially performed as described. Assembly reactions (120 µl) contained 40–60 µl of *Drosophila* embryo extract, 1 µg of plasmid DNA, McNap buffer (3 mM ATP, 30 mM creatine phosphate, 1 µg/ml creatine kinase, 1mM DTT and 1mM MgCl₂). Assembly reactions were incubated for 6 h at 26°C and the assembly was tested by MNase digest. The digest was visualized in SyBr Safe stained agarose gels.

6.2.7.3. Assembly by salt gradient dialysis

Nucleosomes were assembled from DNA and histones by the salt gradient dialysis technique according to Rhodes [Rhodes and Laskey, 1989]. The assembly reaction was performed in the lid of siliconized 1.5 ml tubes (Biozym). Dialysis membranes with a MWCO of 3.5 kD (Spectrapor) were pre-incubated for 5 min in high salt buffer (10mM Tris/HCl pH 7.6, 2M NaCl, 1mM EDTA, 0.05% NP40, 1mM β-mercaptoethanol). This membrane was placed over the lid of a 1.5 ml tube with a big hole (O-ring). The membrane was fixed with a second tube, where the bottom was cut and the lid removed. The tubes were placed (in a styrofoam floater) into a 3 l beaker filled with 300 ml high salt buffer (containing a magnetic stirrer). Air bubbles below the membrane were removed with a bent pasteur pipette. Finally the assembly reaction were pipetted into the lid. 3 l of low salt buffer (10mM Tris/HCl pH 7.6, 50mM NaCl, 1mM EDTA, 0.05% NP40, 1mM β-mercaptoethanol) were pumped into this beaker with a flow rate of 300 ml per hour at room temperature. Hence salt concentration decreased slowly from 2M to 227mM allowing a specific assembly of the histone octamers onto the given DNA fragment. For a test assembly reaction typically 5 µg of DNA (were mixed with different amounts of histone octamers, varying from 3 to 6 µg, in a final volume of 50 µl high salt buffer, supplemented with 200 ng/µl BSA. After the optimal histon:DNA ratio had been determined, nucleosomes were assembled in large scale. In general 25 µg of DNA was mixed with an optimal amount of histones in 250 µl high salt buffer, supplemented with 200 ng/µl BSA.

The assembly mix was split into 5x 50 µl before loading into the dialysis chambers. To control assembly of poly-nucleosomes on plasmid DNA a partial MNase digested had to be done. The digest was visualized in SyBr Safe stained agarose gels.

6.2.7.4. Sucrose gradient sedimentation assay:

Sucrose gradients were used to determine the conformation of chromatin. Long 15%-40% sucrose gradients were prepared in cold, sterile Ex80 buffer. The middle of the polyallomer tube (Beckman Coulter) was marked by the use of the SW40 marking helper. 15% sucrose solution filled up to the mark was underlaid by 40% sucrose solution. The polyallomer tubes were sealed with a lid and the long gradient was adjusted by the Gradient Master™ (Biocomp). The chromatin samples were added on top of the gradients. The run in the Beckman ultracentrifuge supplied with an evenly balanced SW40 rotor lasted 12h, at 7500rpm, 4°C, maximum acceleration and without brake. The gradients were harvested by fractionation of 16-17 fractions (each 650-700µl). The fractions were, dependently on the down-stream application, RNase A/DNase I (37°C, 2h) or proteinase K (55°C, 2h) digested. For nucleic acid visualisation, the proteinase K treated samples were precipitated by ammoniumacetat/ethanol and linearized for 1 hour with 0,5µl XbaI in NEB 4 and BSA per reaction. The nucleic acids were visualised by agarose gelelectrophoresis and EtBr staining.

For protein visualisation, the RNase A/DNase I treated fractions were TCA precipitated and visualised by SDS page and Coomassie staining.

6.2.7.5. Size exclusion by gelfiltration:

Empty gel columns (BioRad) were filled with Sephacryl 300HR and the gelfiltration column was washed twice with 4 column volumes cold Ex80 buffer. The chromatin samples (up to 300µl) were added on top of the size exclusion column matrix and the centrifugation was performed at 200g, 4°C for 1 min. The flowthrough was discarded and the first elution fraction (300µl) was used for later analysis.

6.2.7.6. DNA supercoiling analysis

For 1D and 2D supercoiling analysis DNA purified from *in vitro* reconstituted chromatin was separated on 1.3% agarose gels in Tris/Glycine buffer (pH 8.3). The running conditions of the first dimension were 80 V, 8 h, room temperature. For the second dimension, the gel was soaked for 2 h in a buffer containing 3,9 µM chloroquine and the electrophoresed at 90 V for 9 h at room temperature. Afterwards the DNA was stained with ethidium bromide.

6.2.7.7. Microscale thermophoresis

All microscale thermophoresis measurements were performed at 27°C using Monolith NT™ standard Capillaries and the Monolith NT.015T/NT.115 device (NanoTemper) with the laser being on for 40 s, resulting in a temperature increase of 6K. Binding reactions took place in the chromatin assembly buffer described above. Nucleic acid samples were fluorescently labelled with Cy5, FAM or Cy3 and used at a concentration of 50 nM. For each binding analysis, a titration series was prepared with varying concentrations of Df31, as indicated in the plots (Microscale thermophoresis was performed in cooperation with the company 2bind GmbH (Regensburg, Germany). All curves were plotted with the KaleidaGraph software and the thermophoresis signals were fitted with the Hill equation corrected for the minimum (*Min*) and maximum (*Max*) values of the binding curve: $Y(c) = Min + (Max - Min) / (1 + EC_{50} / c_{pep}^0)^n$, with $Y(c)$ being the thermophoresis signal, c_{pep}^0 the variable concentration of the respective peptide. Under the used experimental conditions K_d is the concentration where half of the oligonucleotide is bound. Thermophoresis signals were normalized to the fraction bound (*X*) by $X = (Y(c) - Min) / (Max - Min)$ and fitted as described above.

6.2.7.8. Knock down of Df31 in *Drosophila* S2R+ cells

Df31 was knocked down by dsRNA incubation as described elsewhere (Worby et al., 2001). Df31 exon sequence was amplified by PCR and flanked by T7 promoter sites with the following primer:

Primer 1 for TTAATACGACTCACTATAGGGAGAATGGCTGATGTGGCTGAG
 CAAAAGAATG

Primer 1 rev TTAATACGACTCACTATAGGGAGATTAGGCGGCCAC
 TTCGCTAGCCTC

The PCR product was used for *in vitro* transcription (Ambion MEGAscript T7 kit) to get suitable amounts of dsRNA. 0.75×10^6 *Drosophila* S2 cells were grown in 6 well plates with 1 ml DMEM medium without FCS and supplied with 10 µg dsRNA. After 1 h incubation, 2 ml of DMEM containing FCS was added. Knock down efficiency was tested after 5 days by qPCR using the following primer pairs:

DF31_qPCR for 1	ACTGTTTCTTTTGCCGCC
DF31_qPCR rev 1	CTTCGCTGCTCTCTTTTTTG
DF31_qPCR for 2	TGACTCAACAGATGCTCCC
DF31_qPCR rev 2	CCCCATTCTGAACCTCATCC

6.2.7.9. Microscopic analysis of *Drosophila* S2R+ and HeLa cells

For the microscopic analysis the cells were grown on glass slides and washed twice with 1xPBS followed by PFA fixation. Cells were permeabilized with PBS containing 0.5% Triton (0°C) and washed twice with PBS. After DNA or antibody staining, cells were washed twice in PBS and mounted overnight with Vectashield (Vector Laboratories). For detailed microscopic analysis a Zeiss Axiovert 200M microscope containing a Zeiss Imager ApoTome 2 device was used.

6.2.7.10. RNA sequencing and data analysis

Total RNA from embryonic extracts was isolated by phenol/chloroform extraction and chromatin associated RNA were isolated after fractionation of chromatin on a sucrose gradient. Isolated RNA was enriched for fragments < 200 bp and strand-specific cDNA libraries were prepared using the ExactStart Small RNA Cloning Kit (Epicentre). Libraries included small coding as well as non-coding RNAs and fragments of longer primary transcripts were created. The cDNA was amplified with hybrid primers containing sequences required for the

Illumina platform. PCR products were cleaned up with AMPure XP beads (Beckman Coulter) and subjected to 1x72 bp sequencing on an Illumina GAXII. We received 23 million sequences for the embryonic transcriptome and 33, 41 and 43 million reads for individual sucrose gradient purified fractions, respectively. All analysis steps were carried out on the Galaxy public server. First, the reads were filtered by quality (cut-off: 20, minimum percentage / read: 80), resulting in 3-8% of discarded reads. The remaining 92-97% of the reads were mapped to *dm3*/BDGP R5 using TopHat v1.2.0 generating a minimum of 92% mapped reads. Transcripts were assembled using Cufflinks v1.0.3 and all transcripts with a lower coverage than 3x were removed. A reference file from the embryonic transcriptome was created and fold-enrichments of caRNA fractions in comparison to it were calculated. Library preparation and data analysis was performed by Sarah Diermeier.

6.2.7.11. Proteome analysis

Linearized and biotinylated DNA containing a repeat of 5S rDNA sequences was immobilized using 1.8 mg paramagnetic streptavidin beads (DynaM280, Invitrogen). DNA bound beads were blocked for 30 min with BSA (1.5 µg/µl) in EX100 (10 mM HEPES pH7.6, 100 mM NaCl, 1.5 mM MgCl₂, 0.5 mM EGTA, 10% (v/v) glycerol, 0.2 mM PMSF, 1 mM DTT). 2 µg of DNA was concentrated using a magnetic particle concentrator (DynaM) and resuspended in a total volume of 240 µl, containing 120 µl *Drosophila* embryo extract and an ATP regenerating system (3 mM ATP, 30 mM creatine phosphate, 2.4 µg creatine phosphate kinase, 3 mM MgCl₂, 1 mM DTT). The reaction was rotated at 26°C for 6 h, washed once with EX100 and resuspended in 200 µl EX100. To remove caRNAs RNaseA was added to a final concentration of 1 µg/µl. After rotating for another 2 h at 26 °C beads were again washed with EX100. For the proteomic analysis a total amount 5 µg of chromatin were subjected to SDS-PAGE and subsequent LC MS/MS mass spectrometry while one microgram was subjected to MNase digestion to validate chromatin reconstitution. Proteins were quantified in label free manner using the Proteome discoverer software package (Thermo Scientific). The calculated intensities were normalized to the total ion current (TIC) and protein ratios calculated as $R = I(-RNaseA) / I(+RNase)$ where I represents the average intensity

of the two most intense ions used for identification in the LC MS/MS analysis. Proteome analysis was performed by Miriam Pusch and Prof. Dr. Axel Imhof, LMU Munich.

7. References

- Allen, T. A., Von Kaenel, S., Goodrich, J. A., and Kugel, J. F. (2004). The SINE-encoded mouse B2 RNA represses mRNA transcription in response to heat shock. *Nat Struct Mol Biol* 11, 816-821.
- Arnold, E. A., and Young, K. E. (1972). Low molecular weight chromatin-associated RNA from rat liver. *Biochim Biophys Acta* 269, 252-258.
- Arya, G., Zhang, Q., and Schlick, T. (2006). Flexible histone tails in a new mesoscopic oligonucleosome model. *Biophys J* 91, 133-150.
- Avvakumov, N., Nourani, A., and Cote, J. (2011). Histone chaperones: modulators of chromatin marks. *Mol Cell* 41, 502-514.
- Baaske, P., Wienken, C. J., Reineck, P., Duhr, S., and Braun, D. (2010). Optical thermophoresis for quantifying the buffer dependence of aptamer binding. *Angew Chem Int Ed Engl* 49, 2238-2241.
- Bachellerie, J. P., Cavaille, J., and Huttenhofer, A. (2002). The expanding snoRNA world. *Biochimie* 84, 775-790.
- Becker, P. B., and Wu, C. (1992). Cell-free system for assembly of transcriptionally repressed chromatin from *Drosophila* embryos. *Mol Cell Biol* 12, 2241-2249.
- Belgrader, P., Siegel, A. J., and Berezney, R. (1991). A comprehensive study on the isolation and characterization of the HeLa S3 nuclear matrix. *J Cell Sci* 98 (Pt 3), 281-291.
- Belmont, A. S., Braunfeld, M. B., Sedat, J. W., and Agard, D. A. (1989). Large-scale chromatin structural domains within mitotic and interphase chromosomes in vivo and in vitro. *Chromosoma* 98, 129-143.
- Belmont, A. S., and Bruce, K. (1994). Visualization of G1 chromosomes: a folded, twisted, supercoiled chromonema model of interphase chromatid structure. *J Cell Biol* 127, 287-302.
- Bernstein, E., Duncan, E. M., Masui, O., Gil, J., Heard, E., and Allis, C. D. (2006). Mouse polycomb proteins bind differentially to methylated histone H3 and RNA and are enriched in facultative heterochromatin. *Mol Cell Biol* 26, 2560-2569.
- Birchler, J. A., Kavi, H. H., and Fernandez, H. R. (2004). Heterochromatin: RNA points the way. *Curr Biol* 14, R759-761.
- Blower, M. D., Nachury, M., Heald, R., and Weis, K. (2005). A Rae1-containing ribonucleoprotein complex is required for mitotic spindle assembly. *Cell* 121, 223-234.

- Bonner, J., and Widholm, J. (1967). Molecular complementarity between nuclear DNA and organ-specific chromosomal RNA. *Proc Natl Acad Sci USA* 57, 1379-1385.
- Bouvier, D., Hubert, J., Seve, A. P., and Bouteille, M. (1985). Structural aspects of intranuclear matrix disintegration upon RNase digestion of HeLa cell nuclei. *Eur J Cell Biol* 36, 323-333.
- Bratkovic, T., and Rogelj, B. (2011). Biology and applications of small nucleolar RNAs. *Cell Mol Life Sci* 68, 3843-3851.
- Britten, R. J., and Davidson, E. H. (1969). Gene regulation for higher cells: a theory. *Science* 165, 349-357.
- Brockdorff, N., Ashworth, A., Kay, G. F., McCabe, V. M., Norris, D. P., Cooper, P. J., Swift, S., and Rastan, S. (1992). The product of the mouse Xist gene is a 15 kb inactive X-specific transcript containing no conserved ORF and located in the nucleus. *Cell* 71, 515-526.
- Brower-Toland, B., Findley, S. D., Jiang, L., Liu, L., Yin, H., Dus, M., Zhou, P., Elgin, S. C., and Lin, H. (2007). Drosophila PIWI associates with chromatin and interacts directly with HP1a. *Genes Dev* 21, 2300-2311.
- Brunner, E., Ahrens, C. H., Mohanty, S., Baetschmann, H., Loevenich, S., Potthast, F., Deutsch, E. W., Panse, C., de Lichtenberg, U., Rinner, O., *et al.* (2007). A high-quality catalog of the Drosophila melanogaster proteome. *Nat Biotechnol* 25, 576-583.
- Cai, S., Lee, C. C., and Kohwi-Shigematsu, T. (2006). SATB1 packages densely looped, transcriptionally active chromatin for coordinated expression of cytokine genes. *Nat Genet* 38, 1278-1288.
- Carter, D., Chakalova, L., Osborne, C. S., Dai, Y. F., and Fraser, P. (2002). Long-range chromatin regulatory interactions in vivo. *Nat Genet* 32, 623-626.
- Catez, F., Yang, H., Tracey, K. J., Reeves, R., Misteli, T., and Bustin, M. (2004). Network of dynamic interactions between histone H1 and high-mobility-group proteins in chromatin. *Mol Cell Biol* 24, 4321-4328.
- Caudron-Herger, M., Muller-Ott, K., Mallm, J. P., Marth, C., Schmidt, U., Fejes-Toth, K., and Rippe, K. (2011). Coding RNAs with a non-coding function: Maintenance of open chromatin structure. *Nucleus* 2, 410-424.
- Chambeyron, S., and Bickmore, W. A. (2004). Chromatin decondensation and nuclear reorganization of the HoxB locus upon induction of transcription. *Genes Dev* 18, 1119-1130.
- Chow, J., and Heard, E. (2009). X inactivation and the complexities of silencing a sex chromosome. *Curr Opin Cell Biol* 21, 359-366.

- Clemson, C. M., Hutchinson, J. N., Sara, S. A., Ensminger, A. W., Fox, A. H., Chess, A., and Lawrence, J. B. (2009). An architectural role for a nuclear noncoding RNA: NEAT1 RNA is essential for the structure of paraspeckles. *Mol Cell* 33, 717-726.
- Cook, P. R. (1999). The organization of replication and transcription. *Science* 284, 1790-1795.
- Corona, D. F., Siriaco, G., Armstrong, J. A., Snarskaya, N., McClymont, S. A., Scott, M. P., and Tamkun, J. W. (2007). ISWI regulates higher-order chromatin structure and histone H1 assembly in vivo. *PLoS Biol* 5, e232.
- Cremer, T., Cremer, C., Schneider, T., Baumann, H., Hens, L., and Kirsch-Volders, M. (1982). Analysis of chromosome positions in the interphase nucleus of Chinese hamster cells by laser-UV-microirradiation experiments. *Hum Genet* 62, 201-209.
- Cremer, T., Kreth, G., Koester, H., Fink, R. H., Heintzmann, R., Cremer, M., Solovei, I., Zink, D., and Cremer, C. (2000). Chromosome territories, interchromatin domain compartment, and nuclear matrix: an integrated view of the functional nuclear architecture. *Crit Rev Eukaryot Gene Expr* 10, 179-212.
- Crevel, G., and Cotterill, S. (1995). DF 31, a sperm decondensation factor from *Drosophila melanogaster*: purification and characterization. *EMBO J* 14, 1711-1717.
- Crevel, G., Huikeshoven, H., and Cotterill, S. (2001). Df31 is a novel nuclear protein involved in chromatin structure in *Drosophila melanogaster*. *J Cell Sci* 114, 37-47.
- Cui, Y., and Bustamante, C. (2000). Pulling a single chromatin fiber reveals the forces that maintain its higher-order structure. *Proc Natl Acad Sci U S A* 97, 127-132.
- Dekker, J., Rippe, K., Dekker, M., and Kleckner, N. (2002). Capturing chromosome conformation. *Science* 295, 1306-1311.
- Desiere, F., Deutsch, E. W., Nesvizhskii, A. I., Mallick, P., King, N. L., Eng, J. K., Aderem, A., Boyle, R., Brunner, E., Donohoe, S., *et al.* (2005). Integration with the human genome of peptide sequences obtained by high-throughput mass spectrometry. *Genome Biol* 6, R9.
- Deuring, R., Fanti, L., Armstrong, J. A., Sarte, M., Papoulas, O., Prestel, M., Daubresse, G., Verardo, M., Moseley, S. L., Berloco, M., *et al.* (2000). The ISWI chromatin-remodeling protein is required for gene expression and the maintenance of higher order chromatin structure in vivo. *Mol Cell* 5, 355-365.

- Dion, M. F., Altschuler, S. J., Wu, L. F., and Rando, O. J. (2005). Genomic characterization reveals a simple histone H4 acetylation code. *Proc Natl Acad Sci U S A* *102*, 5501-5506.
- Dorigo, B., Schalch, T., Bystricky, K., and Richmond, T. J. (2003). Chromatin fiber folding: requirement for the histone H4 N-terminal tail. *J Mol Biol* *327*, 85-96.
- Dorigo, B., Schalch, T., Kulangara, A., Duda, S., Schroeder, R. R., and Richmond, T. J. (2004). Nucleosome arrays reveal the two-start organization of the chromatin fiber. *Science* *306*, 1571-1573.
- Dunker, A. K., Lawson, J. D., Brown, C. J., Williams, R. M., Romero, P., Oh, J. S., Oldfield, C. J., Campen, A. M., Ratliff, C. M., Hipps, K. W., *et al.* (2001). Intrinsically disordered protein. *J Mol Graph Model* *19*, 26-59.
- Eitoku, M., Sato, L., Senda, T., and Horikoshi, M. (2008). Histone chaperones: 30 years from isolation to elucidation of the mechanisms of nucleosome assembly and disassembly. *Cell Mol Life Sci* *65*, 414-444.
- Ender, C., Krek, A., Friedlander, M. R., Beitzinger, M., Weinmann, L., Chen, W., Pfeffer, S., Rajewsky, N., and Meister, G. (2008). A human snoRNA with microRNA-like functions. *Mol Cell* *32*, 519-528.
- Erdel, F., Schubert, T., Marth, C., Langst, G., and Rippe, K. (2010). Human ISWI chromatin-remodeling complexes sample nucleosomes via transient binding reactions and become immobilized at active sites. *Proc Natl Acad Sci U S A* *107*, 19873-19878.
- Ernst, J., and Kellis, M. (2010). Discovery and characterization of chromatin states for systematic annotation of the human genome. *Nat Biotechnol* *28*, 817-825.
- Ernst, J., Kheradpour, P., Mikkelsen, T. S., Shores, N., Ward, L. D., Epstein, C. B., Zhang, X., Wang, L., Issner, R., Coyne, M., *et al.* (2011). Mapping and analysis of chromatin state dynamics in nine human cell types. *Nature* *473*, 43-49.
- Eskiw, C. H., and Bazett-Jones, D. P. (2002). The promyelocytic leukemia nuclear body: sites of activity? *Biochem Cell Biol* *80*, 301-310.
- Fan, J. Y., Rangasamy, D., Luger, K., and Tremethick, D. J. (2004). H2A.Z alters the nucleosome surface to promote HP1alpha-mediated chromatin fiber folding. *Mol Cell* *16*, 655-661.
- Fan, Y., Nikitina, T., Morin-Kensicki, E. M., Zhao, J., Magnuson, T. R., Woodcock, C. L., and Skoultschi, A. I. (2003). H1 linker histones are essential for mouse development and affect nucleosome spacing in vivo. *Mol Cell Biol* *23*, 4559-4572.

- Fedorov, A., Cao, X., Saxonov, S., de Souza, S. J., Roy, S. W., and Gilbert, W. (2001). Intron distribution difference for 276 ancient and 131 modern genes suggests the existence of ancient introns. *Proc Natl Acad Sci U S A* 98, 13177-13182.
- Felsenfeld, G. (1978). Chromatin. *Nature* 271, 115-122.
- Felsenfeld, G., and Groudine, M. (2003). Controlling the double helix. *Nature* 421, 448-453.
- Filion, G. J., van Bommel, J. G., Braunschweig, U., Talhout, W., Kind, J., Ward, L. D., Brugman, W., de Castro, I. J., Kerkhoven, R. M., Bussemaker, H. J., and van Steensel, B. (2010). Systematic protein location mapping reveals five principal chromatin types in *Drosophila* cells. *Cell* 143, 212-224.
- Finch, J. T., and Klug, A. (1976). Solenoidal model for superstructure in chromatin. *Proc Natl Acad Sci U S A* 73, 1897-1901.
- Fischle, W., Tseng, B. S., Dormann, H. L., Ueberheide, B. M., Garcia, B. A., Shabanowitz, J., Hunt, D. F., Funabiki, H., and Allis, C. D. (2005). Regulation of HP1-chromatin binding by histone H3 methylation and phosphorylation. *Nature* 438, 1116-1122.
- Fletcher, T. M., and Hansen, J. C. (1995). Core histone tail domains mediate oligonucleosome folding and nucleosomal DNA organization through distinct molecular mechanisms. *J Biol Chem* 270, 25359-25362.
- Fox, A. H., Bond, C. S., and Lamond, A. I. (2005). P54nrb forms a heterodimer with PSP1 that localizes to paraspeckles in an RNA-dependent manner. *Mol Biol Cell* 16, 5304-5315.
- Francis, N. J., Kingston, R. E., and Woodcock, C. L. (2004). Chromatin compaction by a polycomb group protein complex. *Science* 306, 1574-1577.
- Franke, A., and Baker, B. S. (1999). The rox1 and rox2 RNAs are essential components of the compensasome, which mediates dosage compensation in *Drosophila*. *Mol Cell* 4, 117-122.
- Georgel, P. T., Horowitz-Scherer, R. A., Adkins, N., Woodcock, C. L., Wade, P. A., and Hansen, J. C. (2003). Chromatin compaction by human MeCP2. Assembly of novel secondary chromatin structures in the absence of DNA methylation. *J Biol Chem* 278, 32181-32188.
- Gerstein, M. B., Lu, Z. J., Van Nostrand, E. L., Cheng, C., Arshinoff, B. I., Liu, T., Yip, K. Y., Robilotto, R., Rechtsteiner, A., Ikegami, K., *et al.* (2010). Integrative analysis of the *Caenorhabditis elegans* genome by the modENCODE project. *Science* 330, 1775-1787.
- Getz, M. J., and Saunders, G. F. (1973). Origins of human leukocyte chromatin-associated RNA. *Biochim Biophys Acta* 312, 555-573.

- Gilbert, N., Boyle, S., Fiegler, H., Woodfine, K., Carter, N. P., and Bickmore, W. A. (2004). Chromatin architecture of the human genome: gene-rich domains are enriched in open chromatin fibers. *Cell* 118, 555-566.
- Godde, J. S., and Ura, K. (2008). Cracking the enigmatic linker histone code. *J Biochem* 143, 287-293.
- Gordon, F., Luger, K., and Hansen, J. C. (2005). The core histone N-terminal tail domains function independently and additively during salt-dependent oligomerization of nucleosomal arrays. *J Biol Chem* 280, 33701-33706.
- Greaves, I. K., Rangasamy, D., Ridgway, P., and Tremethick, D. J. (2007). H2A.Z contributes to the unique 3D structure of the centromere. *Proc Natl Acad Sci U S A* 104, 525-530.
- Gregg, C., Zhang, J., Weissbourd, B., Luo, S., Schroth, G. P., Haig, D., and Dulac, C. (2010). High-resolution analysis of parent-of-origin allelic expression in the mouse brain. *Science* 329, 643-648.
- Grewal, S. I., and Jia, S. (2007). Heterochromatin revisited. *Nat Rev Genet* 8, 35-46.
- Grigoryev, S. A., Arya, G., Correll, S., Woodcock, C. L., and Schlick, T. (2009). Evidence for heteromorphic chromatin fibers from analysis of nucleosome interactions. *Proc Natl Acad Sci U S A* 106, 13317-13322.
- Grigoryev, S. A., and Woodcock, C. L. (2012). Chromatin organization - The 30nm fiber. *Exp Cell Res*.
- Guelen, L., Pagie, L., Brasset, E., Meuleman, W., Faza, M. B., Talhout, W., Eussen, B. H., de Klein, A., Wessels, L., de Laat, W., and van Steensel, B. (2008). Domain organization of human chromosomes revealed by mapping of nuclear lamina interactions. *Nature* 453, 948-951.
- Guillebault, D., and Cotterill, S. (2007). The *Drosophila* Df31 protein interacts with histone H3 tails and promotes chromatin bridging in vitro. *J Mol Biol* 373, 903-912.
- Guruharsha, K. G., Rual, J. F., Zhai, B., Mintseris, J., Vaidya, P., Vaidya, N., Beekman, C., Wong, C., Rhee, D. Y., Cenaj, O., *et al.* (2011). A protein complex network of *Drosophila melanogaster*. *Cell* 147, 690-703.
- Guttman, M., Amit, I., Garber, M., French, C., Lin, M. F., Feldser, D., Huarte, M., Zuk, O., Carey, B. W., Cassady, J. P., *et al.* (2009). Chromatin signature reveals over a thousand highly conserved large non-coding RNAs in mammals. *Nature* 458, 223-227.

- Hake, S. B., and Allis, C. D. (2006). Histone H3 variants and their potential role in indexing mammalian genomes: the "H3 barcode hypothesis". *Proc Natl Acad Sci U S A* *103*, 6428-6435.
- Hall, I. M., Shankaranarayana, G. D., Noma, K., Ayoub, N., Cohen, A., and Grewal, S. I. (2002). Establishment and maintenance of a heterochromatin domain. *Science* *297*, 2232-2237.
- Hansen, J. C., Kreider, J. I., Demeler, B., and Fletcher, T. M. (1997). Analytical ultracentrifugation and agarose gel electrophoresis as tools for studying chromatin folding in solution. *Methods* *12*, 62-72.
- Hatton, D., and Gray, J. C. (1999). Two MAR DNA-binding proteins of the pea nuclear matrix identify a new class of DNA-binding proteins. *Plant J* *18*, 417-429.
- Hendzel, M. J., Lever, M. A., Crawford, E., and Th'ng, J. P. (2004). The C-terminal domain is the primary determinant of histone H1 binding to chromatin in vivo. *J Biol Chem* *279*, 20028-20034.
- Holoubek, V., Deacon, N. J., Buckle, D. W., and Naora, H. (1983). A small chromatin-associated RNA homologous to repetitive DNA sequences. *Eur J Biochem* *137*, 249-256.
- Holzmann, K., Gerner, C., Korosec, T., Poltl, A., Grimm, R., and Sauermann, G. (1998). Identification and characterization of the ubiquitously occurring nuclear matrix protein NMP 238. *Biochem Biophys Res Commun* *252*, 39-45.
- Horowitz, R. A., Agard, D. A., Sedat, J. W., and Woodcock, C. L. (1994). The three-dimensional architecture of chromatin in situ: electron tomography reveals fibers composed of a continuously variable zig-zag nucleosomal ribbon. *J Cell Biol* *125*, 1-10.
- Huang, R. C., and Bonner, J. (1965). Histone-bound RNA, a component of native nucleohistone. *Proc Natl Acad Sci USA* *54*, 960-967.
- Huang, R. C., and Huang, P. C. (1969). Effect of protein-bound RNA associated with chick embryo chromatin on template specificity of the chromatin. *J Mol Biol* *39*, 365-378.
- Iborra, F. J., Jackson, D. A., and Cook, P. R. (2001). Coupled transcription and translation within nuclei of mammalian cells. *Science* *293*, 1139-1142.
- Ikura, T., Ogryzko, V. V., Grigoriev, M., Groisman, R., Wang, J., Horikoshi, M., Scully, R., Qin, J., and Nakatani, Y. (2000). Involvement of the TIP60 histone acetylase complex in DNA repair and apoptosis. *Cell* *102*, 463-473.
- Imhof, A. (2006). Epigenetic regulators and histone modification. *Briefings in functional genomics & proteomics* *5*, 222-227.

- Jeffery, L., and Nakielny, S. (2004). Components of the DNA methylation system of chromatin control are RNA-binding proteins. *J Biol Chem* 279, 49479-49487.
- Jonsson, Z. O., Dhar, S. K., Narlikar, G. J., Auty, R., Wagle, N., Pellman, D., Pratt, R. E., Kingston, R., and Dutta, A. (2001). Rvb1p and Rvb2p are essential components of a chromatin remodeling complex that regulates transcription of over 5% of yeast genes. *J Biol Chem* 276, 16279-16288.
- Kan, P.-Y., Caterino, T. L., and Hayes, J. J. (2009). The H4 tail domain participates in intra- and internucleosome interactions with protein and DNA during folding and oligomerization of nucleosome arrays. *Mol Cell Biol* 29, 538-546.
- Kan, P. Y., Lu, X., Hansen, J. C., and Hayes, J. J. (2007). The H3 tail domain participates in multiple interactions during folding and self-association of nucleosome arrays. *Mol Cell Biol* 27, 2084-2091.
- Kanduri, C. (2011). Kcnq1ot1: a chromatin regulatory RNA. *Semin Cell Dev Biol* 22, 343-350.
- Kanehisa, T., Fujitani, H., Sano, M., and Tanaka, T. (1971). Studies on low molecular weight RNA of chromatin. Effects of template activity of chick liver chromatin. *Biochim Biophys Acta* 240, 46-55.
- Kanemaki, M., Makino, Y., Yoshida, T., Kishimoto, T., Koga, A., Yamamoto, K., Yamamoto, M., Moncollin, V., Egly, J. M., Muramatsu, M., and Tamura, T. (1997). Molecular cloning of a rat 49-kDa TBP-interacting protein (TIP49) that is highly homologous to the bacterial RuvB. *Biochem Biophys Res Commun* 235, 64-68.
- Katayama, S., Tomaru, Y., Kasukawa, T., Waki, K., Nakanishi, M., Nakamura, M., Nishida, H., Yap, C. C., Suzuki, M., Kawai, J., *et al.* (2005). Antisense transcription in the mammalian transcriptome. *Science* 309, 1564-1566.
- Khalil, A. M., Guttman, M., Huarte, M., Garber, M., Raj, A., Rivea Morales, D., Thomas, K., Presser, A., Bernstein, B. E., van Oudenaarden, A., *et al.* (2009). Many human large intergenic noncoding RNAs associate with chromatin-modifying complexes and affect gene expression. *Proc Natl Acad Sci USA* 106, 11667-11672.
- Kim, Y., and Clark, D. J. (2002). SWI/SNF-dependent long-range remodeling of yeast HIS3 chromatin. *Proc Natl Acad Sci U S A* 99, 15381-15386.
- King, T. H., Decatur, W. A., Bertrand, E., Maxwell, E. S., and Fournier, M. J. (2001). A well-connected and conserved nucleoplasmic helicase is required for production of box C/D and H/ACA snoRNAs and localization of snoRNP proteins. *Mol Cell Biol* 21, 7731-7746.
- Kireev, I., Lakonishok, M., Liu, W., Joshi, V. N., Powell, R., and Belmont, A. S. (2008). In vivo immunogold labeling confirms large-scale chromatin folding motifs. *Nat Methods* 5, 311-313.

- Kloc, M., Wilk, K., Vargas, D., Shirato, Y., Bilinski, S., and Etkin, L. D. (2005). Potential structural role of non-coding and coding RNAs in the organization of the cytoskeleton at the vegetal cortex of *Xenopus* oocytes. *Development* **132**, 3445-3457.
- Kornberg, R. D. (1977). Structure of chromatin. *Annu Rev Biochem* **46**, 931-954.
- Kruithof, M., Chien, F. T., Routh, A., Logie, C., Rhodes, D., and van Noort, J. (2009). Single-molecule force spectroscopy reveals a highly compliant helical folding for the 30-nm chromatin fiber. *Nat Struct Mol Biol* **16**, 534-540.
- Lamond, A. I., and Spector, D. L. (2003). Nuclear speckles: a model for nuclear organelles. *Nat Rev Mol Cell Biol* **4**, 605-612.
- Langst, G., Bonte, E. J., Corona, D. F., and Becker, P. B. (1999). Nucleosome movement by CHRAC and ISWI without disruption or trans-displacement of the histone octamer. *Cell* **97**, 843-852.
- Letunic, I., Doerks, T., and Bork, P. (2012). SMART 7: recent updates to the protein domain annotation resource. *Nucleic Acids Res* **40**, D302-305.
- Li, G., and Reinberg, D. (2011). Chromatin higher-order structures and gene regulation. *Curr Opin Genet Dev* **21**, 175-186.
- Liang, X. H., Vickers, T. A., Guo, S., and Crooke, S. T. (2011). Efficient and specific knockdown of small non-coding RNAs in mammalian cells and in mice. *Nucleic Acids Res* **39**, e13.
- Lieberman-Aiden, E., van Berkum, N. L., Williams, L., Imakaev, M., Ragoczy, T., Telling, A., Amit, I., Lajoie, B. R., Sabo, P. J., Dorschner, M. O., *et al.* (2009). Comprehensive mapping of long-range interactions reveals folding principles of the human genome. *Science* **326**, 289-293.
- Ling, X., Harkness, T. A., Schultz, M. C., Fisher-Adams, G., and Grunstein, M. (1996). Yeast histone H3 and H4 amino termini are important for nucleosome assembly in vivo and in vitro: redundant and position-independent functions in assembly but not in gene regulation. *Genes Dev* **10**, 686-699.
- Lu, X., Wontakal, S. N., Emelyanov, A. V., Morcillo, P., Konev, A. Y., Fyodorov, D. V., and Skoultschi, A. I. (2009). Linker histone H1 is essential for *Drosophila* development, the establishment of pericentric heterochromatin, and a normal polytene chromosome structure. *Genes Dev* **23**, 452-465.
- Luger, K. (2006). Dynamic nucleosomes. *Chromosome Res* **14**, 5-16.
- Luger, K., Mader, A. W., Richmond, R. K., Sargent, D. F., and Richmond, T. J. (1997). Crystal structure of the nucleosome core particle at 2.8 Å resolution. *Nature* **389**, 251-260.

- Luger, K., and Richmond, T. J. (1998a). DNA binding within the nucleosome core. *Curr Opin Struct Biol* 8, 33-40.
- Luger, K., and Richmond, T. J. (1998b). The histone tails of the nucleosome. *Curr Opin Genet Dev* 8, 140-146.
- Lunyak, V. V., Prefontaine, G. G., Nunez, E., Cramer, T., Ju, B. G., Ohgi, K. A., Hutt, K., Roy, R., Garcia-Diaz, A., Zhu, X., *et al.* (2007). Developmentally regulated activation of a SINE B2 repeat as a domain boundary in organogenesis. *Science* 317, 248-251.
- Ma, H., Siegel, A. J., and Berezney, R. (1999). Association of chromosome territories with the nuclear matrix. Disruption of human chromosome territories correlates with the release of a subset of nuclear matrix proteins. *J Cell Biol* 146, 531-542.
- Maison, C., Bailly, D., Peters, A. H. F. M., Quivy, J.-P., Roche, D., Taddei, A., Lachner, M., Jenuwein, T., and Almouzni, G. (2002). Higher-order structure in pericentric heterochromatin involves a distinct pattern of histone modification and an RNA component. *Nat Genet* 30, 329-334.
- Marsden, R. L., McGuffin, L. J., and Jones, D. T. (2002). Rapid protein domain assignment from amino acid sequence using predicted secondary structure. *Protein Sci* 11, 2814-2824.
- Mattick, J. S., Amaral, P. P., Dinger, M. E., Mercer, T. R., and Mehler, M. F. (2009). RNA regulation of epigenetic processes. *Bioessays* 31, 51-59.
- Mavrich, T. N., Jiang, C., Ioshikhes, I. P., Li, X., Venters, B. J., Zanton, S. J., Tomsho, L. P., Qi, J., Glaser, R. L., Schuster, S. C., *et al.* (2008). Nucleosome organization in the *Drosophila* genome. *Nature* 453, 358-362.
- McBryant, S. J., Klonoski, J., Sorensen, T. C., Norskog, S. S., Williams, S., Resch, M. G., Toombs, J. A., Hobdey, S. E., and Hansen, J. C. (2009). Determinants of histone H4 N-terminal domain function during nucleosomal array oligomerization: roles of amino acid sequence, domain length, and charge density. *J Biol Chem* 284, 16716-16722.
- McGhee, J. D., and Felsenfeld, G. (1980). Nucleosome structure. *Annu Rev Biochem* 49, 1115-1156.
- McGhee, J. D., Felsenfeld, G., and Eisenberg, H. (1980a). Nucleosome structure and conformational changes. *Biophys J* 32, 261-270.
- McGhee, J. D., Rau, D. C., Charney, E., and Felsenfeld, G. (1980b). Orientation of the nucleosome within the higher order structure of chromatin. *Cell* 22, 87-96.
- Meins, F., Jr., Si-Ammour, A., and Blevins, T. (2005). RNA silencing systems and their relevance to plant development. *Annu Rev Cell Dev Biol* 21, 297-318.

- Mondal, T., Rasmussen, M., Pandey, G. K., Isaksson, A., and Kanduri, C. (2010). Characterization of the RNA content of chromatin. *Genome research*.
- Muller, W. G., Walker, D., Hager, G. L., and McNally, J. G. (2001). Large-scale chromatin decondensation and recondensation regulated by transcription from a natural promoter. *J Cell Biol* *154*, 33-48.
- Nakama, M., Kawakami, K., Kajitani, T., Urano, T., and Murakami, Y. (2012). DNA-RNA hybrid formation mediates RNAi-directed heterochromatin formation. *Genes Cells* *17*, 218-233.
- Németh, A., Guibert, S., Tiwari, V. K., Ohlsson, R., and Längst, G. (2008). Epigenetic regulation of TTF-I-mediated promoter-terminator interactions of rRNA genes. *EMBO J* *27*, 1255-1265.
- Nemeth, A., and Langst, G. (2011). Genome organization in and around the nucleolus. *Trends Genet* *27*, 149-156.
- Nickerson, J. A., Krochmalnic, G., Wan, K. M., and Penman, S. (1989). Chromatin architecture and nuclear RNA. *Proc Natl Acad Sci USA* *86*, 177-181.
- Noll, M., and Kornberg, R. D. (1977). Action of micrococcal nuclease on chromatin and the location of histone H1. *J Mol Biol* *109*, 393-404.
- Olson, M. O., Dundr, M., and Szebeni, A. (2000). The nucleolus: an old factory with unexpected capabilities. *Trends Cell Biol* *10*, 189-196.
- Park, Y. J., and Luger, K. (2008). Histone chaperones in nucleosome eviction and histone exchange. *Curr Opin Struct Biol* *18*, 282-289.
- Paul, J., and Duerksen, J. D. (1975). Chromatin-associated RNA content of heterochromatin and euchromatin. *Mol Cell Biochem* *9*, 9-16.
- Pederson, T. (2000). Half a century of "the nuclear matrix". *Mol Biol Cell* *11*, 799-805.
- Pederson, T., and Bhorjee, J. S. (1979). Evidence for a role of RNA in eukaryotic chromosome structure. Metabolically stable, small nuclear RNA species are covalently linked to chromosomal DNA in HeLa cells. *J Mol Biol* *128*, 451-480.
- Phillips, J. E., and Corces, V. G. (2009). CTCF: master weaver of the genome. *Cell* *137*, 1194-1211.
- Platani, M., Goldberg, I., Swedlow, J. R., and Lamond, A. I. (2000). In vivo analysis of Cajal body movement, separation, and joining in live human cells. *J Cell Biol* *151*, 1561-1574.

- Ploner, A., Ploner, C., Lukasser, M., Niederegger, H., and Huttenhofer, A. (2009). Methodological obstacles in knocking down small noncoding RNAs. *RNA* *15*, 1797-1804.
- Prilusky, J., Felder, C. E., Zeev-Ben-Mordehai, T., Rydberg, E. H., Man, O., Beckmann, J. S., Silman, I., and Sussman, J. L. (2005). FoldIndex: a simple tool to predict whether a given protein sequence is intrinsically unfolded. *Bioinformatics* *21*, 3435-3438.
- Qiu, X. B., Lin, Y. L., Thome, K. C., Pian, P., Schlegel, B. P., Weremowicz, S., Parvin, J. D., and Dutta, A. (1998). An eukaryotic RuvB-like protein (RUVBL1) essential for growth. *J Biol Chem* *273*, 27786-27793.
- Richards, E. J., and Elgin, S. C. (2002). Epigenetic codes for heterochromatin formation and silencing: rounding up the usual suspects. *Cell* *108*, 489-500.
- Rippe, K., Schrader, A., Riede, P., Strohn, R., Lehmann, E., and Längst, G. (2007). DNA sequence- and conformation-directed positioning of nucleosomes by chromatin-remodeling complexes. *Proc Natl Acad Sci USA* *104*, 15635-15640.
- Robinson, P. J., and Rhodes, D. (2006). Structure of the '30 nm' chromatin fibre: a key role for the linker histone. *Curr Opin Struct Biol* *16*, 336-343.
- Rochman, M., Malicet, C., and Bustin, M. (2010). HMGN5/NSBP1: a new member of the HMGN protein family that affects chromatin structure and function. *Biochim Biophys Acta* *1799*, 86-92.
- Rochman, M., Postnikov, Y., Correll, S., Malicet, C., Wincovitch, S., Karpova, T. S., McNally, J. G., Wu, X., Bubunencko, N. A., Grigoryev, S., and Bustin, M. (2009). The interaction of NSBP1/HMGN5 with nucleosomes in euchromatin counteracts linker histone-mediated chromatin compaction and modulates transcription. *Mol Cell* *35*, 642-656.
- Rodríguez-Campos, A., and Azorín, F. (2007). RNA Is an Integral Component of Chromatin that Contributes to Its Structural Organization. *PLoS ONE* *2*, e1182.
- Roudier, F., Ahmed, I., Berard, C., Sarazin, A., Mary-Huard, T., Cortijo, S., Bouyer, D., Caillieux, E., Duvernois-Berthet, E., Al-Shikhley, L., *et al.* (2011). Integrative epigenomic mapping defines four main chromatin states in Arabidopsis. *EMBO J* *30*, 1928-1938.
- Routh, A., Sandin, S., and Rhodes, D. (2008). Nucleosome repeat length and linker histone stoichiometry determine chromatin fiber structure. *Proc Natl Acad Sci U S A* *105*, 8872-8877.
- Rydberg, B., Holley, W. R., Mian, I. S., and Chatterjee, A. (1998). Chromatin conformation in living cells: support for a zig-zag model of the 30 nm chromatin fiber. *J Mol Biol* *284*, 71-84.

- Sarma, K., and Reinberg, D. (2005). Histone variants meet their match. *Nat Rev Mol Cell Biol* 6, 139-149.
- Saxonov, S., Berg, P., and Brutlag, D. L. (2006). A genome-wide analysis of CpG dinucleotides in the human genome distinguishes two distinct classes of promoters. *Proc Natl Acad Sci U S A* 103, 1412-1417.
- Schalch, T., Duda, S., Sargent, D. F., and Richmond, T. J. (2005). X-ray structure of a tetranucleosome and its implications for the chromatin fibre. *Nature* 436, 138-141.
- Schmid, K. J., and Tautz, D. (1997). A screen for fast evolving genes from *Drosophila*. *Proc Natl Acad Sci U S A* 94, 9746-9750.
- Schmitz, K. M., Mayer, C., Postepska, A., and Grummt, I. (2010). Interaction of noncoding RNA with the rDNA promoter mediates recruitment of DNMT3b and silencing of rRNA genes. *Genes Dev* 24, 2264-2269.
- Schotta, G., Ebert, A., and Reuter, G. (2003). SU(VAR)3-9 is a conserved key function in heterochromatic gene silencing. *Genetica* 117, 149-158.
- Sekiguchi, J. M., and Kmiec, E. B. (1992). In vitro chromatin assembly promoted by the *Xenopus laevis* S-150 cell-free extract is enhanced by treatment with RNase A. *Nucleic Acids Res* 20, 889-895.
- Sexton, T., Yaffe, E., Kenigsberg, E., Bantignies, F., Leblanc, B., Hoichman, M., Parrinello, H., Tanay, A., and Cavalli, G. (2012). Three-dimensional folding and functional organization principles of the *Drosophila* genome. *Cell* 148, 458-472.
- Shamovsky, I., Ivannikov, M., Kandel, E. S., Gershon, D., and Nudler, E. (2006). RNA-mediated response to heat shock in mammalian cells. *Nature* 440, 556-560.
- Shen, X., Mizuguchi, G., Hamiche, A., and Wu, C. (2000). A chromatin remodelling complex involved in transcription and DNA processing. *Nature* 406, 541-544.
- Shimojo, H., Sano, N., Moriwaki, Y., Okuda, M., Horikoshi, M., and Nishimura, Y. (2008). Novel structural and functional mode of a knot essential for RNA binding activity of the Esa1 presumed chromodomain. *J Mol Biol* 378, 987-1001.
- Shirakawa, H., Rochman, M., Furusawa, T., Kuehn, M. R., Horigome, S., Haketa, K., Sugita, Y., Inada, T., Komai, M., and Bustin, M. (2009). The nucleosomal binding protein NSBP1 is highly expressed in the placenta and modulates the expression of differentiation markers in placental Rcho-1 cells. *J Cell Biochem* 106, 651-658.
- Shogren-Knaak, M., Ishii, H., Sun, J. M., Pazin, M. J., Davie, J. R., and Peterson, C. L. (2006). Histone H4-K16 acetylation controls chromatin structure and protein interactions. *Science* 311, 844-847.

- Shopland, L. S., Lynch, C. R., Peterson, K. A., Thornton, K., Kepper, N., Hase, J., Stein, S., Vincent, S., Molloy, K. R., Kreth, G., *et al.* (2006). Folding and organization of a contiguous chromosome region according to the gene distribution pattern in primary genomic sequence. *J Cell Biol* 174, 27-38.
- Sie, C. P., and Kuchka, M. (2011). RNA editing adds flavor to complexity. *Biochemistry (Mosc)* 76, 869-881.
- Siriaco, G., Deuring, R., Chioda, M., Becker, P. B., and Tamkun, J. W. (2009). *Drosophila* ISWI regulates the association of histone H1 with interphase chromosomes in vivo. *Genetics* 182, 661-669.
- Soding, J., Biegert, A., and Lupas, A. N. (2005). The HHpred interactive server for protein homology detection and structure prediction. *Nucleic Acids Res* 33, W244-248.
- Splinter, E., Heath, H., Kooren, J., Palstra, R. J., Klous, P., Grosveld, F., Galjart, N., and de Laat, W. (2006). CTCF mediates long-range chromatin looping and local histone modification in the beta-globin locus. *Genes Dev* 20, 2349-2354.
- Stalder, J., Larsen, A., Engel, J. D., Dolan, M., Groudine, M., and Weintraub, H. (1980). Tissue-specific DNA cleavages in the globin chromatin domain introduced by DNAase I. *Cell* 20, 451-460.
- Stewart, A. F., Reik, A., and Schutz, G. (1991). A simpler and better method to cleave chromatin with DNase 1 for hypersensitive site analyses. *Nucleic Acids Res* 19, 3157.
- Strohner, R., Wachsmuth, M., Dachauer, K., Mazurkiewicz, J., Hochstatter, J., Rippe, K., and Längst, G. (2005). A 'loop recapture' mechanism for ACF-dependent nucleosome remodeling. *Nat Struct Mol Biol* 12, 683-690.
- Szollosi, E., Bokor, M., Bodor, A., Perczel, A., Klement, E., Medzihradszky, K. F., Tompa, K., and Tompa, P. (2008). Intrinsic structural disorder of DF31, a *Drosophila* protein of chromatin decondensation and remodeling activities. *J Proteome Res* 7, 2291-2299.
- Talbert, P. B., and Henikoff, S. (2010). Histone variants--ancient wrap artists of the epigenome. *Nat Rev Mol Cell Biol* 11, 264-275.
- Tanaka, T., and Kanehisa, T. (1972). Low molecular-weight RNA associated with chromatin. Its interaction with histone. *J Biochem* 72, 1273-1275.
- Terribilini, M., Sander, J. D., Lee, J. H., Zaback, P., Jernigan, R. L., Honavar, V., and Dobbs, D. (2007). RNABindR: a server for analyzing and predicting RNA-binding sites in proteins. *Nucleic Acids Res* 35, W578-584.

- Thoma, F., Koller, T., and Klug, A. (1979). Involvement of histone H1 in the organization of the nucleosome and of the salt-dependent superstructures of chromatin. *J Cell Biol* 83, 403-427.
- Tolhuis, B., Palstra, R. J., Splinter, E., Grosveld, F., and de Laat, W. (2002). Looping and interaction between hypersensitive sites in the active beta-globin locus. *Mol Cell* 10, 1453-1465.
- Tresaugues, L., Dehe, P. M., Guerois, R., Rodriguez-Gil, A., Varlet, I., Salah, P., Pamblanco, M., Luciano, P., Quevillon-Cheruel, S., Sollier, J., *et al.* (2006). Structural characterization of Set1 RNA recognition motifs and their role in histone H3 lysine 4 methylation. *J Mol Biol* 359, 1170-1181.
- Tsai, M. C., Manor, O., Wan, Y., Mosammaparast, N., Wang, J. K., Lan, F., Shi, Y., Segal, E., and Chang, H. Y. (2010). Long noncoding RNA as modular scaffold of histone modification complexes. *Science* 329, 689-693.
- Tumbar, T., Sudlow, G., and Belmont, A. S. (1999). Large-scale chromatin unfolding and remodeling induced by VP16 acidic activation domain. *J Cell Biol* 145, 1341-1354.
- van Eekelen, C. A., and van Venrooij, W. J. (1981). hnRNA and its attachment to a nuclear protein matrix. *J Cell Biol* 88, 554-563.
- van Steensel, B., Delrow, J., and Henikoff, S. (2001). Chromatin profiling using targeted DNA adenine methyltransferase. *Nat Genet* 27, 304-308.
- van-Holde, K. E. (1989). *Chromatin*. Springer Verlag, 497.
- Varga-Weisz, P. D., and Becker, P. B. (2006). Regulation of higher-order chromatin structures by nucleosome-remodelling factors. *Curr Opin Genet Dev* 16, 151-156.
- Verschure, P. J., van der Kraan, I., de Leeuw, W., van der Vlag, J., Carpenter, A. E., Belmont, A. S., and van Driel, R. (2005). In vivo HP1 targeting causes large-scale chromatin condensation and enhanced histone lysine methylation. *Mol Cell Biol* 25, 4552-4564.
- Vitali, P., Basyuk, E., Le Meur, E., Bertrand, E., Muscatelli, F., Cavaille, J., and Huttenhofer, A. (2005). ADAR2-mediated editing of RNA substrates in the nucleolus is inhibited by C/D small nucleolar RNAs. *J Cell Biol* 169, 745-753.
- von Heyden, H. W., and Zachau, H. G. (1971). Characterization of RNA in fractions of calf thymus chromatin. *Biochim Biophys Acta* 232, 651-660.
- Wang, G. G., Allis, C. D., and Chi, P. (2007). Chromatin remodeling and cancer, Part I: Covalent histone modifications. *Trends Mol Med* 13, 363-372.

- Wang, K. C., Yang, Y. W., Liu, B., Sanyal, A., Corces-Zimmerman, R., Chen, Y., Lajoie, B. R., Protacio, A., Flynn, R. A., Gupta, R. A., *et al.* (2011). A long noncoding RNA maintains active chromatin to coordinate homeotic gene expression. *Nature* 472, 120-124.
- Wang, L., and Brown, S. J. (2006). BindN: a web-based tool for efficient prediction of DNA and RNA binding sites in amino acid sequences. *Nucleic Acids Res* 34, W243-248.
- Wang, X., and Hayes, J. J. (2008). Acetylation mimics within individual core histone tail domains indicate distinct roles in regulating the stability of higher-order chromatin structure. *Mol Cell Biol* 28, 227-236.
- Wang, Y., Fischle, W., Cheung, W., Jacobs, S., Khorasanizadeh, S., and Allis, C. D. (2004). Beyond the double helix: writing and reading the histone code. *Novartis Found Symp* 259, 3-17; discussion 17-21, 163-169.
- Wass, M. N., and Sternberg, M. J. (2008). ConFunc--functional annotation in the twilight zone. *Bioinformatics* 24, 798-806.
- Widom, J., and Klug, A. (1985). Structure of the 300A chromatin filament: X-ray diffraction from oriented samples. *Cell* 43, 207-213.
- Wilkins, M. R., Gasteiger, E., Bairoch, A., Sanchez, J. C., Williams, K. L., Appel, R. D., and Hochstrasser, D. F. (1999). Protein identification and analysis tools in the ExPASy server. *Methods Mol Biol* 112, 531-552.
- Willingham, A. T., Orth, A. P., Batalov, S., Peters, E. C., Wen, B. G., Aza-Blanc, P., Hogenesch, J. B., and Schultz, P. G. (2005). A strategy for probing the function of noncoding RNAs finds a repressor of NFAT. *Science* 309, 1570-1573.
- Wilusz, J. E., Sunwoo, H., and Spector, D. L. (2009). Long noncoding RNAs: functional surprises from the RNA world. *Genes Dev* 23, 1494-1504.
- Wolffe, A. P. (1997). Histone H1. *Int J Biochem Cell Biol* 29, 1463-1466.
- Wolffe, A. P., Khochbin, S., and Dimitrov, S. (1997). What do linker histones do in chromatin? *Bioessays* 19, 249-255.
- Woodcock, C. L. (1994). Chromatin fibers observed in situ in frozen hydrated sections. Native fiber diameter is not correlated with nucleosome repeat length. *J Cell Biol* 125, 11-19.
- Woodcock, C. L., and Ghosh, R. P. (2010). Chromatin higher-order structure and dynamics. *Cold Spring Harb Perspect Biol* 2, a000596.
- Worby, C. A., Simonson-Leff, N., and Dixon, J. E. (2001). RNA interference of gene expression (RNAi) in cultured *Drosophila* cells. *Sci STKE* 2001, pl1.

Zheng, C., Lu, X., Hansen, J. C., and Hayes, J. J. (2005). Salt-dependent intra- and internucleosomal interactions of the H3 tail domain in a model oligonucleosomal array. *J Biol Chem* 280, 33552-33557.

8. Appendix

8.1. Curriculum vitae

Name: Schubert
 First Name: Thomas
 Nationality: German
 Date of birth: 29. May 1983
 Place of birth: Regensburg, Germany

Education:

9/2008 – 8/2012 **PhD student** at the institute of Biochemistry III, University of Regensburg, Head Prof. Herbert Tschochner, Supervisor Prof. Dr. Gernot Längst

9/2007 – 6/2008 **Diploma student** at the institute of Physiology, University of Regensburg, Head Prof. Armin Kurtz, Supervisor Vladimir Todorov

9/2003 – 8/2007 **Studies of Biology** at the university of Regensburg

9/2002 - 6/2003 **Civil Service**, Regensburger Krankentransporte

6/2002 **High school diploma** (Abitur), Gymnasium Neutraubling

Work experience:

9/2006 – 3/2007 Institute of environmental microbiology and astrobiology, University of New South Wales, Sydney
 Head and Supervisor Prof Dr. Brett A. Neilan

8.2. List of publications

Df31 protein and snoRNAs maintain accessible higher order structures of chromatin.

Schubert T, Pusch M, Diermeier S, Benes V, Imhof A, Längst A
(In revision) **Mol Cell**, 2012 march

Human ISWI chromatin-remodelling complexes sample nucleosomes via transient binding reactions and become immobilized at active sites.

Erdel F, **Schubert T**, Marth C, Längst G, Rippe K.
Proc Natl Acad Sci U S A. 2010 Nov

PPARgamma-dependent regulation of adenylate cyclase 6 amplifies the stimulatory effect of cAMP on renin gene expression.

Desch M, **Schubert T**, Schreiber A, Mayer S, Friedrich B, Artunc F, Todorov VT.
Mol Endocrinol. 2010 Nov

The Pal3 promoter sequence is critical for the regulation of human renin gene transcription by peroxisome proliferator-activated receptor-gamma,

Todorov VT, Desch M, **Schubert T**, Kurtz A.
Endocrinology 2008 Sep

8.3. Active participation at conferences

Oral presentation, selected speaker:

1. RIGeL summer academy on cellular Biochemistry and Biophysics
25.9.-26.9.2010, Kostenz, Germany

Chromatin: structure and function, Abcam meeting,
5.12.-8.12.2011, Aruba

Poster presentation:

The Non-Coding Genome Conference,
13.10.2010-16.10.2010, EMBL, Heidelberg, Germany

62.Mosbacher Kolloquium, mechanisms of RNA-mediated regulation
7.4.2011-9.4.2011, Mosbach, Germany

2. RIGeL summer academy on cellular Biochemistry and Biophysics
26.9.-27.9.2011, Kostenz, Germany

8.4. Grants and awards

6/2006		DAAD internship travel grant, UNSW, Sydney
9/2011		DAAD conference travel grant, Abcam meeting, Aruba
10/2010	1. Poster Award	EMBO Meeting Heidelberg, „the Non-Coding Genome“ conference
4/2011	1. Poster Award	62. Mosbacher Kolloquium, GBM meeting, Mosbach „mechanisms of RNA-mediated regulation“
9/2011	1. Poster Prize	2. RIGeL summer academy on cellular Biochemistry and Biophysics

9. Eidesstattliche Erklärung

Hiermit erkläre ich, Thomas Friedrich Schubert, geboren am 29.Mai.1983 in Regensburg, an Eides statt, die vorliegende Promotionsarbeit mit dem Titel:

„Df31 and chromatin associated RNAs maintain accessible higher order structures of chromatin“

selbstständig verfasst zu haben, unter alleiniger Verwendung der angegebenen Hilfsmittel. Die aus anderen Quellen direkt oder indirekt übernommenen Daten oder Konzepte sind unter Angabe des Literatur- bzw. Personenzitats gekennzeichnet.

Die Arbeit wurde bisher weder im In- noch im Ausland in gleicher oder ähnlicher Form einer anderen Prüfungsbehörde vorgelegt.

Regensburg, den

(Thomas Schubert)

10. Acknowledgements

It is a pleasure for me, to thank all the people who made this thesis possible.

First of all, I owe sincere and earnest thankfulness to Prof. Dr. Gernot Längst. I am very grateful for the amazing topic I could work on. Thanks for all support you offered me, the financial, the technical, the scientific and the intellectual help. In this fruitful atmosphere I was able to learn a lot!

Furthermore, I would like to thank the dissertation committee, Prof. Dr. Herbert Tschochner, Prof. Dr. Michael Rehli and Prof. Dr. Gunter Meister for the examination of my thesis and the constructive suggestions.

I would like to show my gratitude to all collaboration partners. Thanks to Axel Imhof and Miriam for their fantastic work; I enjoyed every day in your lab. Thanks to Karsten Rippe, Fabian and Maiwen in Heidelberg for the ideas and the fruitful collaborations. Last but not least, I would like to thank Sarah Diermeier for all her efforts in the project.

It is a great pleasure to thank the whole team of the House of the Ribosome. Thank you for all the help, support, discussions and all the fun we shared. Special thanks to Gisela Pöll, not just your fantastic cakes saved me several times.

I am truly indebted and thankful to the Längst team. You made it very easy to join the group and I very soon felt accepted as member. Thanks for all help and support you offered as well as all the fun we got together.

Furthermore I would like to thank the commando centre upstairs. We were a great team. Special thanks to Dr. Attila Nemeth for all the „5 minutes“ you had for me. Michi, Karina, Josef, Stefan and Attila you are the reason for an incredible good atmosphere in the small lab.

My very special gratitude is due to my family, for their loving support. You always gave me the freedom as well as the security that I needed.

I owe my loving thanks to my wife Evi. Without your encouragement and understanding it would have been impossible for me to finish this work. You are a constant source of strength and endurance for me.

